

USAFSAM-TR-89-32

AD-A223 757

**ADSORPTION AND DIFFUSION OF OXYGEN, NITROGEN,
METHANE AND ARGON IN MOLECULAR SIEVE CARBONS**

Yi Hua Ma, Sc.D.
Weiruo Sun, M.S.
Maruti Bhandarkar, Ph.D.
Jinqu Wang, M.S.

DTIC
ELECTE
JUL 06 1990
S D D

Department of Chemical Engineering
Worcester Polytechnic Institute
Worcester, MA 01609

April 1990

Final Report for Period 1 March 1988 - 30 September 1989

Approved for public release; distribution is unlimited.

Prepared for
USAF SCHOOL OF AEROSPACE MEDICINE
Human Systems Division (AFSC)
Brooks Air Force Base, TX 78235-5301



50 0. 0 018

NOTICES

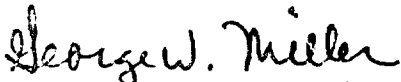
This final report was submitted by Worcester Polytechnic Institute, 100 Institute Road, Worcester, MA, under contract F33615-87-D-0627, job order 7930-11-8A, with the USAF School of Aerospace Medicine, Human Systems Division, AFSC, Brooks AFB, Texas, Major George W. Miller (USAFSAM/VNL) was the Laboratory Project Scientist-in-Charge.

When Government drawings, specifications, or other data are used for any purpose other than in connection with a definitely Government-related procurement, the United States Government incurs no responsibility or any obligation whatsoever. The fact that the Government may have formulated or in any way supplied the said drawings, specifications, or other data, is not to be regarded by implication, or otherwise in any manner construed, as licensing the holder or any other person or corporation; or as conveying any rights or permission to manufacture, use, or sell any patented invention that may in any way be related thereto.

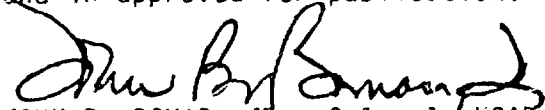
This effort was funded wholly through the LDIR Program.

The Office of Public Affairs has reviewed this report, and it is releasable to the National Technical Information Service, where it will be available to the general public, including foreign nationals.

This report has been reviewed and is approved for publication.



GEORGE W. MILLER, Major, USAF
Project Scientist



JOHN B. BOMAR, JR., Colonel, USAF, BSC
Supervisor



GEORGE E. SCHWENDER, Colonel, USAF, MC, CFS
Commander

UNCLASSIFIED

SECURITY CLASSIFICATION OF THIS PAGE

REPORT DOCUMENTATION PAGE				Form Approved OMB No. 0704-0188		
1a. REPORT SECURITY CLASSIFICATION <u>Unclassified</u>			1b. RESTRICTIVE MARKINGS			
2a. SECURITY CLASSIFICATION AUTHORITY			3. DISTRIBUTION/AVAILABILITY OF REPORT Approved for public release; distribution is unlimited.			
2b. DECLASSIFICATION/DOWNGRADING SCHEDULE						
4. PERFORMING ORGANIZATION REPORT NUMBER(S)			5. MONITORING ORGANIZATION REPORT NUMBER(S) USAFSAM-TR-89-32			
6a. NAME OF PERFORMING ORGANIZATION Worcester Polytechnic Institute		6b. OFFICE SYMBOL (If applicable)		7a. NAME OF MONITORING ORGANIZATION USAF School of Aerospace Medicine (VNL)		
6c. ADDRESS (City, State, and ZIP Code) 100 Institute Road Worcester, MA 01609			7b. ADDRESS (City, State, and ZIP Code) Human Systems Division (AFSC) Brooks AFB, Texas 78235-5301			
8a. NAME OF FUNDING/SPONSORING ORGANIZATION		8b. OFFICE SYMBOL (If applicable)		9. PROCUREMENT INSTRUMENT IDENTIFICATION NUMBER F33615-87-D-0627/0001		
8c. ADDRESS (City, State, and ZIP Code)			10. SOURCE OF FUNDING NUMBERS			
			PROGRAM ELEMENT NO 61101F	PROJECT NO. 7930	TASK NO 11	WORK UNIT ACCESSION NO 8A
11. TITLE (Include Security Classification) Adsorption and Diffusion of Oxygen, Nitrogen, Methane and Argon in Molecular Sieve Carbons						
12. PERSONAL AUTHOR(S) Ma, Yi Hua; Sun, Weiruo; Bhandarkar, Maruti; and Wang, Jinqu						
13a. TYPE OF REPORT Final		13b. TIME COVERED FROM 88/03 TO 89/09		14. DATE OF REPORT (Year, Month, Day) 1990, April		
15. PAGE COUNT 98						
16. SUPPLEMENTARY NOTATION						
17. COSATI CODES			18. SUBJECT TERMS (Continue on reverse if necessary and identify by block number)			
FIELD	GROUP	SUB-GROUP	Adsorption; Diffusion Rate; Molecular Sieve Carbons; Langmuir Equation; Vacancy Solution Model; Kinetic Data; Isotherm; Isosteric Heat of Adsorption. (TES)LE			
07	04					
11	07					
19. ABSTRACT (Continue on reverse if necessary and identify by block number) Equilibrium adsorption and diffusion data for oxygen, nitrogen, methane and argon in carbon molecular sieves 3A and 5A at 0°C, 30°C and 50°C were obtained at pressures up to 13 Bar using a high-pressure Cahn electrobalance. On a molar basis, methane had the highest adsorption capacity among the four gases studied both in 3A and 5A molecular sieve carbons. Oxygen and nitrogen had approximately the same equilibrium adsorption capacity. Equilibrium adsorption data were represented by a Langmuir equation and the Vacancy Solution Model (VSM). The VSM appears to give a good fit of the experimental data while the representation of the experimental data by the Langmuir equation showed deviation, especially at high pressures. The isosteric heats of adsorption were found to increase slightly with an increase in surface coverage. The values were slightly higher on 3A than on 5A for all the gases except argon. Kinetic data showed that oxygen has the highest diffusion rate and methane the lowest. Diffusivities increased with temperature. At low temperature the diffusivity for nitrogen increased with pressure. No pressure dependency was observed for the diffusivity of the other gases.						
20. DISTRIBUTION/AVAILABILITY OF ABSTRACT <input checked="" type="checkbox"/> UNCLASSIFIED/UNLIMITED <input type="checkbox"/> SAME AS RPT <input type="checkbox"/> DTIC USERS			21. ABSTRACT SECURITY CLASSIFICATION Unclassified			
22a. NAME OF RESPONSIBLE INDIVIDUAL George W. Miller, Major, USAF			22b. TELEPHONE (Include Area Code) (512) 536-3361		22c. OFFICE SYMBOL USAFSAM/VNL	

CONTENTS

	Page
INTRODUCTION.....	1
EXPERIMENTAL.....	2
RESULTS AND DISCUSSION.....	7
Activation Procedure.....	7
Single Component Adsorption.....	10
Model Differentiation.....	10
The Langmuir isotherm.....	10
The vacancy solution model.....	11
Adsorption on 5A and 3A MSC.....	12
Adsorption of O ₂	12
Adsorption of CH ₄	13
Adsorption of N ₂	18
Adsorption of Ar.....	21
Comparison with previous studies.....	21
Isosteric Heat of Adsorption.....	21
Single Component Diffusion.....	30
Mathematical Model.....	30
Comparison of Diffusivity Values.....	31
Variation of Diffusivity with Temperature and Pressure.....	36
Multicomponent Adsorption.....	38
Original Design of the Multicomponent Adsorption Setup.....	38
Difficulty in the Original Design.....	40
New Design.....	41
CONCLUSIONS.....	41
RECOMMENDATIONS FOR FUTURE WORK.....	44
Measurement of Adsorption and Diffusion of Binary Gases.....	44

Model Prediction for Multicomponent Adsorption from Single Component Adsorption Data.....	44
Mathematical Modeling for Multicomponent Diffusion....	45
NOMENCLATURE.....	45
REFERENCES.....	46
APPENDIX A: Adsorption Data.....	49
APPENDIX B: Computer Program for VSM Calculations.....	83

List of Figures

Figure No.	Page
1. High pressure (0-10,000 Torr) adsorption unit.....	3
2. Photographs of the high pressure adsorption unit.....	4
3. Schematic of the low pressure (0-760 Torr) adsorption system.....	5
4. Photographs of the low pressure adsorption system...	6
5. Scanning electron micrographs of the molecular sieve carbons.....	8
6. Weight change during initial pump-down.....	9
7. O ₂ adsorption and desorption isotherms.....	14
8. Uptake curves during O ₂ adsorption (low pressure)....	14
9. Uptake curves during O ₂ adsorption (high pressure)...	15
10. O ₂ adsorption isotherm on 5A MSC.....	15
11. O ₂ adsorption isotherm on 3A MSC.....	16
12. O ₂ adsorption isotherm on 5A MSC.....	16
13. O ₂ adsorption isotherm on 3A MSC.....	17
14. CH ₄ adsorption and desorption isotherm on 5A MSC.....	17
15. CH ₄ adsorption and desorption isotherm on 3A MSC.....	18
16. CH ₄ adsorption isotherm on 5A MSC.....	19
17. CH ₄ adsorption isotherm on 3A MSC.....	19
18. CH ₄ adsorption isotherm on 5A MSC.....	20
19. CH ₄ adsorption isotherm on 3A MSC.....	20
20. N ₂ adsorption and desorption isotherm on 5A MSC.....	22
21. N ₂ adsorption isotherm on 5A MSC.....	22
22. N ₂ adsorption isotherm on 3A MSC.....	23
23. Ar adsorption isotherm on 5A MSC.....	23
24. Ar adsorption isotherm on 3A MSC.....	24
25. Adsorption capacities of different samples.....	24
26. CH ₄ adsorption on various samples.....	25
27. O ₂ adsorption on various samples.....	25
28. N ₂ adsorption on various samples.....	26
29. Ar adsorption on various samples.....	26
30. Plot of ln P vs 1/T for Ar on 5A MSC.....	28
31. Plot of ln P vs 1/T for Ar on 3A MSC.....	28
32. Isosteric heat of adsorption as a function of coverage.....	29

33.	Uptake curves of gases on 3A MSC at 0°C.....	34
34.	Uptake curves of gases on 3A MSC at 30°C.....	34
35.	Uptake curves of gases on 3A MSC at 50°C.....	35
36.	Uptake curves at different temperatures.....	35
37.	The variation of diffusivity of Ar with pressure.....	37
38.	The variation of diffusivity of O ₂ with pressure.....	37
39.	Schematic of the well-stirred reactor.....	39
40.	Calibration curve of O ₂ in He (at 100 Torr).....	40
41.	New design for the well-stirred reactor.....	42
42.	Photographs of the well-stirred reactor.....	43

List of Tables

Table No.

1.	Properties of the MSC Samples.....	7
2.	Langmuir Equation Constants.....	12
3.	Isotherm Parameters for the VSM.....	13
4.	Isosteric Heat of Adsorption for Gases on 5A MSC.....	27
5.	Isosteric Heat of Adsorption for Gases on 3A MSC.....	27
6.	Diffusivity of Gases in 3A MSC.....	32
7.	Diffusivity of Gases in 5A MSC.....	33
8.	Activation Energy of Diffusion in 5A and 3A MSC.....	36

Accession For	
NTIS CRA&I	<input checked="checked" type="checkbox"/>
DTIC TAB	<input type="checkbox"/>
Unannounced	<input type="checkbox"/>
Justification _____	
By _____	
Distribution /	
Availability Codes	
Dist	Avail and/or Special
A-1	



SUMMARY

An important development in adsorption technology is pressure swing adsorption (PSA) in which periodical regeneration of the adsorbent is accomplished by reducing total pressure. Large throughputs can generally be obtained from a small-scale PSA adsorber by using a short cycle time (in minutes or seconds) which results in rapid pressure cycling. Small-scale PSA adsorbers are presently used to produce breathable oxygen on board military aircraft. The mechanisms for separation in PSA are mainly based on kinetic or equilibrium effects although the use of the steric effect is also possible (e.g. molecular sieve). Consequently, understanding both equilibrium and kinetic data is essential in designing a better PSA process. This report describes the technical efforts to compile the equilibrium and kinetic data of several gases in molecular sieve carbons (MSC) with the objective that the results can be applied to the design of a PSA process for air separation.

Equilibrium adsorption and diffusion of oxygen, nitrogen, methane and argon in carbon molecular sieves 3A and 5A were investigated. Equilibrium as well as kinetic data were compiled during the adsorption experiments in two different gravimetric setups, one for high pressures and the other for low pressures, although most runs were made in the high pressure unit. The experimental data are tabulated in the Appendix. The adsorbate pressure was varied over a wide range, viz., 0-10,000 Torr at three temperatures, 0°C, 30°C and 50°C. Both high pressure and low pressure adsorption experiments were carried out gravimetrically.

On a molar basis, methane had the highest adsorption capacity among the four gases studied in both 3A and 5A molecular sieve carbons. Oxygen and nitrogen had approximately the same equilibrium adsorption capacity. Equilibrium adsorption data are represented by a Langmuir equation and the vacancy solution model (VSM). The VSM model appears to give a good fit to the experimental data. Experimental evidences also showed that MSC adsorbed relatively small amounts of water when it was exposed to ambient air for an extended period. This hydrophobic property of MSC makes it especially suitable for air separation in a pressure swing operation.

The isosteric heats of adsorption were found to increase slightly with increases in the surface coverage. The values are slightly higher on 3A than on 5A for all the gases except argon, indicating that 3A MSC showed a greater energetic heterogeneity than 5A MSC although both MSCs showed a relatively low energetic heterogeneity.

Kinetic data showed that oxygen had the highest diffusion rate while methane had the lowest rate. Methane adsorption in 3A was considerably slower than in 5A MSC. The adsorption of oxygen

in both 5A and 3A occurred at about the same rate. Nitrogen and argon adsorption in 3A was slower than in 5A. The diffusivity values obtained from the kinetic data showed no dependency on pressure but increased with increasing temperature as expected.

The high adsorption rate of oxygen in both 3A and 5A MSC coupled with the fact that both argon and nitrogen had a slower adsorption rate in 3A than in 5A implies that 3A may be a better adsorbent for kinetic separation of air components in a pressure swing operation.

Recommendations are made for a follow-up program to employ the newly designed multicomponent adsorption setup to collect data for the adsorption and diffusion of binary gases at 0°C, 30°C, and 50°C in a pressure range of 0-10,000 Torr. Both the effects of co-adsorption of binary gases and the displacement phenomena should be investigated. Furthermore, it is also recommended to continue the investigation of model prediction for multicomponent adsorption from single component adsorption data. The Langmuir, VSM, IAST and modified Langmuir-Sips isotherm equations should be used to predict multicomponent adsorption isotherms from single component data. The mixture adsorption isotherms developed from the model should be compared with those developed from experimental measurements. Furthermore, the development of a mathematical model for multicomponent diffusion is recommended.

ADSORPTION AND DIFFUSION OF OXYGEN, NITROGEN, METHANE AND ARGON IN MOLECULAR SIEVE CARBONS

I. INTRODUCTION

It is well known that coals and their carbonized product show molecular sieve properties although their adsorption capacities are generally too low to have any practical use. There is, however, considerable information in the literature about the production of carbons with both molecular sieve properties and high adsorption capacity from carbonization of organic polymers (1-3). Carbons with molecular sieving properties were first observed by Franklin (4) who reported that heat treated coals excluded fluids according to their molecular sizes. Dacey and Thomas (5) later reported an extensive study on the properties of a hard, highly porous charcoal prepared by the pyrolysis of polyvinylidene chloride. Their results clearly showed the molecular sieving properties of the charcoal. Extensive reviews on the subject have been reported by Walker et al (6) and Spencer and Bond (7). As an adsorbent, carbon molecular sieves may be preferred to inorganic molecular sieves due not only to their stability at higher temperatures and in acidic media but also due to their lower affinity to water (6). Furthermore, from a practical point of view, molecular sieve carbons are attractive because they can be easily obtained by pyrolysis of many thermosetting polymers such as poly (vinylidene chloride) (PVDC) (5, 8), poly (furfuryl alcohol) (9), cellulose (10), cellulose triacetate (11), saran copolymer (12), poly (di vinylbenzene) (13), and various coals such as anthracite (14) and the bamboo (15). Thus, the fact that the effective pore size can be adjusted by the conditions of the manufacturing process makes it relatively easy to tailor a carbon sieve for a specific separation. However, the difficulty involved in achieving absolute reproducibility between different batches (16) and the existence of a distribution of pore size, even if narrow, make the molecular sieving selectivity of a carbon sieve not as good as that of a zeolite sieve. Nevertheless, the remarkably high kinetic selectivity which may be attained with a well-prepared carbon sieve coupled with its low water affinity makes carbon sieve a prime adsorbent for air separation.

A number of current and proposed applications of carbon sieves has been reviewed by Jüntgen (17). It should be pointed out that currently the most important large-scale application for carbon sieve is in air separation. It should further be pointed out that its deterioration due to oxidation does not appear to be a significant problem. Other potential applications include the clean-up of the off-gases from nuclear facilities and the production of pure hydrogen from gas streams containing small

amounts of hydrocarbons. However, a wider range of process applications will emerge as the technology of producing carbon sieves is further developed.

The present study reports an investigation of the adsorption and diffusion of nitrogen (N_2), oxygen (O_2), methane (CH_4) and argon (Ar) in 5A and 3A molecular sieve carbons. The prime objective was to investigate the effects of molecular size on the equilibrium adsorption and diffusion property of these molecular sieve carbons. It is anticipated that the results obtained in the present study can be applied to the design of a pressure swing adsorption (PSA) process for air separation.

II. EXPERIMENTAL

The adsorption of pure gases by 5A and 3A MSC (20-40 mesh) was studied at 0°, 30°, and 50°C. The adsorbate pressure was varied over a wide range, *viz.*, 0-10,000 Torr. Equilibrium as well as kinetic data were compiled during the adsorption experiments in two different gravimetric setups, one for high pressures and the other for low pressures although most runs were made in the high pressure unit.

The high-pressure adsorption experiments were carried out in a gravimetric setup constructed using mainly 316 stainless steel. A Cahn 1000 electrobalance was placed inside a stainless steel casing; it was connected to a gas reservoir, gas supply tank and a pumping system using thick-walled stainless steel tubing and precision Nupro valves. Pressures up to 50 Bars could be safely reached in the setup shown schematically in Figure 1. Photographs of the high pressure unit are shown in Figure 2.

The entire system could be evacuated to a pressure less than 10^{-3} Torr by means of an oil-free turbo pump (Varian V80A) in conjunction with a mechanical roughing pump. The weight change during experiments could be determined with an accuracy of 0.5 micrograms. The weight, temperature, and pressure could be monitored continuously with an AT&T personal computer. The pressure was measured using MKS Baratron gauges. Omega digital controllers were used for temperature control and measurement.

Additional experiments in the subatmospheric pressure range (0-760 Torr) were also carried out in an all-glass unit housed in an insulated box free from any kind of disturbance, either mechanical or thermal. The apparatus is shown schematically in Figure 3. Photographs of the unit are shown in Figure 4. The setup consisted of a Cahn 2000 electrobalance mounted inside a glass chamber that could be evacuated to a pressure less than 10^{-4} Torr by means of an oil-free turbo pump (Varian V80A) in conjunction with a mechanical roughing pump. The change in the weight of the sample during experiments could be determined with an accuracy of 0.5 micrograms. The weight, temperature, and

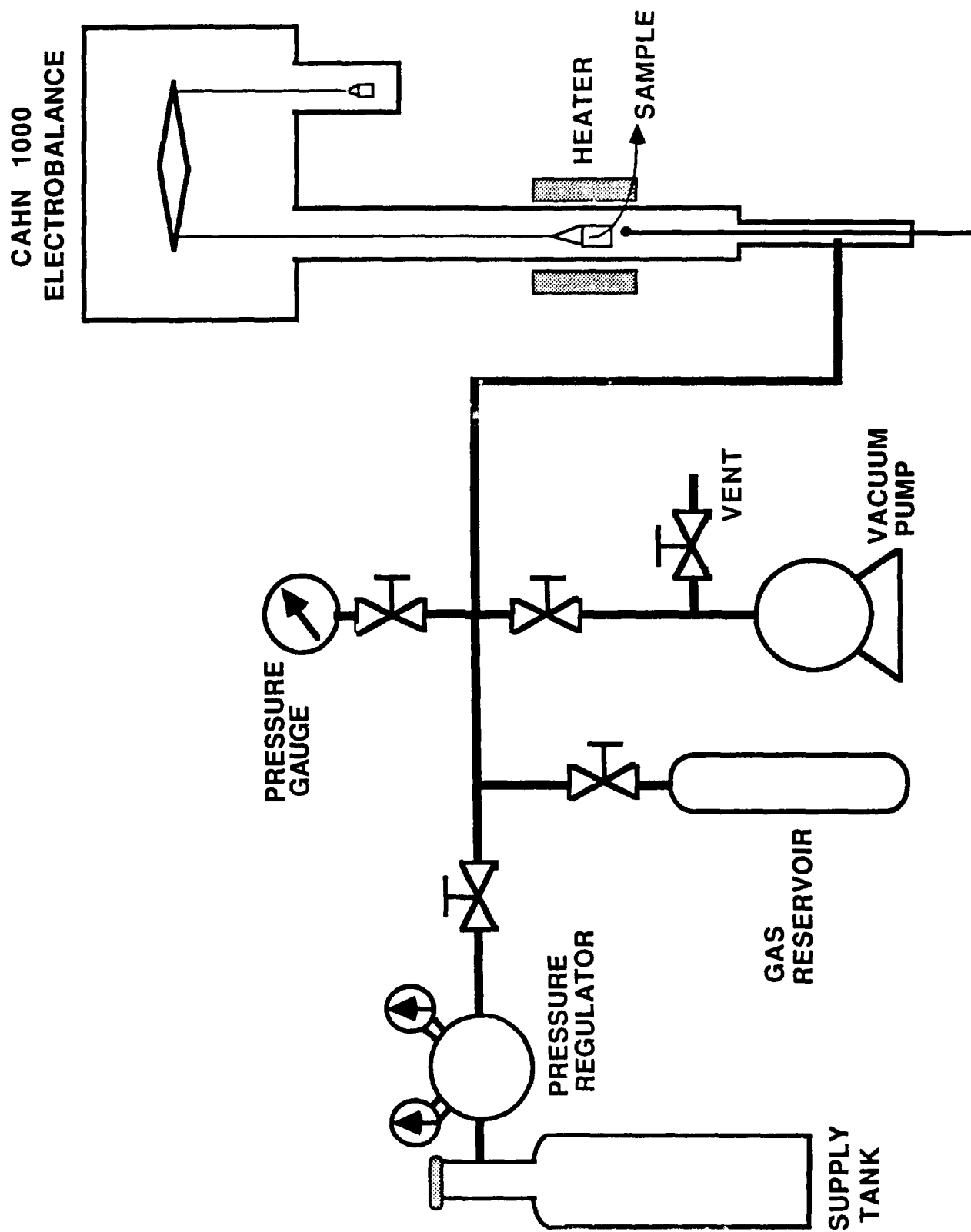


Figure 1. High pressure (0-10,000 Torr) adsorption unit.

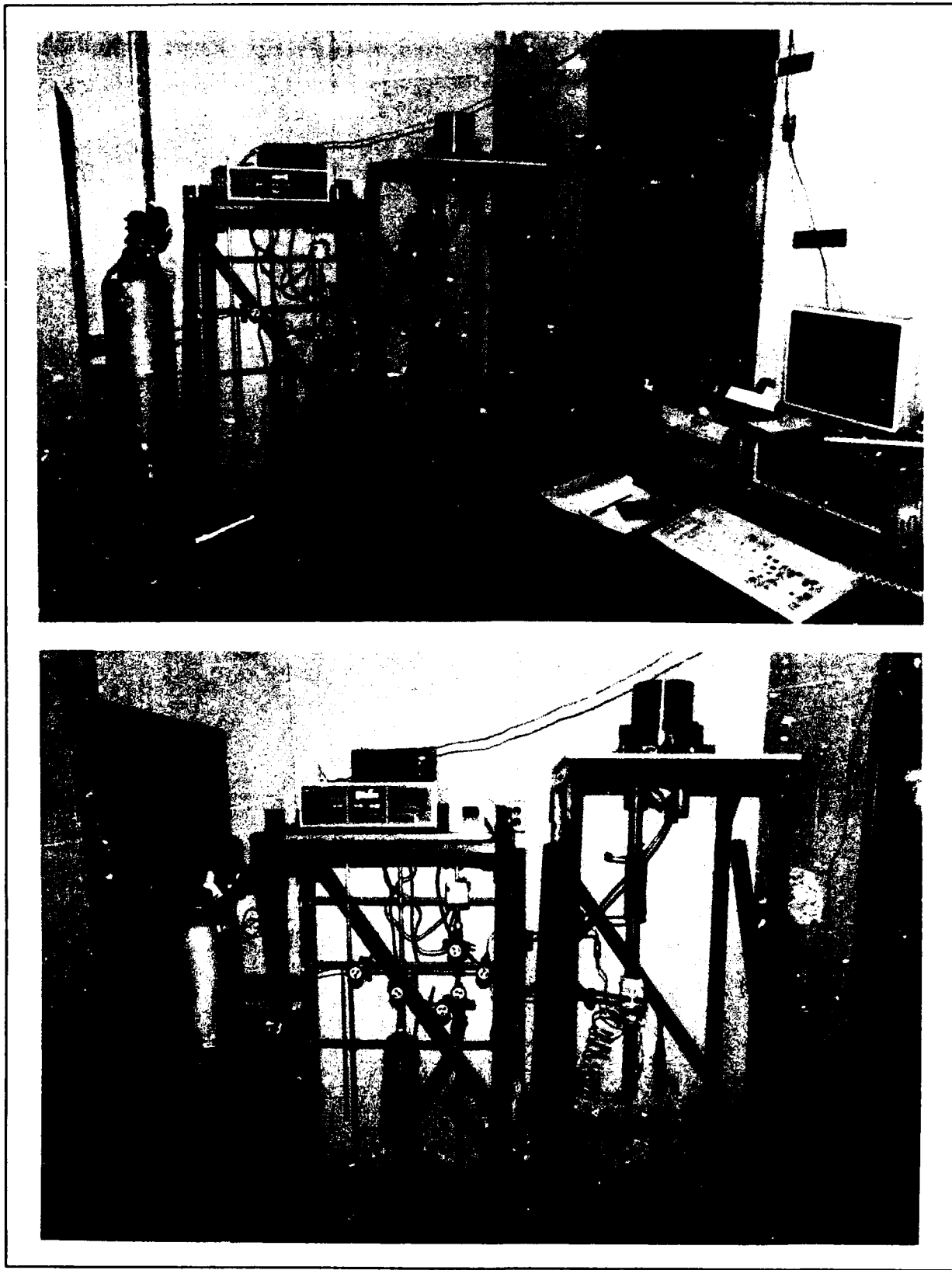
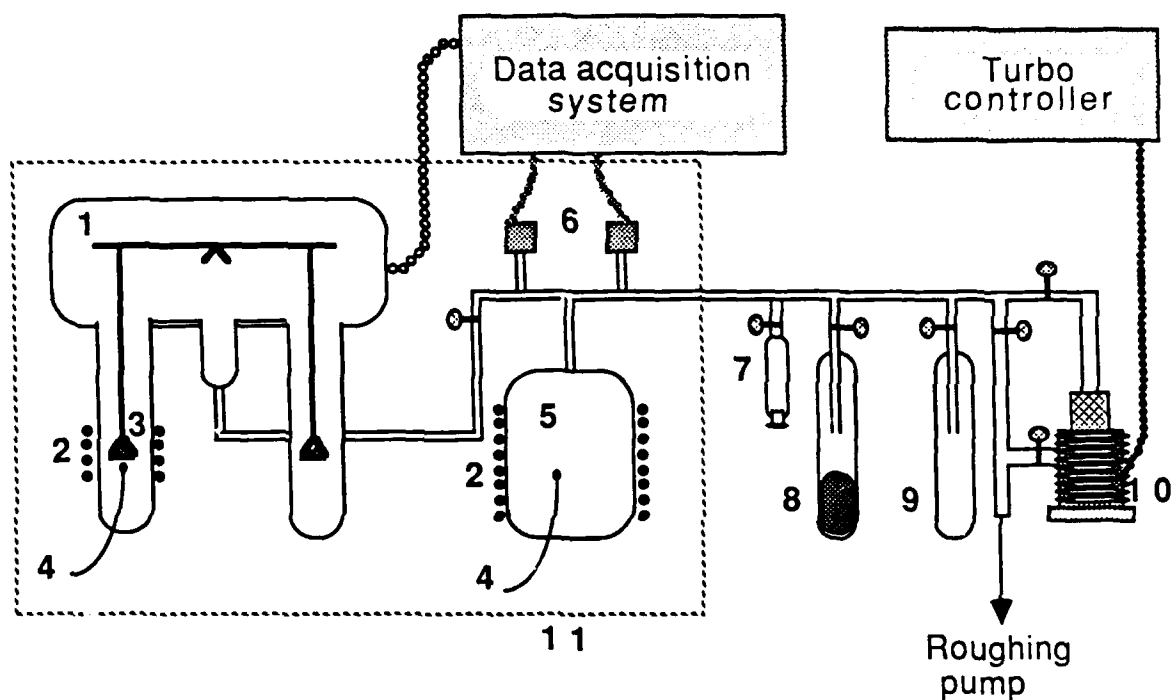


Figure 2. Photographs of the high pressure adsorption unit.



- | | |
|-----------------------|-------------------------|
| 1. Balance assembly | 6. Pressure sensors |
| 2. Controlled heaters | 7. Injection assembly |
| 3. Sample | 8. Zeolite trap |
| 4. Thermocouples | 9. Cold trap |
| 5. Gas reservoir | 10. Turbomolecular pump |
| 11. Insulated box | |

Figure 3. Schematic of the low-pressure (0 - 760 Torr) adsorption system.

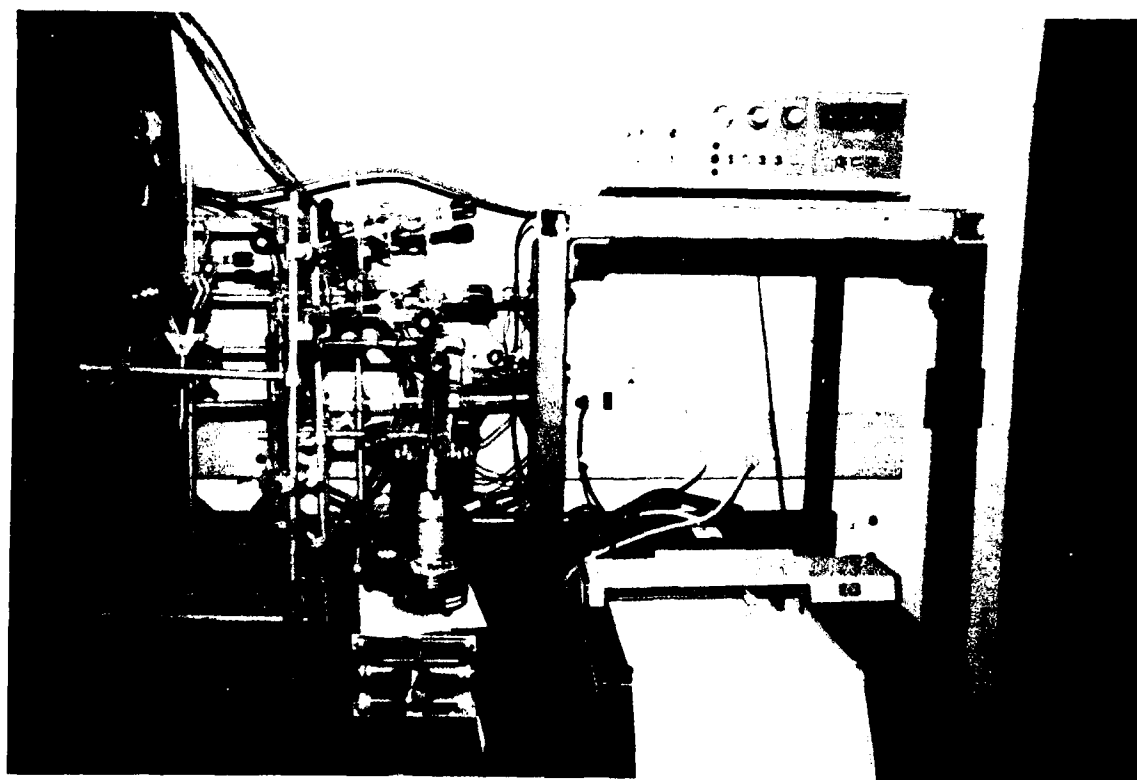


Figure 4. Photographs of the low pressure adsorption unit.

pressure could be monitored continuously using a three-channel chart recorder. The pressure was measured using MKS Baratron gauges. Omega 4002 digital controllers were used for temperature control and measurement.

The sample was activated at 300°C under vacuum for an extended period (6 h). After activation, the sample was allowed to cool to the desired temperature. The gas in the gas reservoir was then expanded into the adsorption system and the weight increase of the sample was continuously recorded. After equilibrium was reached, additional gas was admitted to the adsorption system for a second equilibrium adsorption measurement. The process was repeated until the system reached its final pressure (760 Torr for the subatmospheric unit and approximately 5,000-10,000 Torr for the high pressure unit). Multiple runs were made to assure the reproducibility of the data, which were generally very good as shown in the figures.

The experimental data are given in Appendix A. Each data set contains brief information regarding the experimental conditions. Adsorption isotherms presented in figures were obtained from the pressure vs. equilibrium adsorption amounts tabulated in Appendix A with a reference to the corresponding figure. Uptake rate data giving adsorbed amounts vs. time are also given in Appendix A.

The 3A and 5A molecular sieve carbons (MSC) were manufactured by Takeda Chemical Industries, LTD of Tokyo, Japan, and provided by TIGG Corporation of Pittsburgh, PA. Some of the pertinent information on the MSC samples are summarized in Table 1. The scanning electron micrographs of both 3A and 5A MSC are shown in Figure 5.

TABLE 1. PROPERTIES OF THE MSC SAMPLES

Particle size:	20 - 40 mesh
Bulk density:	0.59 g/cm ³
Sample weight:	~ 80 mg
Activation temperature:	300°C under vacuum
Duration of activation:	6 hours

III. RESULTS AND DISCUSSION

Activation Procedure

To examine the effect of activation on the initial sample weight loss, about 86 mg of sample (5A MSC, 20-40 mesh) was placed in the electrobalance of the low-pressure unit; its weight-loss was monitored as evacuation proceeded at room

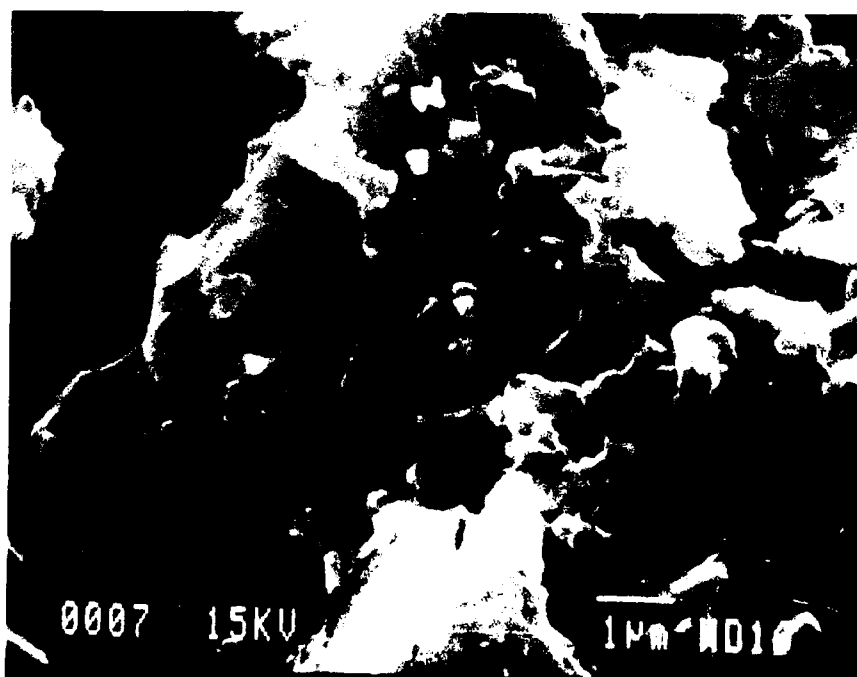
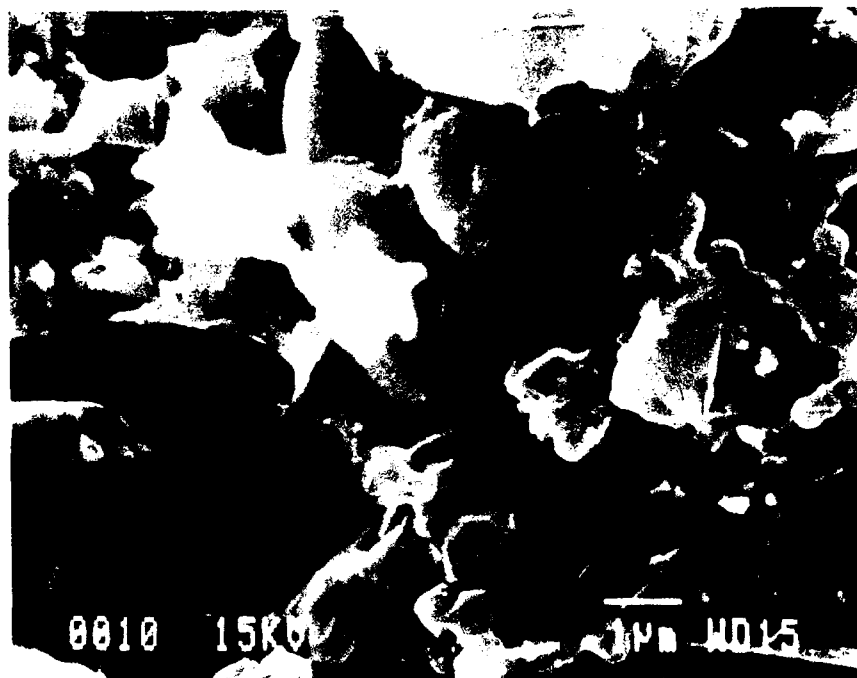


Figure 5. Scanning electron micrographs of molecular sieve carbon 5A (top) and 3A (bottom).

temperature. Figure 6 shows the weight measurements (expressed as a percentage of initial weight) obtained at various stages during the pump-down. The weight-loss was, roughly speaking, linearly proportional to the pressure decrease from the initial one atmosphere. Calculations showed that if Henry's law ($w = K'P$, where P is the pressure in Torr, w is the adsorbed amount in mg/g and K' is a constant in mg/g·Torr), as applied to adsorption, were employed to model the equilibrium desorption data for 5A MSC in Figure 6, the constant K' was equal to 58.9 (mg/g of adsorbed weight per Torr). This value was close to that obtained later for the adsorption of N_2 or O_2 ($K' = 66.2$), indicating that the sample mostly adsorbed air while it was under room conditions. Total weight loss during desorption at room temperature was about 1.5% (= 15 mg/g). After a pressure below 10^{-4} Torr was reached in the system, the sample was activated at 100°C, 200°C, and 300°C, successively, each time for 6 hours. After cooling the sample down to room temperature it was observed that there was virtually no additional weight loss during these activation (heating) steps. Figure 6 also shows the weight loss during pump down for 3A MSC. A total loss of only 0.9% by this sample clearly indicates that 3A adsorbed even less amounts of gases and vapors than 5A MSC while it was stored under room conditions. Our observation that the MSC adsorbs negligible amounts of moisture is consistent with the hydrophobic property generally observed in MSC.

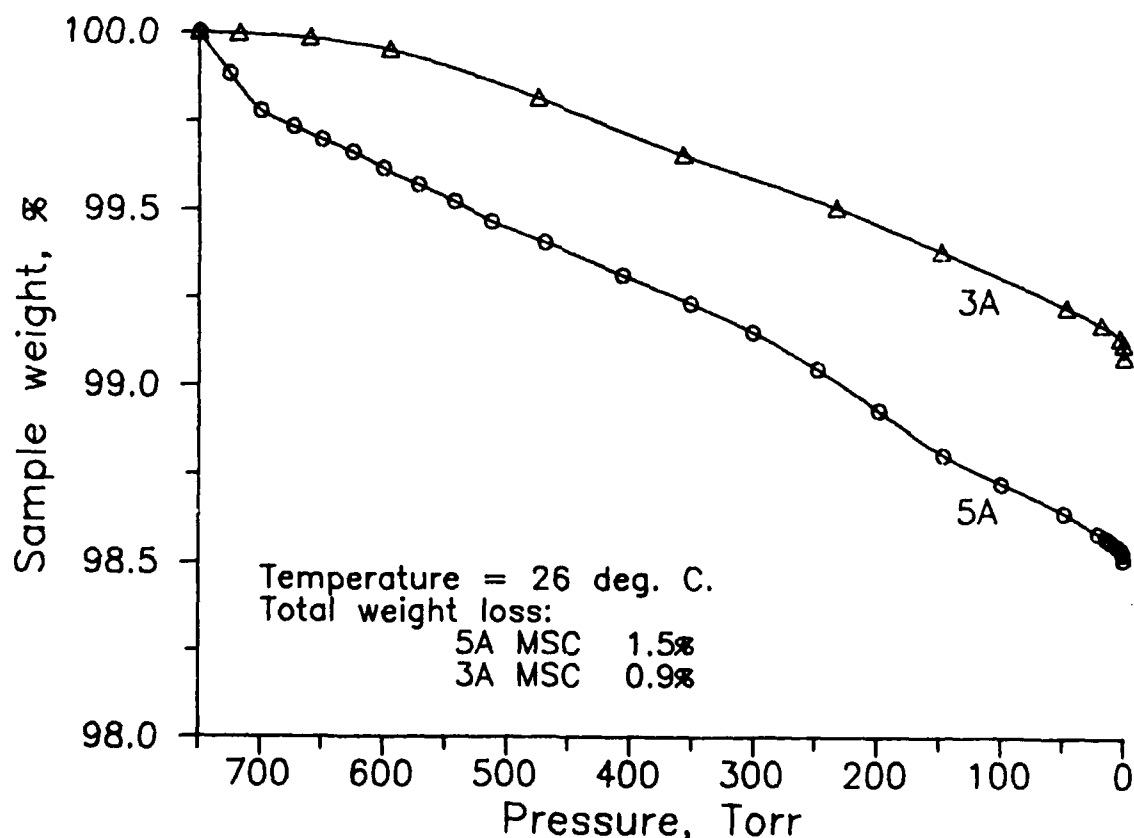


Figure 6. Weight change during initial pump-down.

Experimental evidence from the low pressure unit appears to show that it is unnecessary to activate the sample at high temperature; however, unless stated otherwise, the runs reported here were performed after the samples were activated at a higher temperature (300°C) for 6 hours to ensure uniform sample pretreatment in both the high pressure and low pressure units. It was not possible to completely regenerate the sample without heating after the sample had been exposed to high pressure gases.

Single Component Adsorption

Model Differentiation

The Langmuir Isotherm The Langmuir isotherm exhibits Type I (Brunauer, Deming, Deming and Teller (BDDT) classification) behavior which is generally characterized by a long flat branch normally horizontal. The mathematical representation of the Langmuir isotherm is shown in Eq. (1):

$$\frac{q}{q_m} = \frac{b P}{1 + b P} \quad (1)$$

where q is the adsorption capacity, P is the pressure, q_m is the monolayer coverage, and b is a constant. In this work, the constants q_m and b were determined from experimental adsorption isotherm data by plotting $1/q$ against $1/P$. Equation (1) suggests that such a plot gives a straight line with a slope equal to $1/(q_m b)$ and a y-axis intercept equal to $1/q_m$.

Type I isotherms are frequently encountered with adsorbents such as charcoal and zeolite 13X. The classical interpretation of Type I isotherms is based on the assumptions that the adsorbed layer on the pore wall is only one molecule thick and that the completion of this monolayer gives the plateau of the isotherm. This mechanism was first developed by Langmuir for application to adsorption on an open surface which is freely exposed to the gas phase. The extension of the Langmuir isotherm to microporous adsorbents represents a rather long extrapolation, especially as the channels may be many hundreds or even thousands of molecular diameters in length. Further deviations from the simple Langmuir model can arise from the overlapping of the potential field and from irregularities in the channel producing variations in the extent of overlapping from place to place along the pores. Thus, the assumption of a uniform potential over the entire surface is rarely valid. Nevertheless, the Langmuir isotherm is frequently used to describe an adsorption isotherm exhibiting Type I behavior. One may, thus, regard this as an empirical two-parameter fit of a curve rather than attaching theoretical significance to the fit in the context of the development originally proposed by Langmuir.

The Vacancy Solution Model Suwanayuen and Danner (18) developed a gas adsorption isotherm equation based on vacancy solution theory. The model was later improved by Cochran et al (19, 20). The vacancy solution model (VSM) assumes the existence of a hypothetical solvent called "vacancy" to be filled by adsorbate molecules. Phase equilibrium between the gas and the adsorbed solutions is assumed to exist and excess properties in relation to a dividing surface are used to define the properties of the adsorbed phase. Using the chemical potential expression derived by Lucassen-Reynders (21-23), Danner and his co-workers formulated the following isotherm equation:

$$P = \left| \frac{n_1^\infty}{b_1} \frac{\theta}{1 - \theta} \right| \exp \left| \frac{\alpha_{1V}^2 \theta}{1 + \alpha_{1V} \theta} \right| \quad (2)$$

where $\theta (=n_1/n_1^\infty)$ is the surface coverage.

Danner and his co-workers suggested that the temperature dependence of these parameters can be expressed in the following forms:

$$b_1 = b_{01} \exp \left(- \frac{q_1}{RT} \right) \quad (3)$$

$$n_1^\infty = n_{01}^\infty \exp \left(- \frac{r_1}{T} \right) \quad (4)$$

and

$$\alpha_{1V} = m_1 n_1^\infty - 1 \quad (5)$$

where b_{01} , n_{01}^∞ , q_1 , r_1 and m_1 are assumed to be independent of temperature. b_1 (mmol/g·Torr) is the Henry's law constant of the adsorbate, n_1^∞ (mmol/g) is the limiting amount adsorbed, r_1 (°K) is a temperature-independent constant characterizing adsorbate-adsorbent system, α_{1V} is a parameter describing the nonideality in adsorbed phase induced by interaction between adsorbate and vacancy, q_1 (KJ/mol) is the isosteric heat of adsorption at infinite dilution, m_1 (g/mmol) is a temperature-independent constant of proportionality, R (KJ/mol·°K) is the gas constant, and T (°K) is the temperature of adsorption.

As cautioned by the authors, one should not attach too much physical significance to the regressed parameters although the model was developed by analogy with the Flory-Huggins model (20) for vapor-liquid equilibria. The authors further suggested that the parameters could either be computed using Eq. (2) for n_1^∞ , b_1

and α_{1v} or using Eq. (2), (3), (4), and (5) together with isotherms at different temperatures. In the present study, Eq. (2) was used to obtain n_1^∞ , b_1 and α_{1v} from the experimental adsorption data at one temperature and a least square error regression method. The computer program is listed in Appendix B.

Both Langmuir and VSM isotherm equations were used to describe the adsorption of gases on 3A and 5A molecular sieve carbons in the present study. Both equations were employed to fit all the experimental data in the entire pressure range of 0-10,000 Torr obtained under this contract. The Langmuir constants for all the gases studied are tabulated in Table 2 while the parameters for the VSM are shown in Table 3.

TABLE 2. LANGMUIR EQUATION CONSTANTS

MSC	Gas	0°C		30°C		50°C	
		q_m mmol/g	b 1/Torr	q_m mmol/g	b 1/Torr	q_m mmol/g	b 1/Torr
3A	N ₂	1.90	7.84×10^{-4}	1.97	3.34×10^{-4}	1.68	3.44×10^{-4}
	O ₂	2.32	7.58×10^{-4}	2.01	3.08×10^{-4}	1.37	4.53×10^{-4}
	CH ₄	3.23	7.81×10^{-4}	2.72	1.43×10^{-3}	2.01	1.11×10^{-3}
	Ar	2.38	4.61×10^{-4}	2.02	3.72×10^{-4}	1.61	3.03×10^{-4}
5A	N ₂	2.08	7.44×10^{-4}	2.14	2.95×10^{-4}	1.58	3.65×10^{-4}
	O ₂	2.42	5.25×10^{-4}	2.78	1.69×10^{-4}	1.64	2.87×10^{-4}
	CH ₄	3.12	1.83×10^{-3}	2.62	7.47×10^{-4}	2.35	7.02×10^{-4}
	Ar	2.62	4.12×10^{-4}	1.81	4.06×10^{-4}	2.58	1.26×10^{-4}

P: pressure, Torr

q: adsorption capacity, mmol/g

Adsorption on 5A and 3A MSC

Adsorption of O₂ Both the low pressure adsorption unit and the high pressure adsorption unit were used to study the adsorption of O₂ on 5A MSC at 30°C. For low pressure runs, O₂ was adsorbed on a 5A sample previously activated at 300°C for 6 hours. The amount adsorbed at equilibrium was measured after a step increase in the adsorbate pressure. The data are shown by circles in Figure 7. Adsorption was rapid and equilibrium was achieved quickly as shown in Figures 8 and 9. (The differences in the figures were perhaps due to the differences in the sensitivity between the two apparatuses.) When the adsorption experiment was repeated using the sample that was not activated, but was desorbed completely of O₂ under vacuum (less than 10^{-4} Torr), the adsorption data (squares in Figure 7) were reproducible. O₂ was

TABLE 3. ISOTHERM PARAMETERS FOR THE VACANCY SOLUTION MODEL

MSC	Gas	Temp(°C)	Parameters of VSM		
			n_1^∞ (mmol/g)	b_1 (mmol/g·Torr)	α_{1v}
3A	N ₂	0	2.1183	1.0982×10^{-3}	-3.26×10^{-11}
		30	1.9893	0.6606×10^{-3}	-3.28×10^{-12}
		50	1.8188	0.5321×10^{-3}	-7.14×10^{-11}
	O ₂	0	2.6571	1.3865×10^{-3}	2.31×10^{-12}
		30	2.3844	0.5315×10^{-3}	-1.13×10^{-12}
		50	1.7375	0.4899×10^{-3}	3.92×10^{-10}
	CH ₄	0	3.6728	2.0124×10^{-3}	-2.24×10^{-11}
		30	2.7504	3.7574×10^{-3}	-1.31×10^{-11}
		50	2.0496	2.1960×10^{-3}	-1.14×10^{-11}
	Ar	0	2.6080	0.9472×10^{-3}	1.57×10^{-11}
		30	2.2170	0.6175×10^{-3}	9.01×10^{-14}
		50	1.8223	0.4318×10^{-3}	-1.06×10^{-12}
5A	N ₂	0	2.4625	1.1330×10^{-3}	-1.82×10^{-11}
		30	2.3531	0.5725×10^{-3}	8.14×10^{-12}
		50	1.9027	0.4723×10^{-3}	1.44×10^{-11}
	O ₂	0	2.8299	1.0380×10^{-3}	-1.51×10^{-11}
		30	2.8468	0.4654×10^{-3}	3.29×10^{-10}
		50	2.2330	0.3959×10^{-3}	-3.26×10^{-11}
	CH ₄	0	3.3112	4.7407×10^{-3}	-8.32×10^{-12}
		30	3.0366	1.5465×10^{-3}	-7.64×10^{-11}
		50	2.6299	1.4269×10^{-3}	-1.23×10^{-11}
	Ar	0	2.8879	0.9260×10^{-3}	-7.51×10^{-11}
		30	2.1067	0.6026×10^{-3}	-2.83×10^{-12}
		50	2.8535	0.3075×10^{-3}	-2.34×10^{-11}
BF ^a	N ₂	30	1.5902	0.3831×10^{-3}	-1.03×10^{-11}
	O ₂	30	1.7429	0.5270×10^{-3}	-9.46×10^{-12}
	CH ₄	30	1.7781	1.6974×10^{-3}	1.39×10^{-11}
	Ar	30	1.8889	0.3544×10^{-3}	1.76×10^{-11}

^a BF = Bergbau Forschung

easily desorbed. Figure 7 shows that both the adsorption and the desorption isotherms are fairly linear below 760 Torr. In Figure 10, data obtained using the low-pressure unit were plotted together with those obtained using the high-pressure unit. The excellent agreement between the data obtained from the low pressure unit and those from the high pressure unit is a good indication of the consistency of the adsorption data. Similar observations were made for O₂ on 3A MSC as shown in Figure 11. Figures 12 and 13 are the adsorption isotherms at 0°C, 30°C, and 50°C for O₂ on 5A and 3A MSC, respectively.

Adsorption of CH₄ Following O₂ adsorption on 5A MSC and subsequent complete desorption under vacuum, CH₄ was adsorbed. The amount adsorbed at equilibrium is shown in Figure 14 using

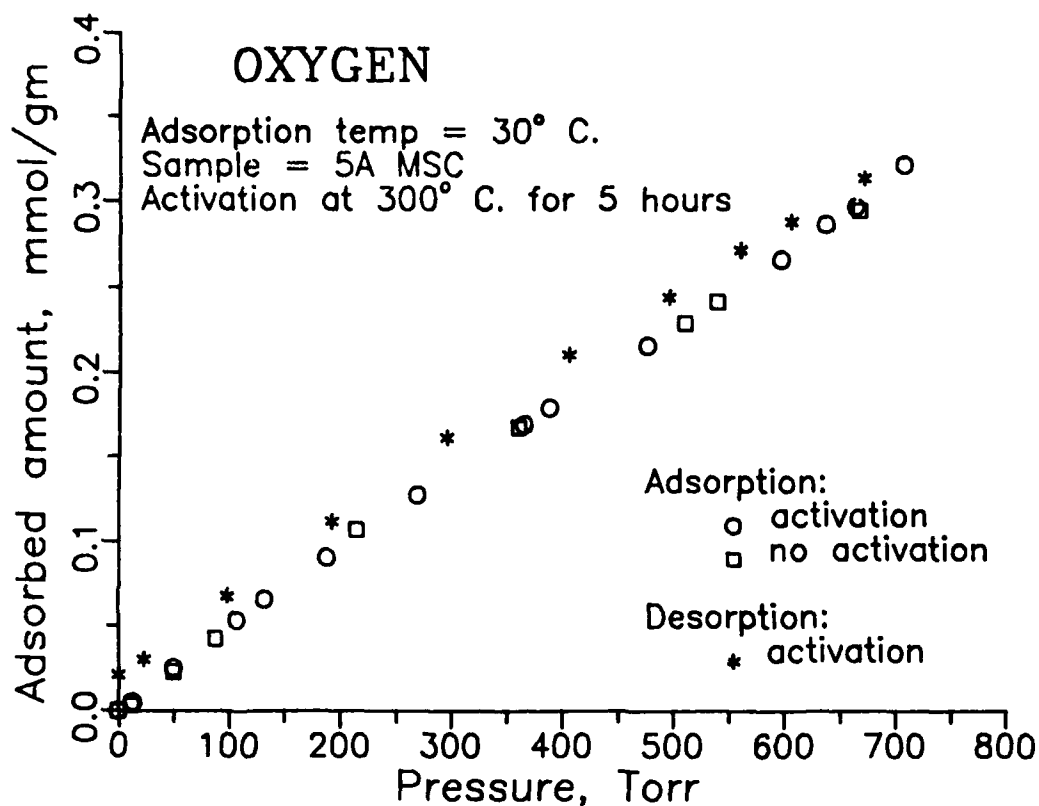


Figure 7. O₂ adsorption and desorption isotherms.

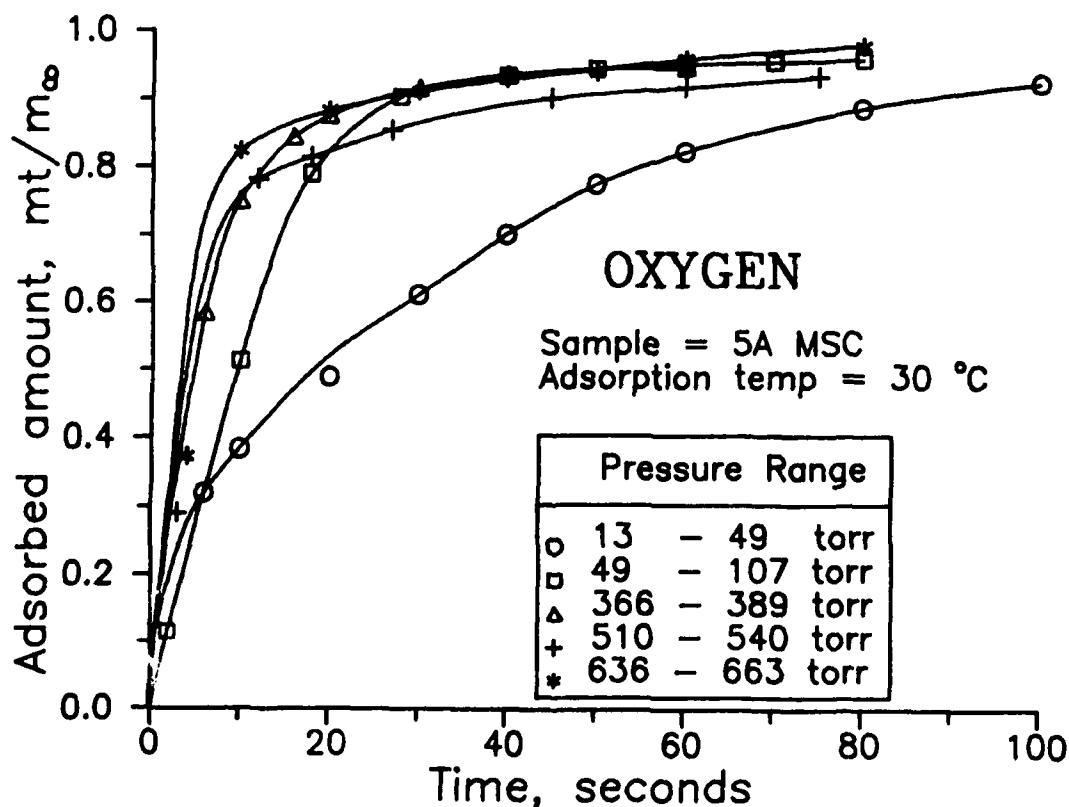


Figure 8. Uptake curves during O₂ adsorption (low pressure).

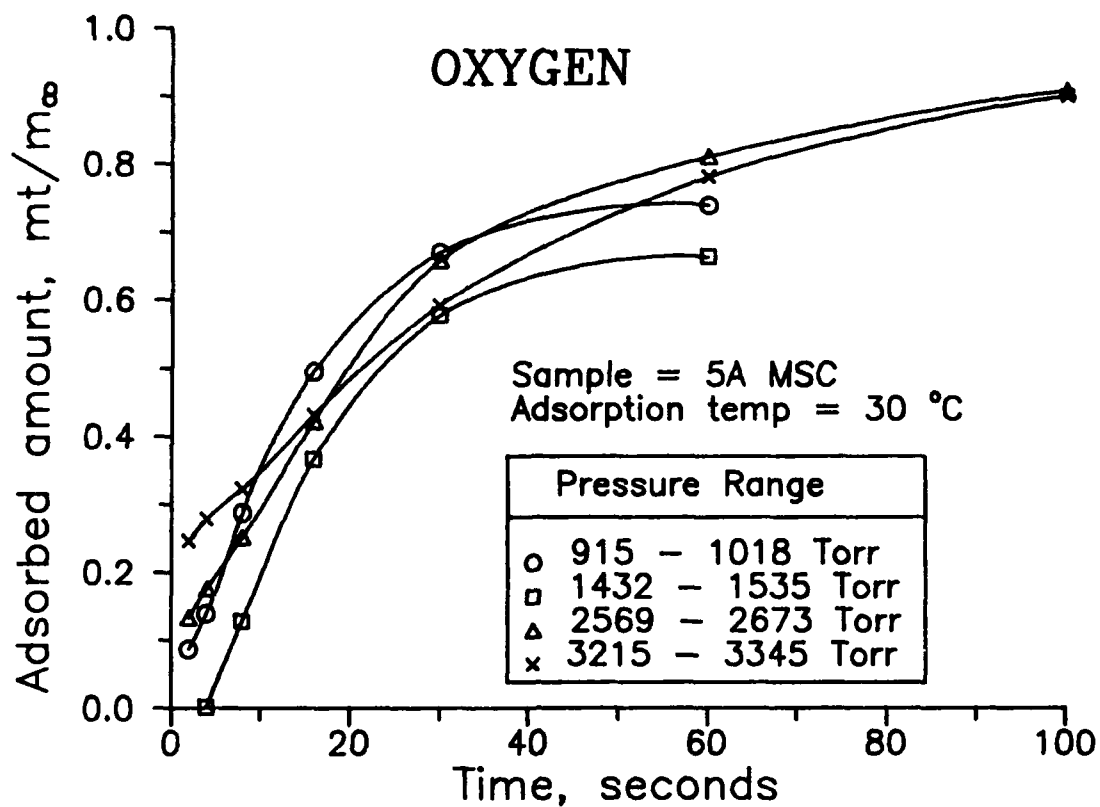


Figure 9. Uptake curves during O₂ adsorption (high pressure).

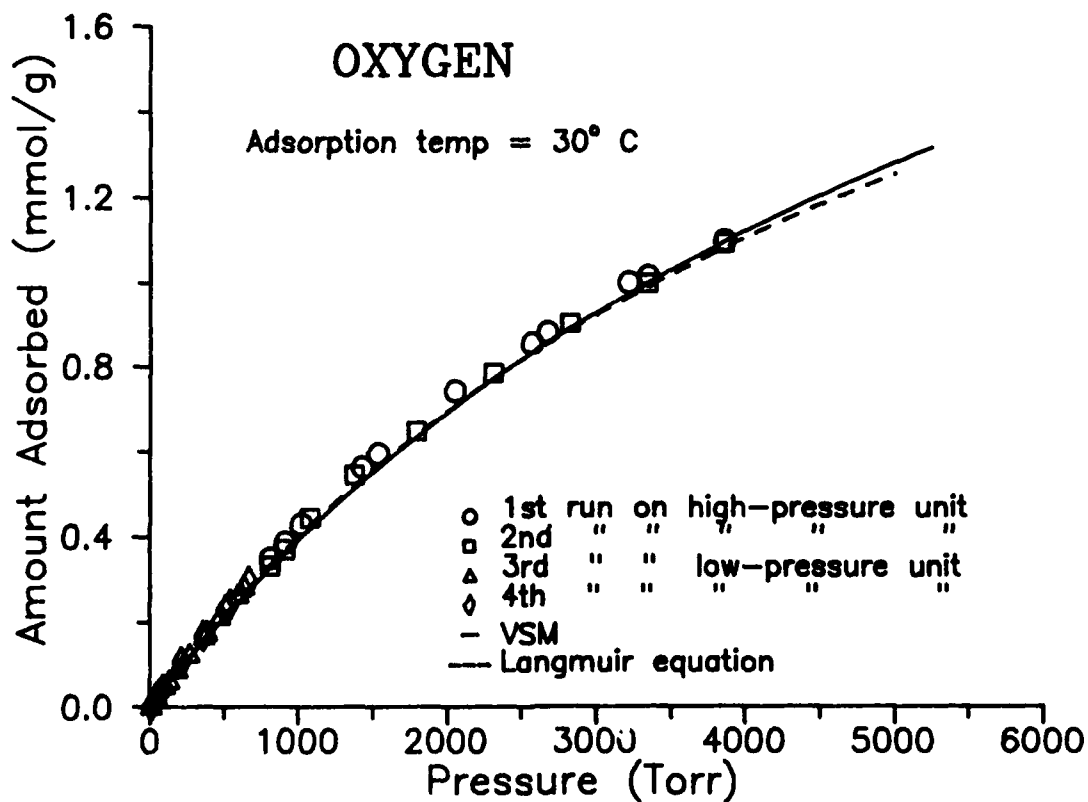


Figure 10. O₂ adsorption isotherm on 5A MSC.

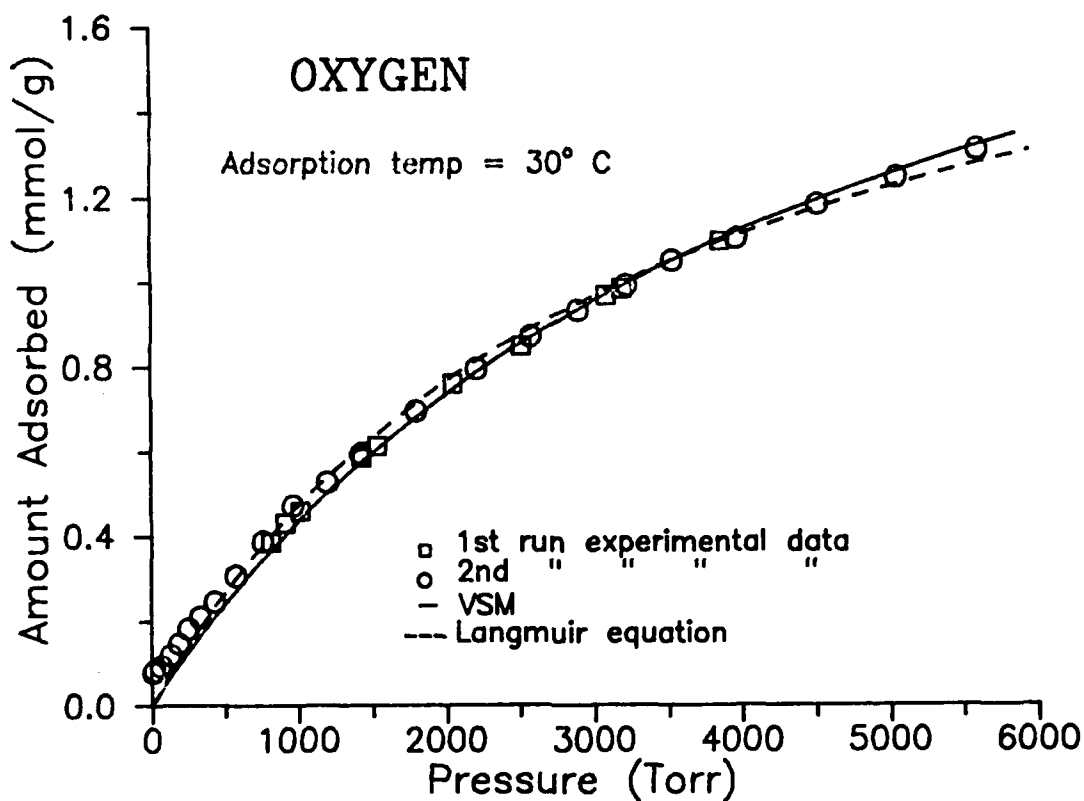


Figure 11. O₂ adsorption isotherm on 3A MSC.

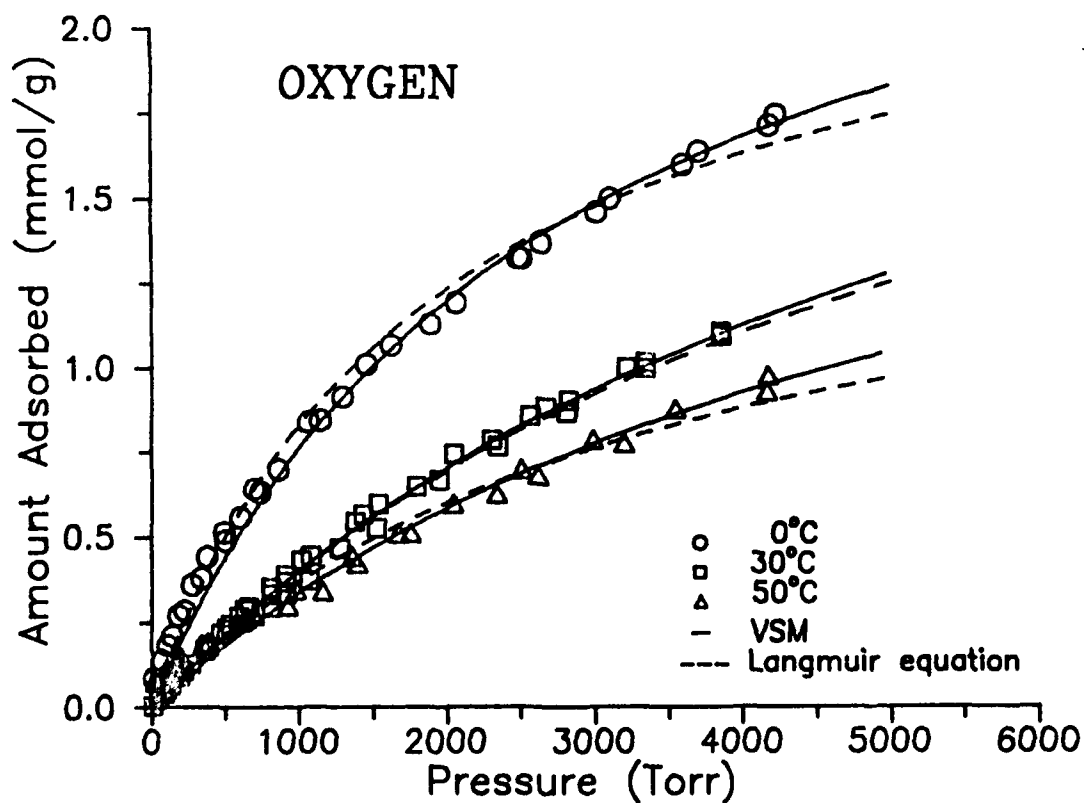


Figure 12. O₂ adsorption isotherm on 5A MSC.

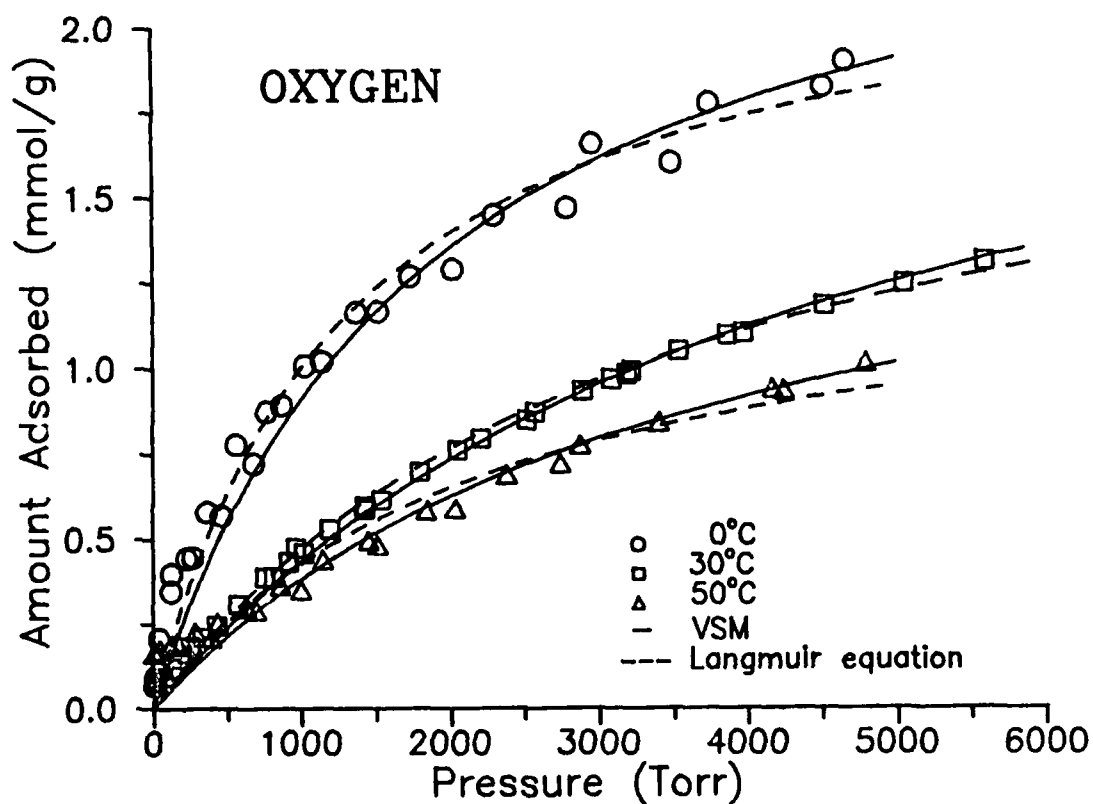


Figure 13. O_2 adsorption isotherm on 3A MSC.

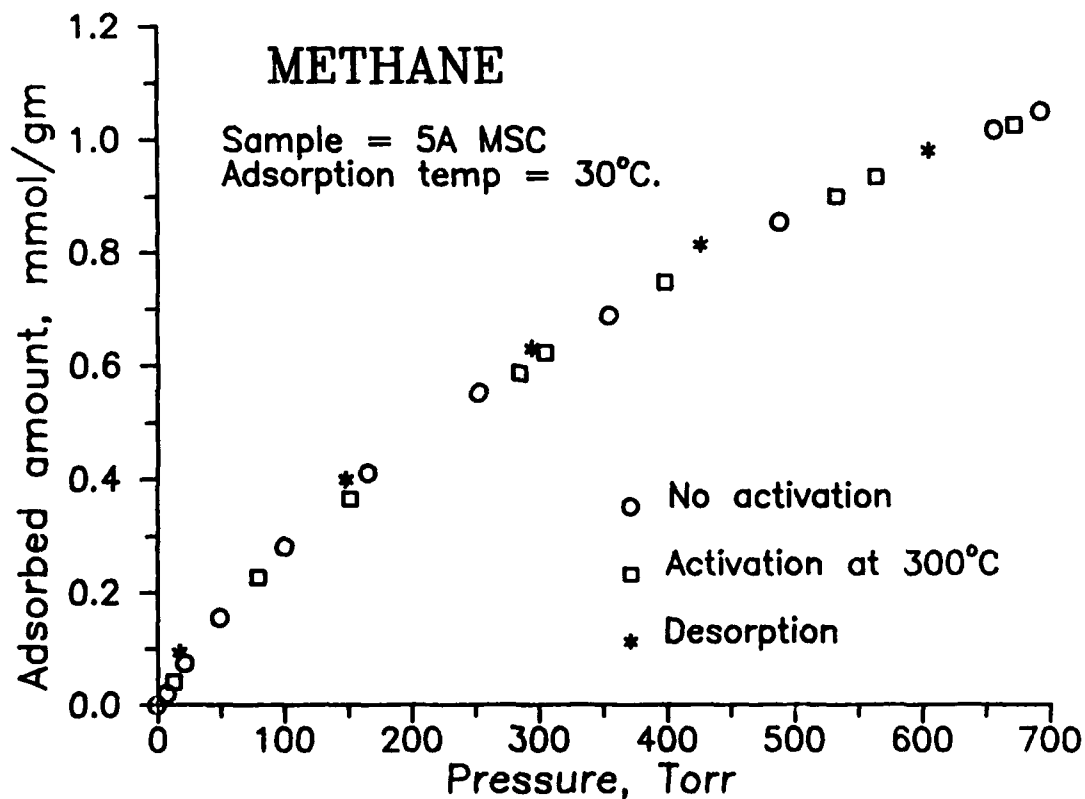


Figure 14. CH_4 adsorption and desorption isotherm on 5A MSC.

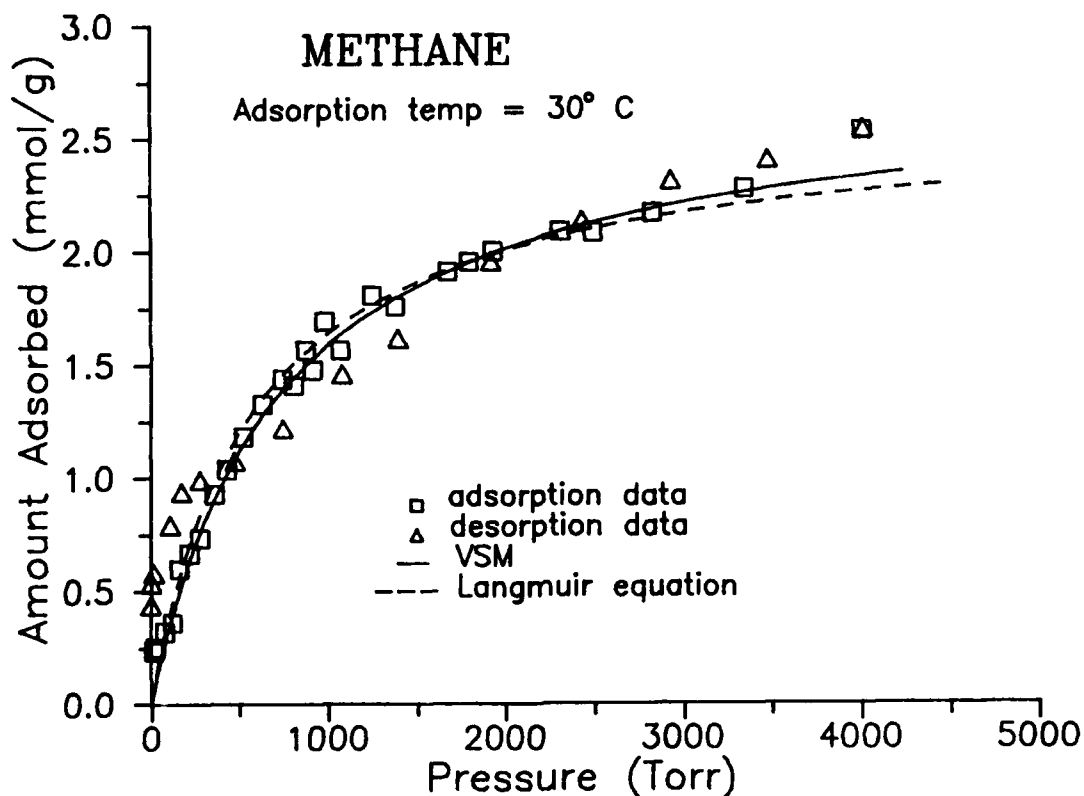


Figure 15. CH_4 adsorption and desorption isotherm on 3A MSC.

circles. Adsorption capacity of the sample was the same when it was activated at 300°C for 6 hours prior to CH_4 adsorption.

At low pressures, the desorption isotherm closely followed the adsorption isotherm as shown in Figure 14. It should, however, be pointed out that it was not possible to obtain complete desorption after the sample had been exposed to high pressure gas as shown in Figure 15. At high pressures, gas molecules may be adsorbed in the finer pores of the MSC making it difficult to desorb without heating. In Figure 16 the data obtained in the low-pressure unit and the high-pressure unit are shown. A similar curve for 3A MSC is shown in Figure 17. The adsorption equilibrium isotherms for CH_4 in 5A and 3A MSC are shown in Figures 18 and 19 respectively at three temperatures, 0°C , 30°C , and 50°C . The behavior of methane adsorption isotherms on 3A was unusual. The equilibrium adsorption capacity at 30°C was higher than at 0°C at pressures less than 2,500 Torr. One possible explanation for this variation is that the adsorption rate for methane at 0°C was very low and equilibrium was never reached. More work is needed to fully understand this apparent anomaly.

Adsorption of N_2 Adsorption of N_2 on 5A MSC was also checked using the sample that was activated at 300°C for 6 hours, and the sample that was simply desorbed of CH_4 but not activated. In both cases the adsorption isotherms were identical. Further, the

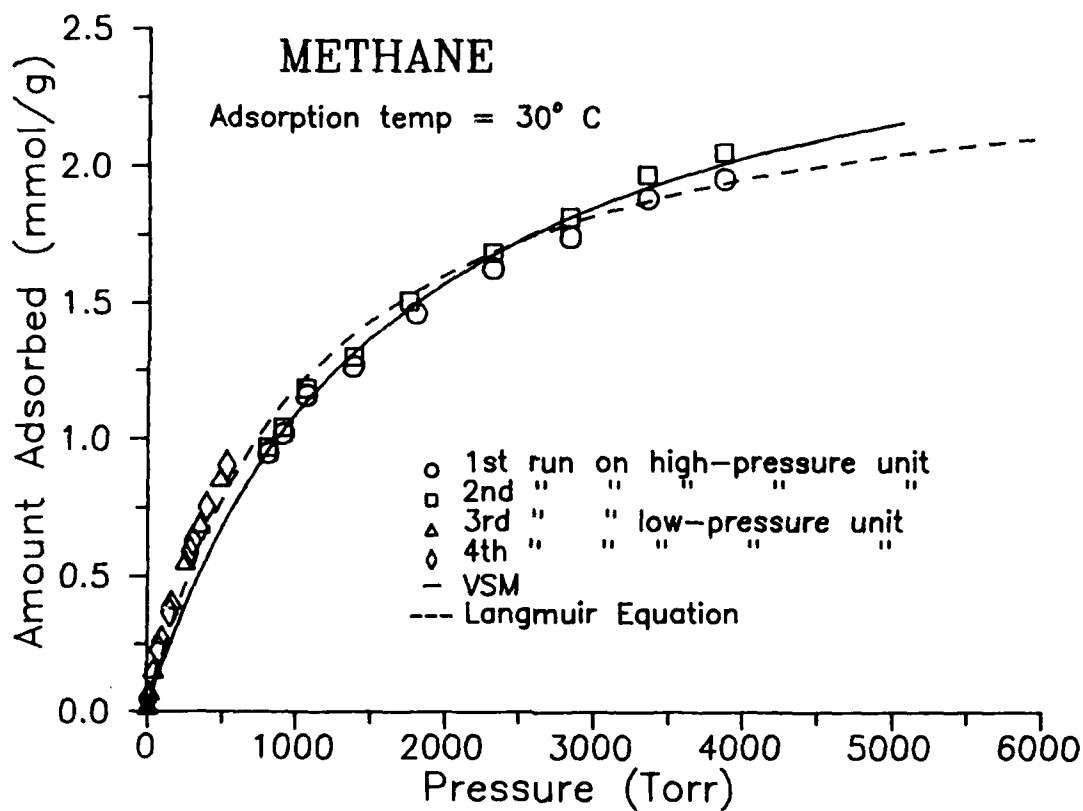


Figure 16. CH₄ adsorption isotherm on 5A MSC.

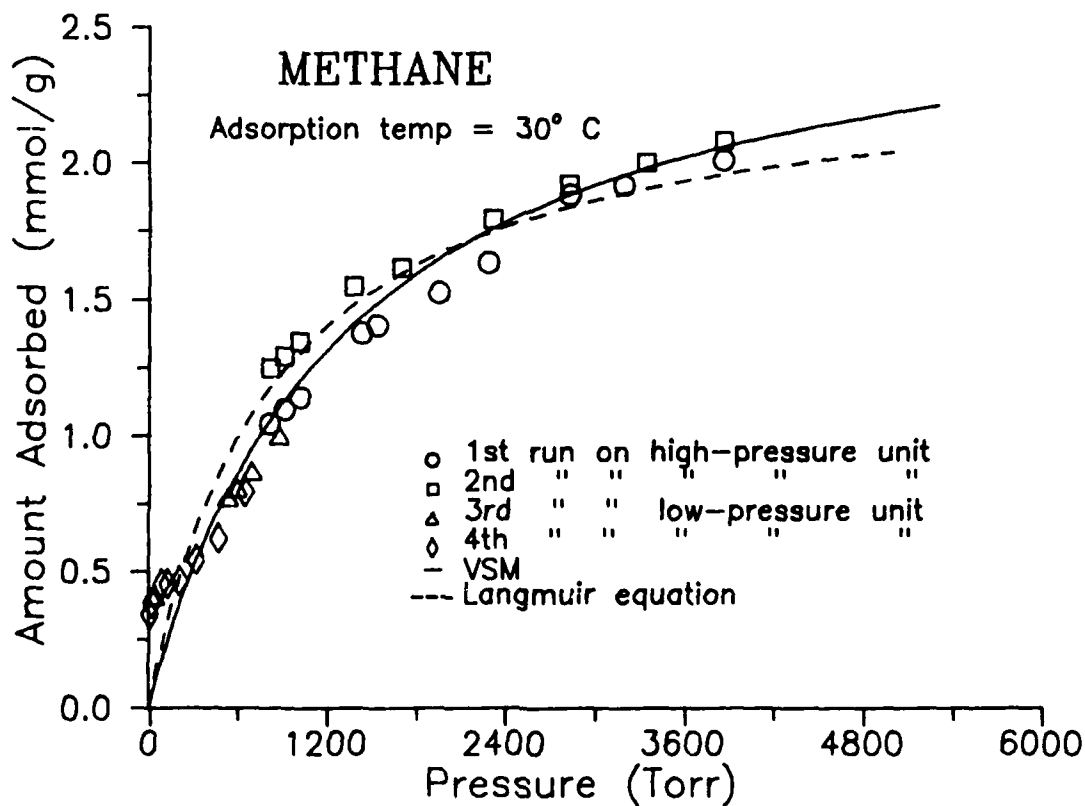


Figure 17. CH₄ adsorption isotherm on 3A MSC.

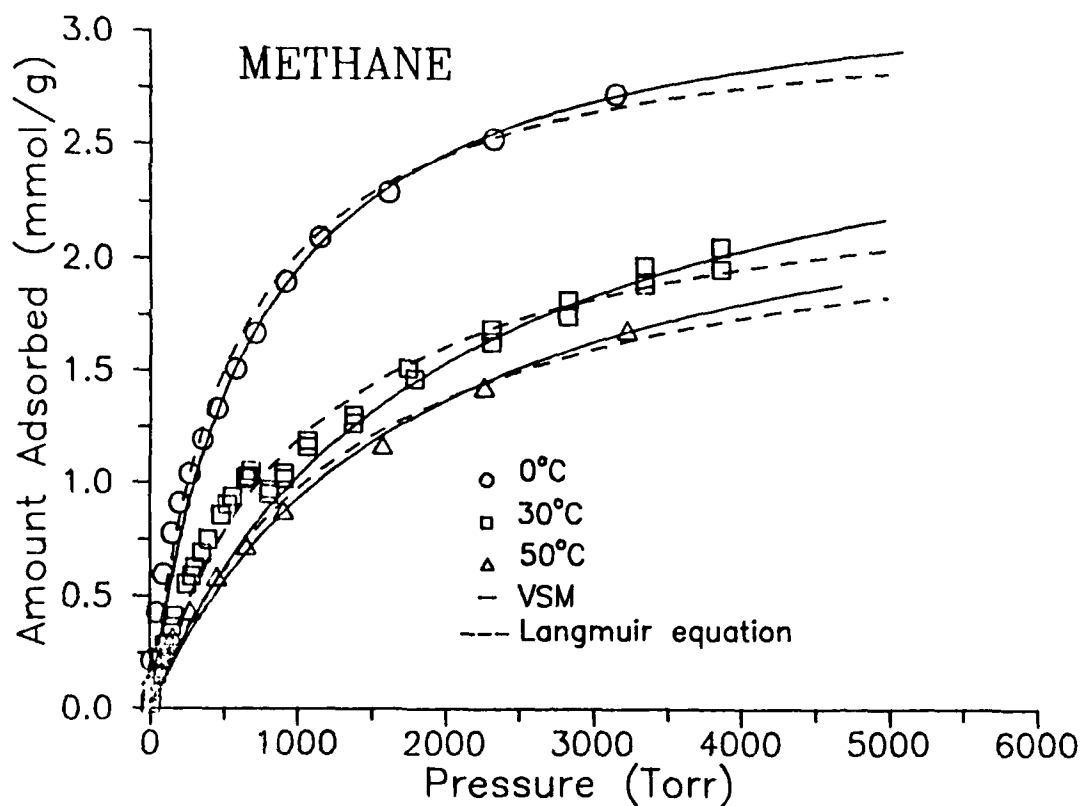


Figure 18. CH₄ adsorption isotherm on 5A MSC.

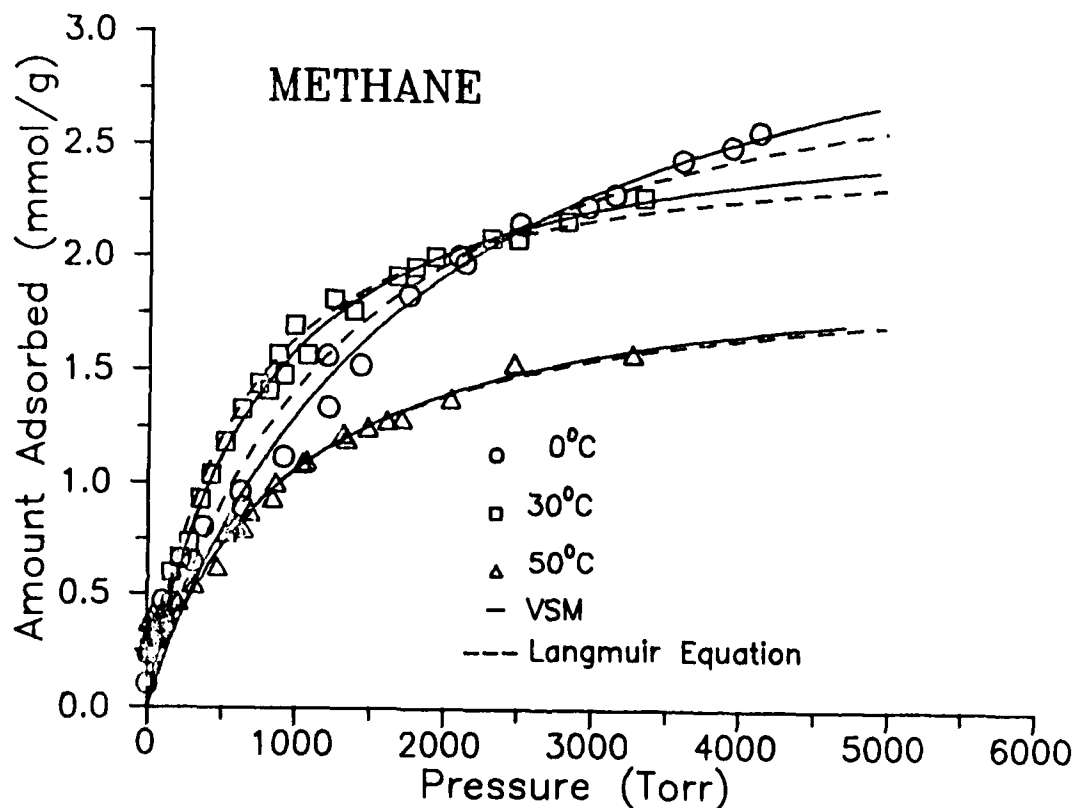


Figure 19. CH₄ adsorption isotherm on 3A MSC.

desorption isotherm was similar to the adsorption isotherm. These data are shown in Figure 20. The adsorption data over the entire pressure range of 0-6,000 Torr are shown in Figure 21. The adsorption equilibrium isotherms for N_2 in 5A and 3A MSC are shown in Figures 21 and 22 respectively at three temperatures, 0°C, 30°C, and 50°C.

Adsorption of Ar Figures 23 and 24 show the equilibrium adsorption isotherms for argon in 5A and 3A MSC at three temperatures, 0°C, 30°C, and 50°C. The VSM appears to give a good fit of the experimental data. The Langmuir equation seems to be adequate for the description of the isotherms although some deviation of the experimental data from the theoretical curve was observed at high pressures.

Comparison with previous studies There are relatively few studies providing equilibrium adsorption isotherms for molecular sieve carbons. Materials from different sources make it even more difficult to make an accurate comparison. Nevertheless, Figure 25 compares the current results for 5A MSC and those reported by Ruthven et al. (24). Although there are some differences between the present study and that of Ruthven et al, the agreement should be regarded as fairly good considering the substantial differences among the materials. Kapoor and Yang (25) found that the adsorption data for methane could be fitted using a Langmuir equation for Bergbau Forschung molecular sieve carbon at 25°C. They obtained a q_m value of 1.92 mmol/g and a b value of $8 \times 10^{-4} \text{ Torr}^{-1}$ which are somewhat different from the results in Table 2. However, considering the fact that the materials used in Kapoor and Yang's work were from Bergbau Forschung, the observed differences probably would be expected.

Additional experiments were performed on the MSC produced by Bergbau Forschung for comparison. The results are shown in Figures 26, 27, 28 and 29 for methane, oxygen, nitrogen and argon, respectively. From these figures, it appears that the 3A MSC from Takeda had, in general, higher capacities than those of Bergbau Forschung.

Isosteric Heat of Adsorption

The temperature dependence of adsorption isotherms can be used to derive the isosteric heat of adsorption which is a differential molar quantity. The derivation of an equation for the isosteric heat of adsorption is similar to the derivation of the Clausius-Clapeyron equation for a phase change in a one-component system. Therefore, the equation for the isosteric heat of adsorption is:

$$\left. \frac{\partial (\ln P)}{\partial (1/T)} \right|_n = - \frac{q^{st}}{R} \quad (6)$$

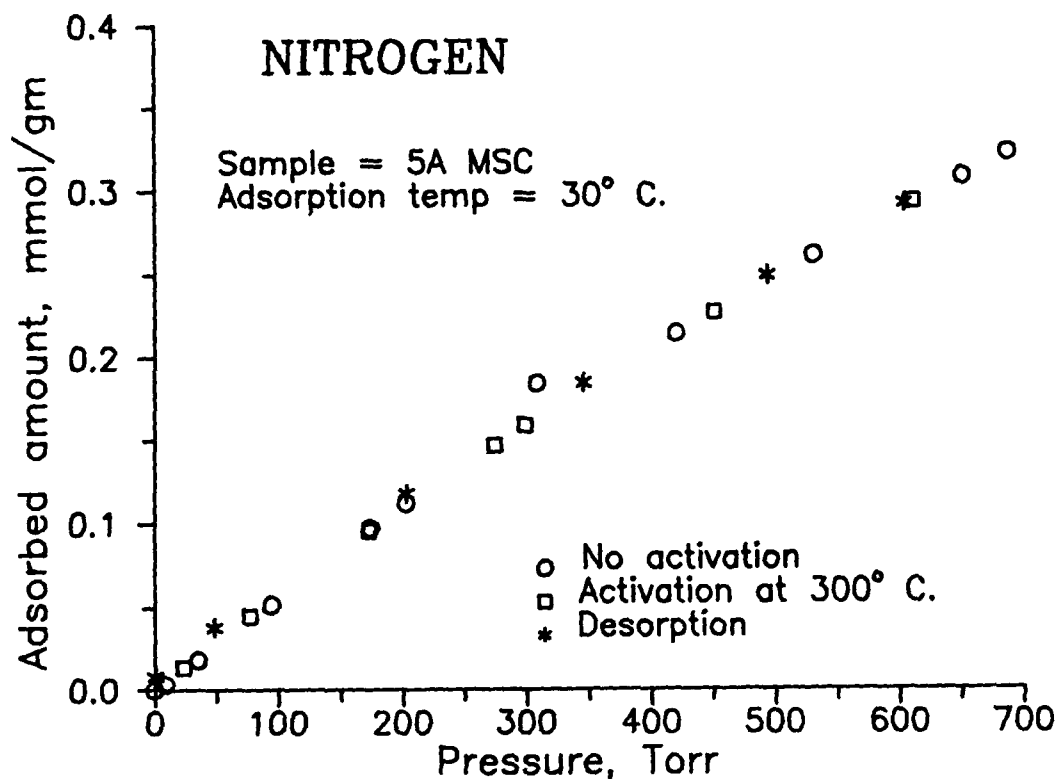


Figure 20. N₂ adsorption and desorption isotherm on 5A MSC.

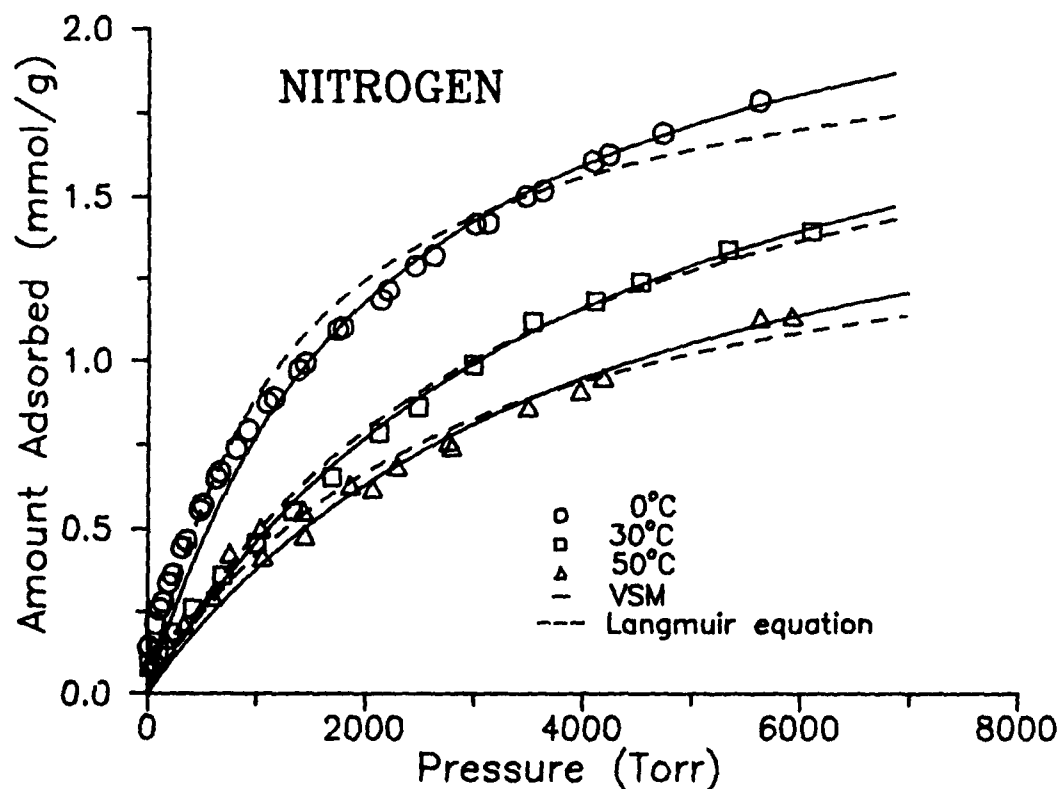


Figure 21. N₂ adsorption isotherm on 5A MSC.

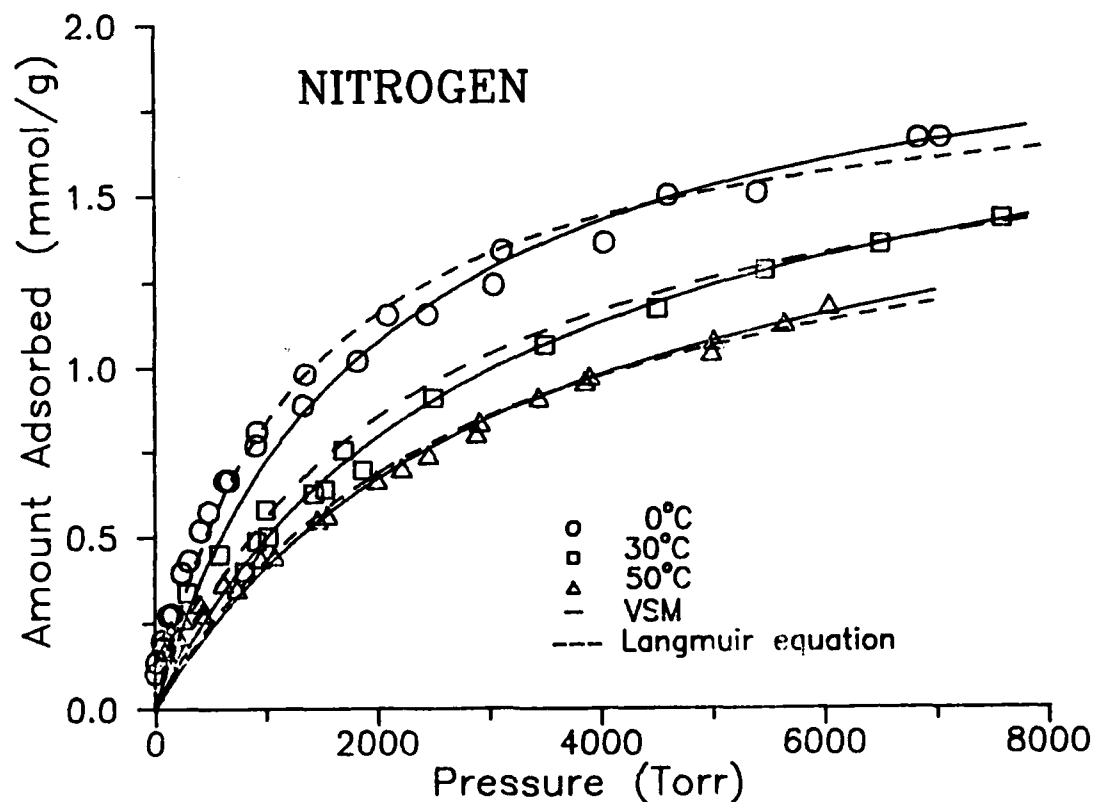


Figure 22. N₂ adsorption isotherm on 3A MSC.

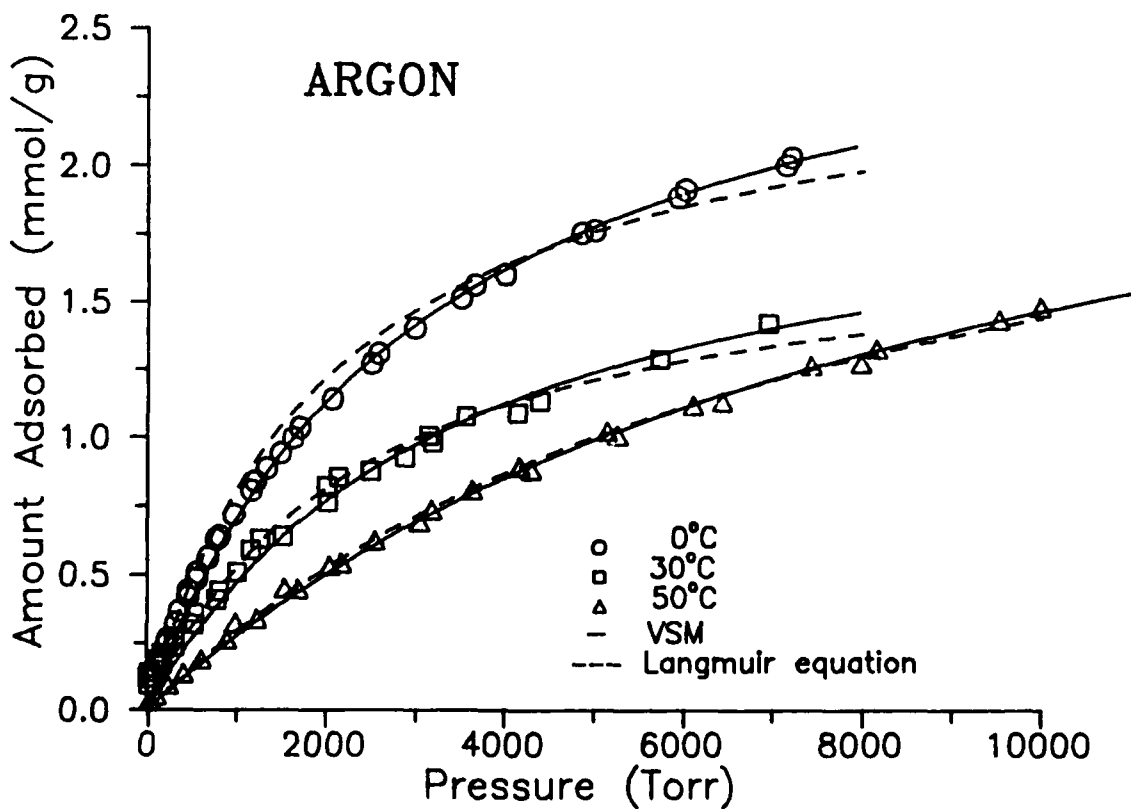


Figure 23. Ar adsorption isotherm on 5A MSC.

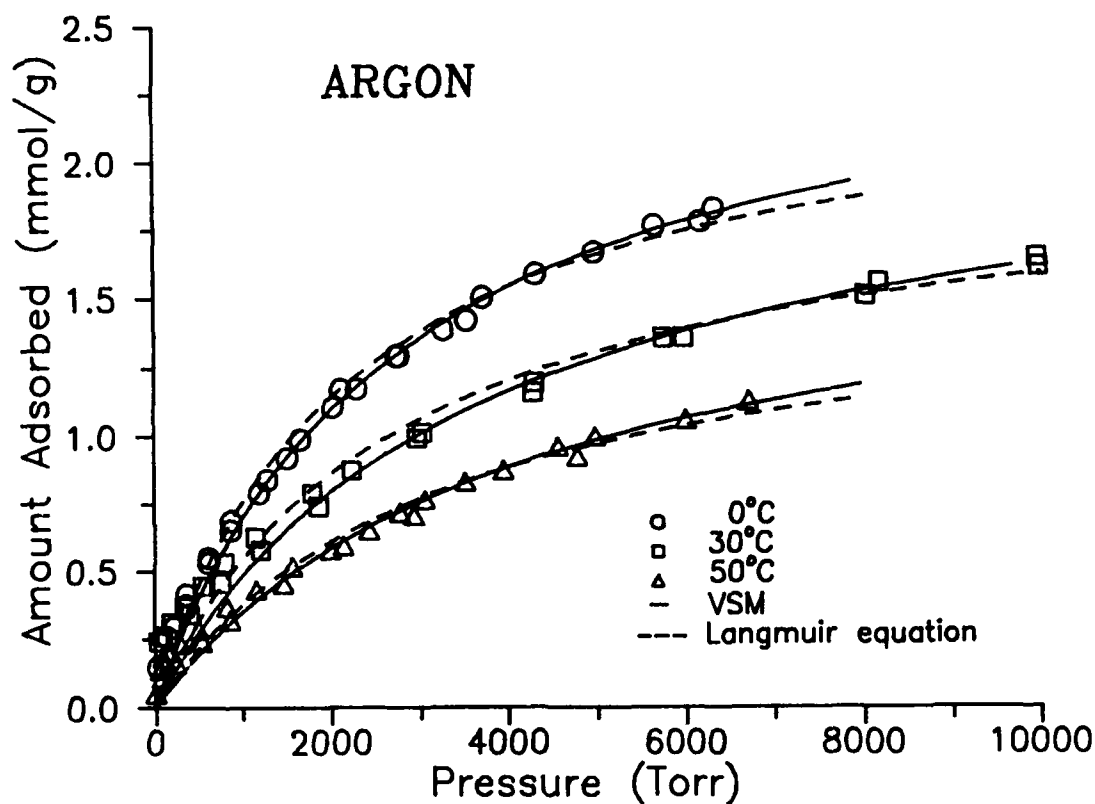


Figure 24. Ar adsorption isotherm on 3A MSC.

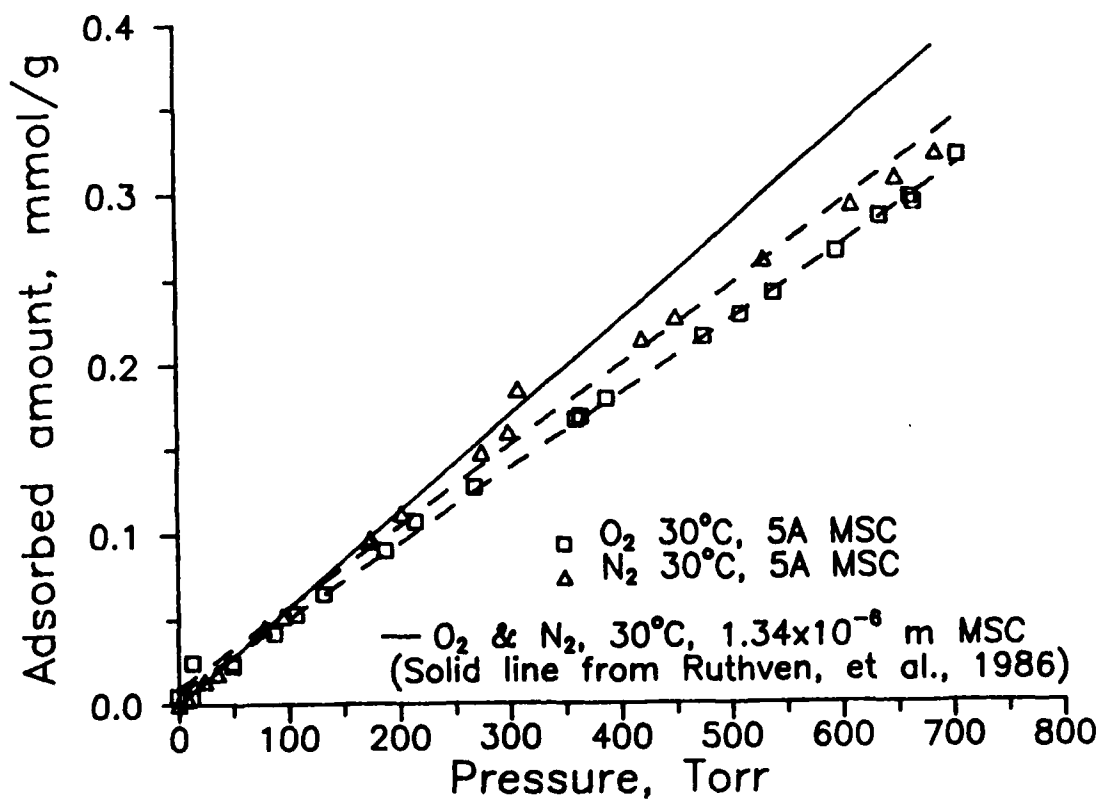


Figure 25. Adsorption capacities of different samples.

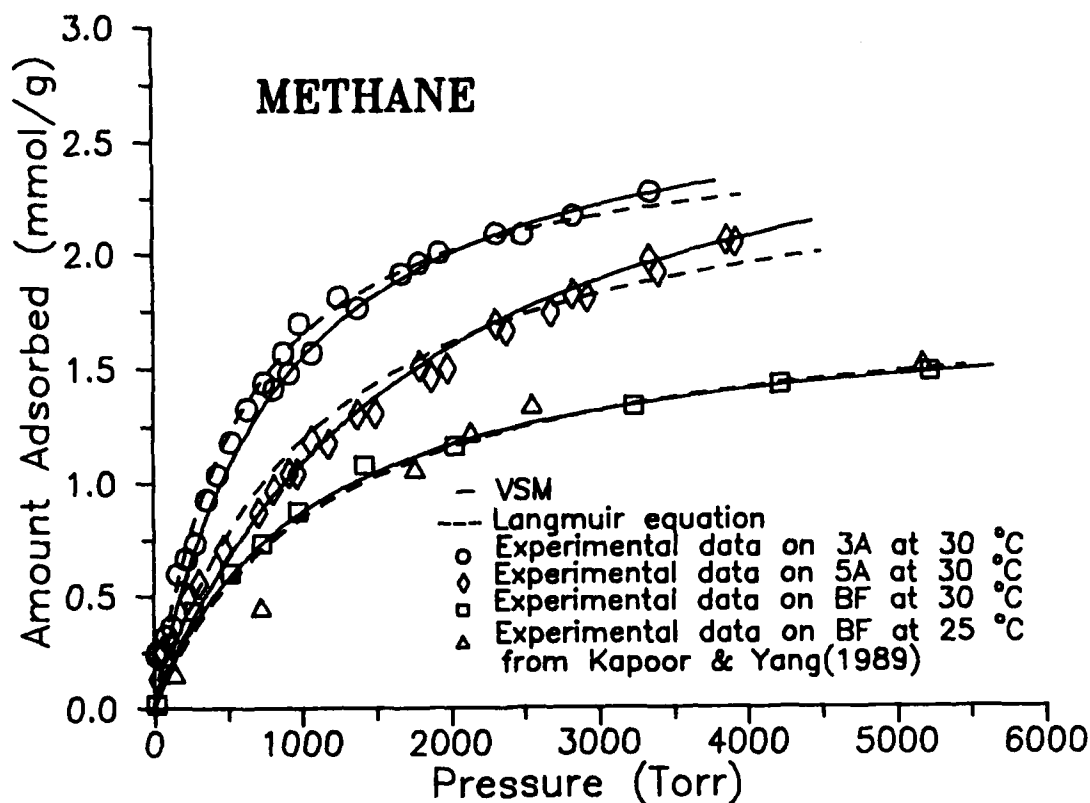


Figure 26. CH_4 adsorption on various samples.

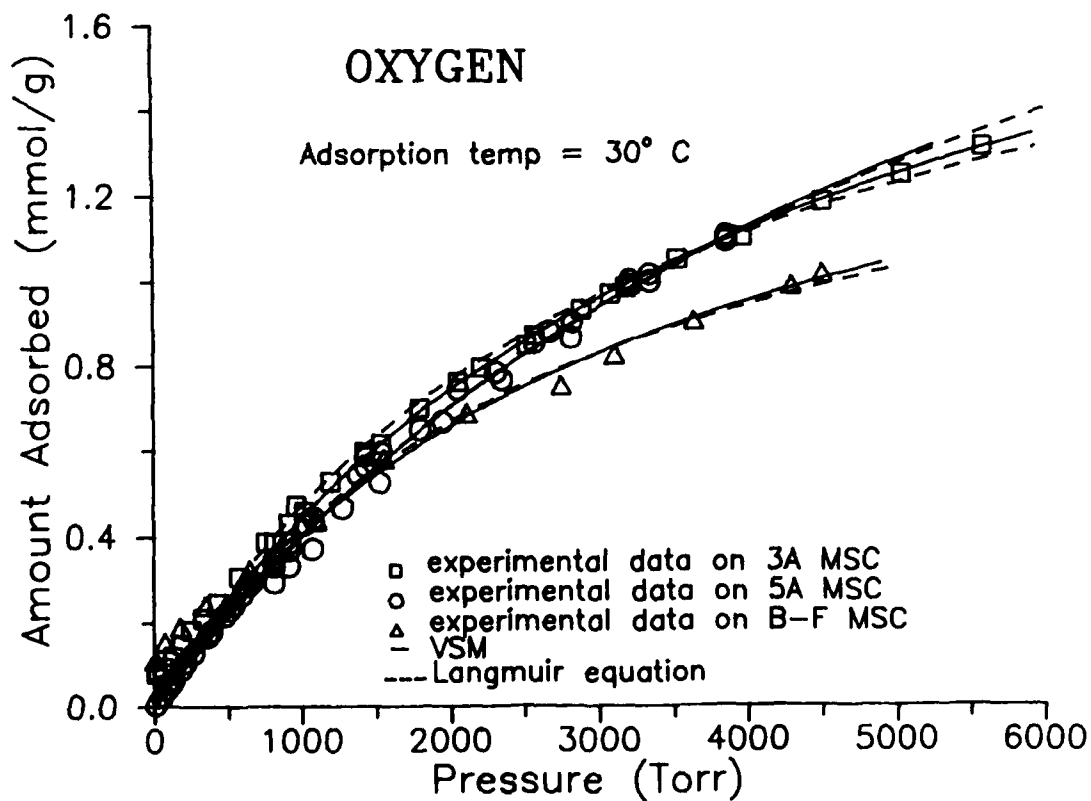


Figure 27. O_2 adsorption on various samples.

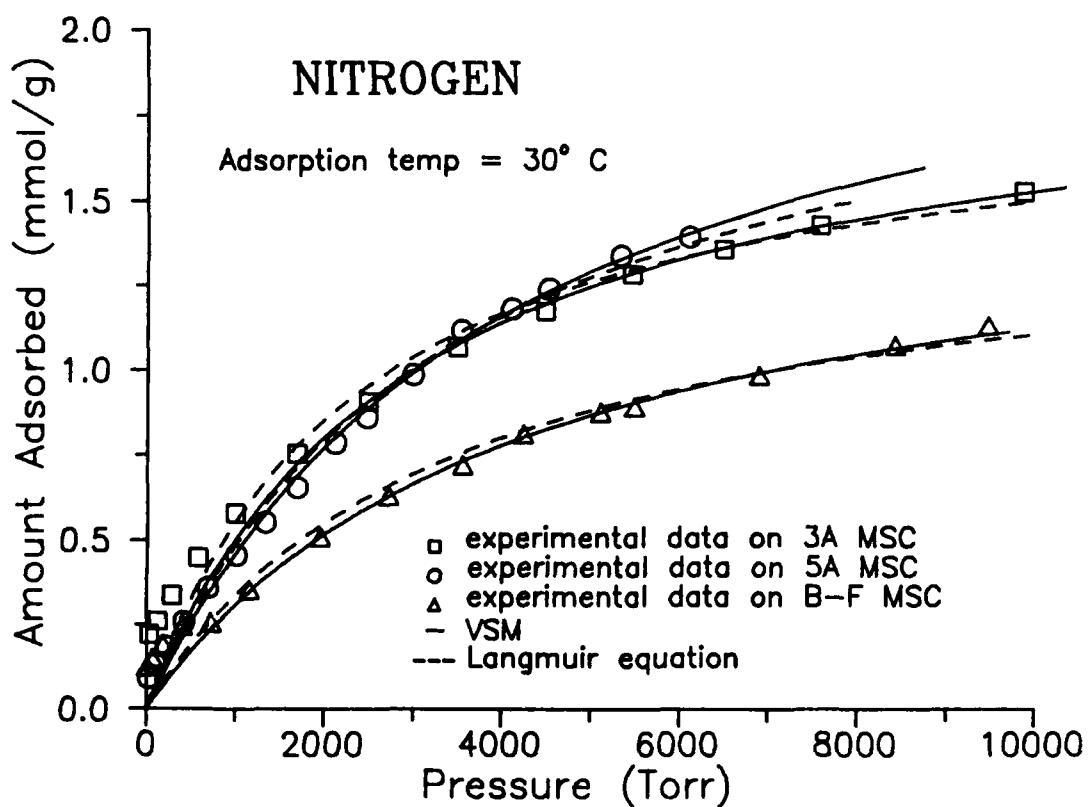


Figure 28. N₂ adsorption on various samples.

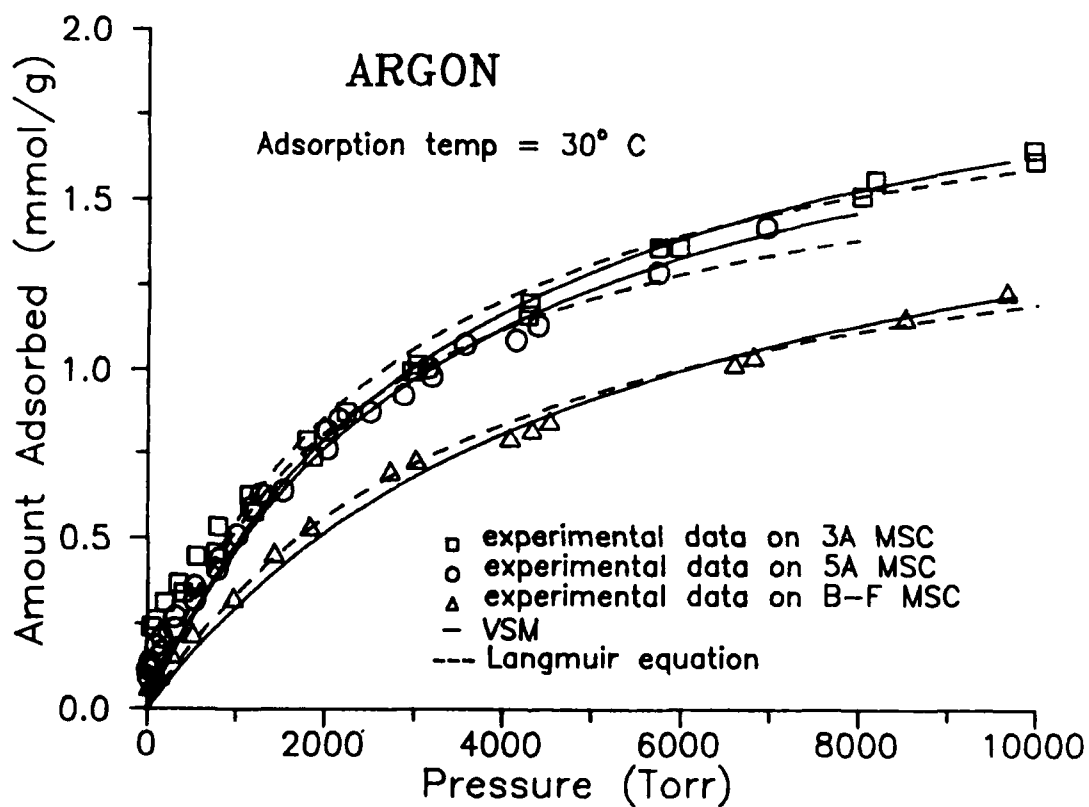


Figure 29. Ar adsorption on various samples.

where q^{st} is the isosteric heat of adsorption, R is the gas constant and n is the amount adsorbed.

From Eq. (6), it is clear that a plot of $\ln P$ vs $1/T$ at a constant adsorbed amount will yield a straight line with the

slope of $-\frac{q^{st}}{R}$. Typical plots are shown in Figures 30 and 31 for argon on both 5A and 3A MSC. Straight lines are obtained for both cases. The isosteric heats of adsorption for all the gases studied are tabulated as a function of the amount adsorbed in Tables 4 and 5 for 5A and 3A MSC respectively and are plotted in Figure 32. It is seen that the values for methane are higher than for other gases. The difference between the values for 3A MSC and 5A MSC is the least in the case of nitrogen, and the most in the case of argon. Further, in the case of argon, the q^{st} values were considerably higher on 5A MSC than on 3A MSC. The

TABLE 4. ISOSTERIC HEAT OF ADSORPTION FOR GASES ON 5A MSC

Gas: N ₂		O ₂		CH ₄		Ar	
q^a mmol/g	$-q^{st}{}^b$ KJ/mol	q mmol/g	$-q^{st}$ KJ/mol	q mmol/g	$-q^{st}$ KJ/mol	q mmol/g	$-q^{st}$ KJ/mol
0.046	12.92	0.055	14.73	0.056	16.31	0.036	15.67
0.114	13.19	0.139	15.01	0.139	16.49	0.089	15.71
0.228	13.69	0.277	15.54	0.278	16.84	0.179	15.79
0.456	14.99	0.554	16.94	0.556	17.66	0.357	15.97
0.684	16.96	0.831	19.10	0.834	18.76	0.536	16.18

a : q =amount adsorbed

b : q^{st} =isosteric heat of adsorption

TABLE 5. ISOSTERIC HEAT OF ADSORPTION FOR GASES ON 3A MSC

Gas: N ₂		O ₂		CH ₄		Ar	
q^a mmol/g	$-q^{st}{}^b$ KJ/mol	q mmol/g	$-q^{st}$ KJ/mol	q mmol/g	$-q^{st}$ KJ/mol	q mmol/g	$-q^{st}$ KJ/mol
0.035	13.12	0.042	17.33	0.534	18.11	0.036	10.99
0.089	13.23	0.104	17.57	0.133	18.38	0.091	11.18
0.177	13.43	0.208	18.02	0.267	18.88	0.182	11.55
0.355	13.92	0.417	19.12	0.534	20.05	0.364	12.41
0.532	14.59	0.625	20.63	0.801	21.57	0.547	13.52

a : q =amount adsorbed

b : q^{st} =isosteric heat of adsorption

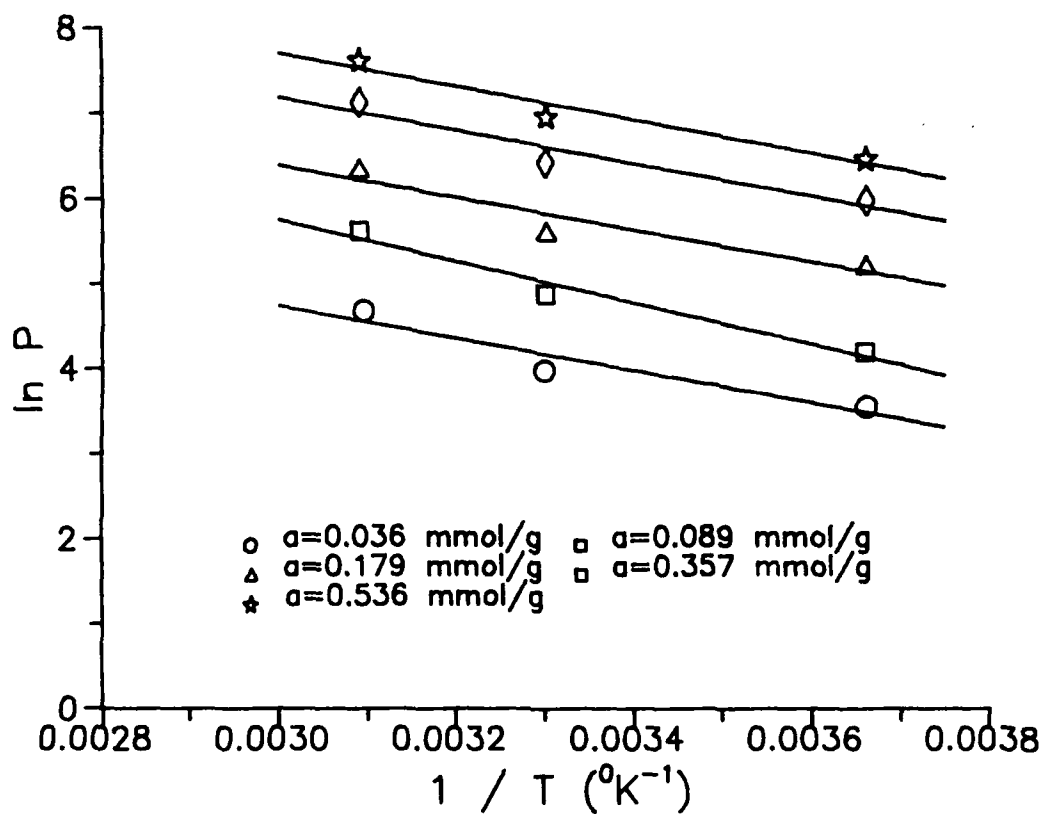


Figure 30. Plot of $(\ln P)$ vs. $(1/T)$ for Ar on 5A MSC.

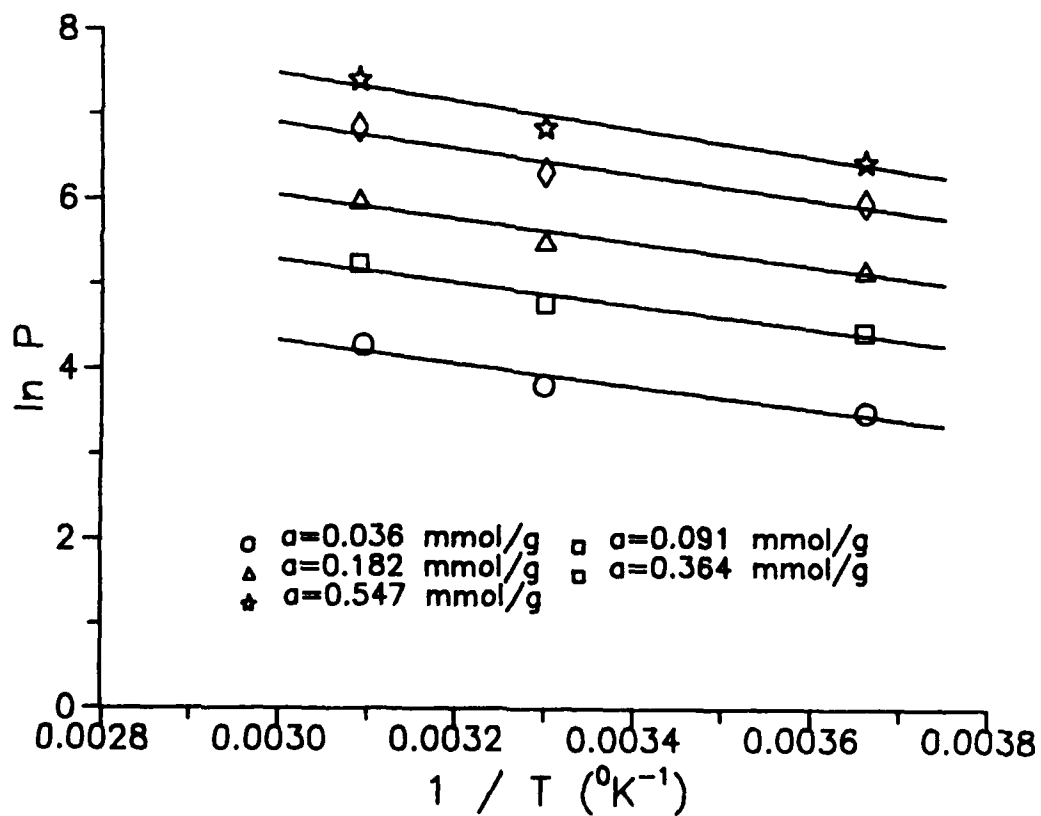


Figure 31. Plot of $(\ln P)$ vs. $(1/T)$ for Ar on 3A MSC.

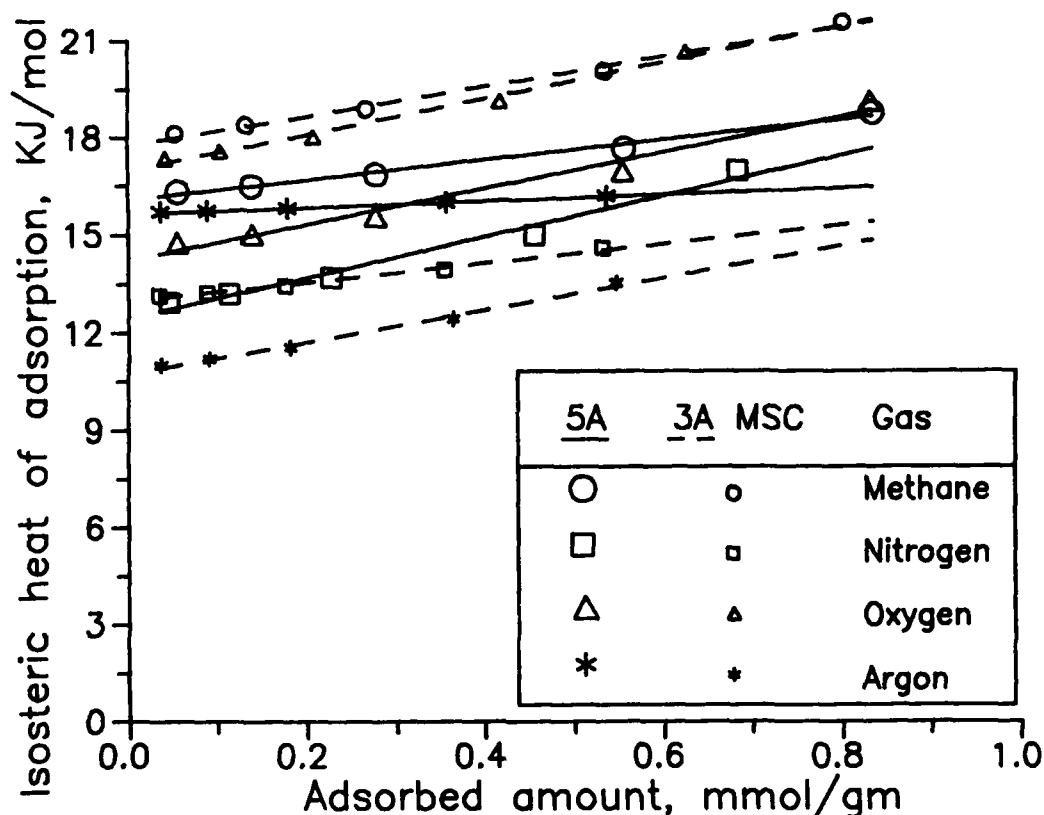


Figure 32. Isosteric heat of adsorption vs. coverage.

reason for the high values is unclear at the present. More work is needed to clarify this point.

From the low surface coverage data reported by Chihara et al. (26) for 5A MSC, the q^{st} values were 18.8, 23.8 and 16.7 KJ/mol, respectively, for nitrogen, methane and argon. Comparing these values with those given in Table 4 we find that the values obtained for methane and nitrogen in the present study are lower, on an average, by about 30%. The values for argon are close in both studies. The isosteric heat of adsorption which is a measure of the interactions between adsorbate molecules and adsorbent lattice atoms, may be used as a measure of the energetic heterogeneity of a surface. Observed differences in the q^{st} values for the same gas on different samples point to the differences in the nature of the sample surfaces. (As already noted, the reproducibility of the MSC from different batches has been difficult.) With the increasing amount of adsorption the adsorbing surface will be progressively covered with more and more adsorbate molecules so that more than one layer of these molecules may be formed and a variation in q^{st} values may be observed with the increasing coverage. In the present study we observe that the q^{st} values increase slightly (except for Argon on 5A) as the surface coverage increases. The fact that the q^{st} values are high for N_2 and CH_4 in the low-coverage study of Chihara et al. suggests that the adsorbent surface (carbon) and the adsorbate molecules have higher (absolute value) attraction

potential than that possessed by two like (adsorbate) molecules. Further, the slight increase in values with increasing adsorption in the present high-coverage study indicates that there is some interaction between the adsorbate molecules.

Single Component Diffusion

Mathematical Model

The diffusion of gases in porous solids is generally assumed to follow Fick's second law. This assumption is valid for the diffusion of gases in molecular sieve carbons. The derivation of the partial differential equation to describe the diffusion process in the MSC is based on the following assumptions:

1. The particles of the MSC are isothermal, uniform and spherical.
2. Fickian diffusion may be used to describe the diffusion process within the pores of the MSC.
3. The diffusion coefficient is constant during the adsorption process.
4. At the gas-solid interface, the concentration of the adsorbate is the same as that in the gas phase.

Utilizing the above described assumptions, a mass balance on a spherical particle (27) yields

$$\frac{\partial C}{\partial t} = D \left(\frac{1}{r^2} \right) \frac{\partial}{\partial r} \left(r^2 \frac{\partial C}{\partial r} \right) \quad (7)$$

with C = concentration of the adsorbate in the solid
 r = radial position
 t = time
 D = diffusion coefficient

Equation (7) can be solved analytically using the following initial and boundary conditions associated with a constant volume, constant pressure system:

$$\begin{aligned} \text{At } t = 0 \quad C(0, r) &= C_0 \\ \text{At } t > 0 \\ \text{at } r = 0 \quad \frac{\partial C(t, 0)}{\partial r} &= 0 \\ \text{at } r = R \quad C(t, R) &= C_\infty \end{aligned} \quad (8)$$

where R is the radius of the MSC particle.

In the present study, the amount of gas adsorbed by the MSC was measured experimentally as a function of time. Therefore, it is more useful to calculate the total amount of gas adsorbed at any time by the following relation:

$$M_t = 4\pi \int_0^R (C - C_0) r^2 dr \quad (9)$$

where M_t = amount adsorbed at any time t .

The solution of Eq. (7) with boundary conditions, Eq.(8), in terms of fractional uptake M_t/M_∞ is given by Crank (28)

$$\frac{M_t}{M_\infty} = 1 - \frac{6}{\pi^2} \sum_{n=1}^{\infty} \frac{1}{n^2} \exp(-n^2 \pi^2 t D / r^2) \quad (10)$$

where D is the diffusivity, M_t is the mass of the sorbate adsorbed in time t , M_∞ is the mass of the sorbate adsorbed at equilibrium, and r is the mean particle diameter.

Comparison of Diffusivity Values

Equation (10) was used to determine the diffusion coefficient of all the gases in both 3A and 5A MSC. The least squares method was used to fit the experimental data with Eq. (10). The diffusion coefficients determined in this manner are shown in Tables 6 and 7 for 3A and 5A MSC respectively. Figures 33, 34, 35, and 36 compare the typical experimental data and the curves computed from Eq. (10) which show, in general, good agreement. The D/r^2 value used for each curve is indicated on the figures. The rates of adsorption of various gases are compared with each other at 0°C, 30°C, and 50°C, respectively, in Figures 33, 34, and 35. The rates for one gas (argon on 3A MSC) are shown at three temperatures in Figure 36.

The diffusivity values range from 10^{-5} for methane at 0°C in 3A MSC to 10^{-2} sec^{-1} for oxygen in 5A MSC at 50°C. Diffusivities in 3A MSC are comparable to those in BF MSC, but lower than in 5A MSC. Among the four gases studied, methane has the lowest diffusional rate and oxygen the highest in all samples. The diffusivity values could be arranged in the following order: $\text{CH}_4 < \text{N}_2 \approx \text{Ar} < \text{O}_2$. On a relative scale if methane was assigned a diffusivity value of 1, the corresponding values for oxygen, nitrogen and argon at 30°C were about 14, 2, and 2, respectively, in the case of 5A MSC. Similarly, in the case of 3A MSC, the relative diffusivity values at 30°C for methane, oxygen, nitrogen and argon were 1, 160, 8, and 13 respectively. Comparing the rates in 3A and 5A MSC for, say, methane, it was found that the gas diffused in 5A about 15 times as fast as in 3A MSC.

TABLE 6. DIFFUSIVITY OF GASES IN 3A MSC

Gas	0°C		30°C		50°C	
	P ^a (Torr)	D/r ² ^b (sec ⁻¹)	P ^a (Torr)	D/r ² ^b (sec ⁻¹)	P ^a (Torr)	D/r ² ^b (sec ⁻¹)
N ₂	73	4.70 x 10 ⁻⁵	85	2.27 x 10 ⁻⁴	130	6.71 x 10 ⁻⁴
	153	5.21 x 10 ⁻⁵	425	2.67 x 10 ⁻⁴	290	5.52 x 10 ⁻⁴
	485	6.92 x 10 ⁻⁵	780	2.13 x 10 ⁻⁴	580	8.14 x 10 ⁻⁴
	907	9.07 x 10 ⁻⁵	1545	2.19 x 10 ⁻⁴	1000	7.14 x 10 ⁻⁴
	1823	1.16 x 10 ⁻⁴	1990	2.22 x 10 ⁻⁴	1700	9.14 x 10 ⁻⁴
	3039	1.59 x 10 ⁻⁴	3440	2.26 x 10 ⁻⁴	3500	1.13 x 10 ⁻³
	4025	1.85 x 10 ⁻⁴	5630	2.32 x 10 ⁻⁴	5470	1.04 x 10 ⁻³
O ₂	42	2.07 x 10 ⁻³	577	4.64 x 10 ⁻³	162	5.40 x 10 ⁻³
	138	1.53 x 10 ⁻³	756	5.86 x 10 ⁻³	283	6.12 x 10 ⁻³
	466	2.37 x 10 ⁻³	1197	5.17 x 10 ⁻³	435	1.27 x 10 ⁻²
	680	1.55 x 10 ⁻³	1424	5.02 x 10 ⁻³	630	1.34 x 10 ⁻²
	1143	2.74 x 10 ⁻³	1797	4.10 x 10 ⁻³	857	1.05 x 10 ⁻²
	1513	2.22 x 10 ⁻³	6591	4.14 x 10 ⁻³	1450	5.74 x 10 ⁻³
	2017	1.76 x 10 ⁻³	8466	4.64 x 10 ⁻³	1840	4.79 x 10 ⁻³
CH ₄	81	8.70 x 10 ⁻⁶	220	4.23 x 10 ⁻⁵	210	7.52 x 10 ⁻⁵
	422	1.35 x 10 ⁻⁵	430	3.69 x 10 ⁻⁵	320	6.27 x 10 ⁻⁵
	717	9.20 x 10 ⁻⁶	634	2.69 x 10 ⁻⁵	471	7.64 x 10 ⁻⁵
	815	1.38 x 10 ⁻⁵	745	2.61 x 10 ⁻⁵	690	9.19 x 10 ⁻⁵
	1192	1.36 x 10 ⁻⁵	877	3.10 x 10 ⁻⁵	920	8.47 x 10 ⁻⁵
	1988	1.18 x 10 ⁻⁵	1250	4.08 x 10 ⁻⁵	1045	8.30 x 10 ⁻⁵
	2583	1.21 x 10 ⁻⁵	2493	3.72 x 10 ⁻⁵	1315	9.19 x 10 ⁻⁵
Ar	227	1.59 x 10 ⁻⁴	200	3.79 x 10 ⁻⁴	240	6.33 x 10 ⁻⁴
	867	1.70 x 10 ⁻⁴	350	3.43 x 10 ⁻⁴	1461	4.85 x 10 ⁻⁴
	877	2.20 x 10 ⁻⁴	500	3.96 x 10 ⁻⁴	2130	6.66 x 10 ⁻⁴
	1196	1.92 x 10 ⁻⁴	800	3.24 x 10 ⁻⁴	2935	5.90 x 10 ⁻⁴
	1512	1.96 x 10 ⁻⁴	1150	3.62 x 10 ⁻⁴	3950	5.47 x 10 ⁻⁴
	2029	1.82 x 10 ⁻⁴	3020	3.93 x 10 ⁻⁴	4560	6.05 x 10 ⁻⁴
	2737	1.95 x 10 ⁻⁴	6000	3.53 x 10 ⁻⁴	4980	6.15 x 10 ⁻⁴

^a P : Pressure

^b D/r² : Diffusivity

Although the adsorption capacity of MSC for nitrogen and oxygen were approximately the same, there was a large difference in adsorption rates, which means that the adsorbent could be employed in a PSA process depending on a kinetic separation to obtain nitrogen, argon and oxygen from air. By comparing our data on 3A MSC, BF MSC and 5A MSC, it appears that either 3A MSC or BF MSC is better suited in air separation processes because the adsorbent may be predicted to show a higher kinetic selectivity when exposed to a mixture of oxygen and nitrogen. Of the three adsorbents, BF MSC appears to give the best kinetic selectivity for the N₂-O₂ mixture, with a diffusivity ratio

TABLE 7. DIFFUSIVITY OF GASES IN 5A MSC

Gas	0°C		30°C		50°C	
	P ^a (Torr)	D/r ² ^b (sec ⁻¹)	P ^a (Torr)	D/r ² ^b (sec ⁻¹)	P ^a (Torr)	D/r ² ^b (sec ⁻¹)
N ₂	79	5.42 x 10 ⁻⁴	227	1.88 x 10 ⁻³	56	3.62 x 10 ⁻³
	143	4.72 x 10 ⁻⁴	1690	1.36 x 10 ⁻³	132	3.06 x 10 ⁻³
	508	2.27 x 10 ⁻⁴	2129	1.11 x 10 ⁻³	594	4.48 x 10 ⁻³
	665	3.00 x 10 ⁻⁴	2483	7.04 x 10 ⁻⁴	1055	5.21 x 10 ⁻³
	924	5.90 x 10 ⁻⁴	2995	1.19 x 10 ⁻³	1438	2.05 x 10 ⁻³
	2624	3.41 x 10 ⁻⁴	4112	9.59 x 10 ⁻⁴	2288	3.44 x 10 ⁻³
	3631	4.80 x 10 ⁻⁴	5330	8.31 x 10 ⁻⁴	4181	2.60 x 10 ⁻³
O ₂	378	1.86 x 10 ⁻³	67	7.23 x 10 ⁻³	101	8.97 x 10 ⁻³
	602	1.22 x 10 ⁻³	505	4.56 x 10 ⁻³	203	1.44 x 10 ⁻²
	1066	1.38 x 10 ⁻³	1022	5.78 x 10 ⁻³	347	1.09 x 10 ⁻²
	1621	1.30 x 10 ⁻³	1235	7.08 x 10 ⁻³	920	1.58 x 10 ⁻²
	2509	1.49 x 10 ⁻³	1917	6.35 x 10 ⁻³	1157	1.10 x 10 ⁻²
	3019	1.15 x 10 ⁻³	2822	6.89 x 10 ⁻³	1358	1.00 x 10 ⁻²
	3598	1.04 x 10 ⁻³	4866	7.59 x 10 ⁻³	2505	1.07 x 10 ⁻²
CH ₄	106	1.95 x 10 ⁻⁴	970	9.38 x 10 ⁻⁴	146	1.22 x 10 ⁻³
	157	3.65 x 10 ⁻⁴	1520	7.66 x 10 ⁻⁴	223	1.39 x 10 ⁻³
	444	2.67 x 10 ⁻⁴	2383	3.00 x 10 ⁻⁴	1225	9.37 x 10 ⁻³
	695	2.14 x 10 ⁻⁴	2682	2.62 x 10 ⁻⁴	2037	1.44 x 10 ⁻³
	1009	1.88 x 10 ⁻⁴	2928	2.76 x 10 ⁻⁴	2805	1.14 x 10 ⁻³
	1932	2.34 x 10 ⁻⁴	3402	4.41 x 10 ⁻⁴	3343	1.21 x 10 ⁻³
	3822	1.97 x 10 ⁻⁴	3922	4.22 x 10 ⁻⁴	555	8.93 x 10 ⁻⁴
Ar	225	5.42 x 10 ⁻⁴	103	9.43 x 10 ⁻⁴	145	2.17 x 10 ⁻³
	810	3.34 x 10 ⁻⁴	174	6.71 x 10 ⁻⁴	407	2.26 x 10 ⁻³
	970	7.59 x 10 ⁻⁴	312	1.16 x 10 ⁻³	610	1.77 x 10 ⁻³
	1342	7.69 x 10 ⁻⁴	1210	1.23 x 10 ⁻³	1533	1.98 x 10 ⁻³
	1496	6.04 x 10 ⁻⁴	2147	7.85 x 10 ⁻⁴	3178	2.34 x 10 ⁻³
	2994	4.39 x 10 ⁻⁴	2586	1.11 x 10 ⁻³	3570	1.63 x 10 ⁻³
	4004	3.29 x 10 ⁻⁴	3661	8.76 x 10 ⁻⁴	3653	1.82 x 10 ⁻³

^a P : Pressure^b D/r² : Diffusivity

(N₂/O₂) of 0.04. Ruthven et al. (24) reported diffusivity values of 1.2x10⁻⁴ and 37x10⁻⁴ sec⁻¹ for nitrogen and oxygen on the BF MSC, respectively, yielding a diffusivity ratio of 0.03. In our study, high kinetic selectivities are also observed for Ar-O₂ and CH₄-O₂ on 3A and BF MSC. Studies involving mixture adsorption are needed to confirm these results.

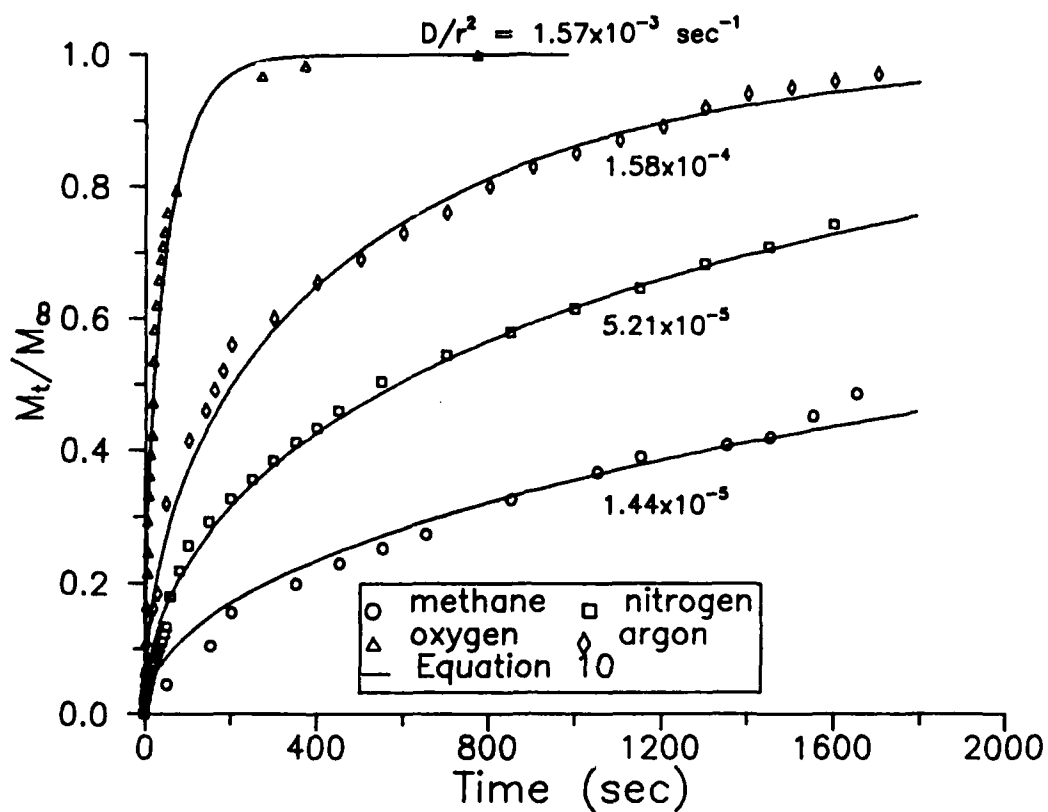


Figure 33. Uptake curves of gases on 3A MSC at 0°C.

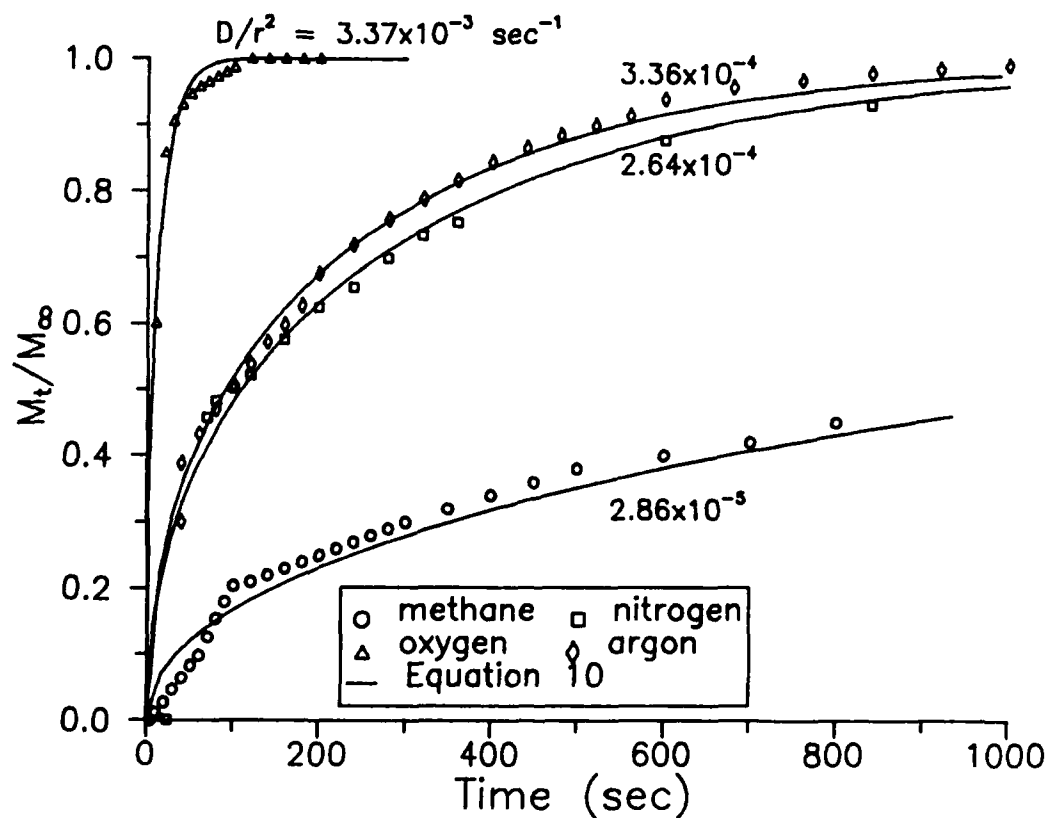


Figure 34. Uptake curves of gases on 3A MSC at 30°C.

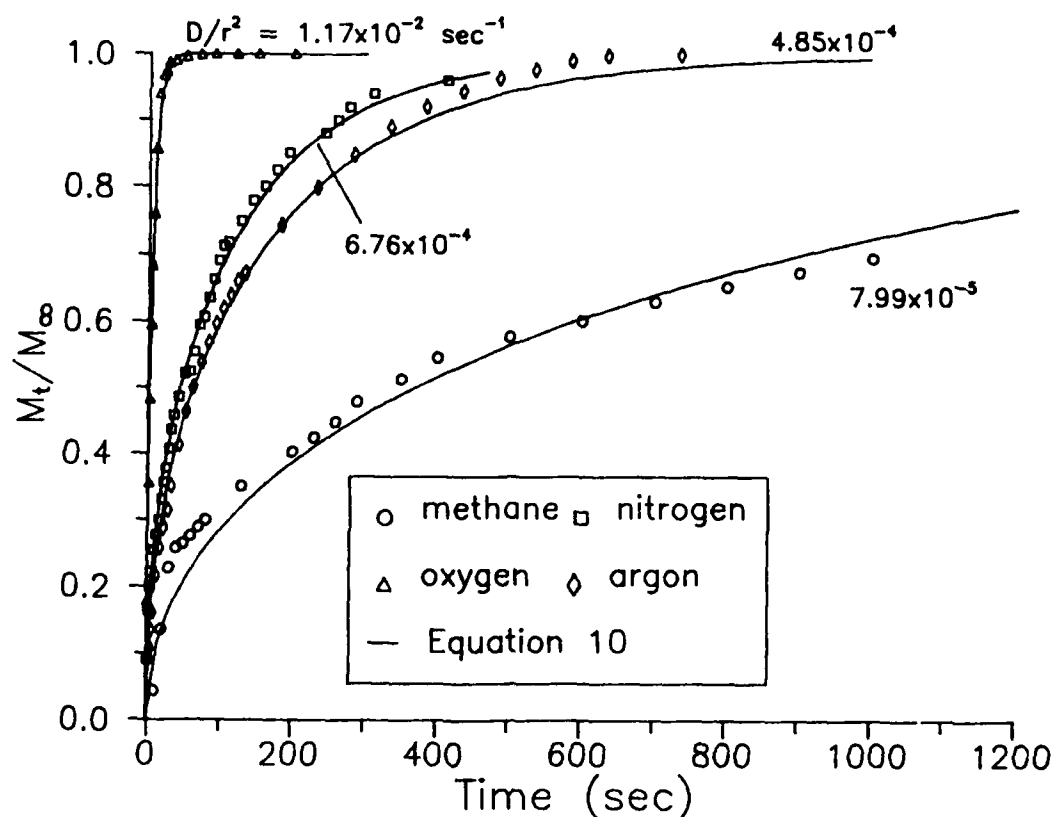


Figure 35. Uptake curves of gases on 3A MSC at 50°C.

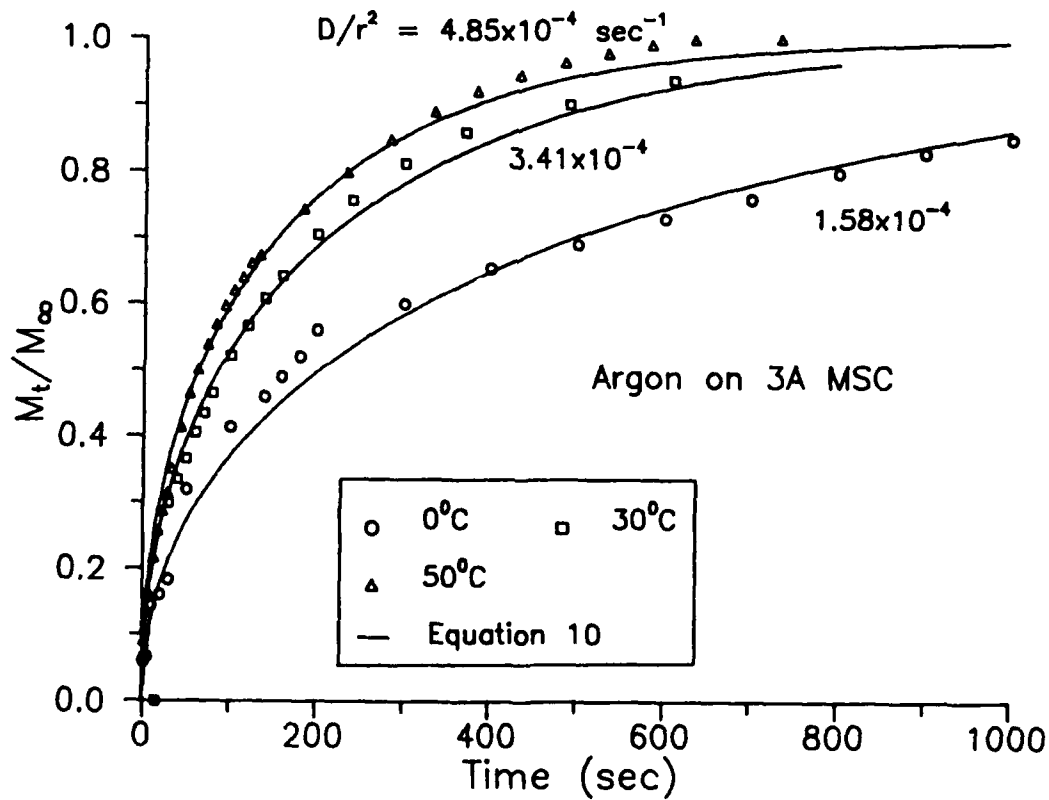


Figure 36. Uptake curves at different temperatures.

Variation of Diffusivity with Temperature and Pressure

The diffusivity values increased with the increasing adsorption temperature, as was expected. Generally speaking, the data obtained in the present study showed that the rate of increase in the diffusivity values was steepest for nitrogen in 3A MSC, and for oxygen in 5A MSC. The values for argon showed a comparatively smaller increase in the diffusivity with increasing temperature. It is interesting to correlate the temperature dependence of the diffusivity (D) using the Arrhenius equation:

$$D = D_0 \exp(-E/RT) \quad (11)$$

where D_0 is the pre-exponential factor, E is the activation energy for diffusion, R is the gas constant, and T is the temperature (Kelvin). From Eq. (11) it is clear that a plot of $\ln(D)$ versus $(1/T)$ will be a straight line. Such plots were constructed from the data for each gas on both 3A and 5A MSC. The activation energies for the adsorption were obtained from the slopes of these plots. The average values are listed in Table 8.

TABLE 8. ACTIVATION ENERGY OF DIFFUSION IN 5A AND 3A MSC

	E (KJ/mol)			
	N ₂	O ₂	CH ₄	Ar
5A MSC	27.7	32.2	22.3	18.6
3A MSC	29.2	20.6	27.8	16.6

The activation energy values were high, comparable to the values for isosteric heats of adsorption (Tables 4 and 5) confirming that the diffusion in MSC is an activated process (26). For argon and methane these values were about 19 and 22 KJ/mol, respectively. The values for argon and methane obtained previously (26) in the case of 5A MSC from chromatographic measurements and a moment analysis were about 16 and 20 KJ/mol, respectively. For nitrogen the value of 16 KJ/mol was reported in the same study, and the value in the present study was high, about 28 KJ/mol. The values of activation energy for diffusion could not be correlated well with the isosteric heats of adsorption, although it should be mentioned that the ratio E/q_{st} was in the range of 1 to 2 for the gases studied. Perhaps, such a correlation would be more useful if the adsorption experiments were carried out at extremely low coverage (Henry's law region) of the adsorbate upon the sample, as was done in previous chromatographic measurements (26) from which a ratio of 0.9 was obtained. However, adsorption at very low coverages would not have much practical interest.

In general, the obtained diffusivity values showed no dependency on adsorbate pressure (Figures 37 and 38). The only

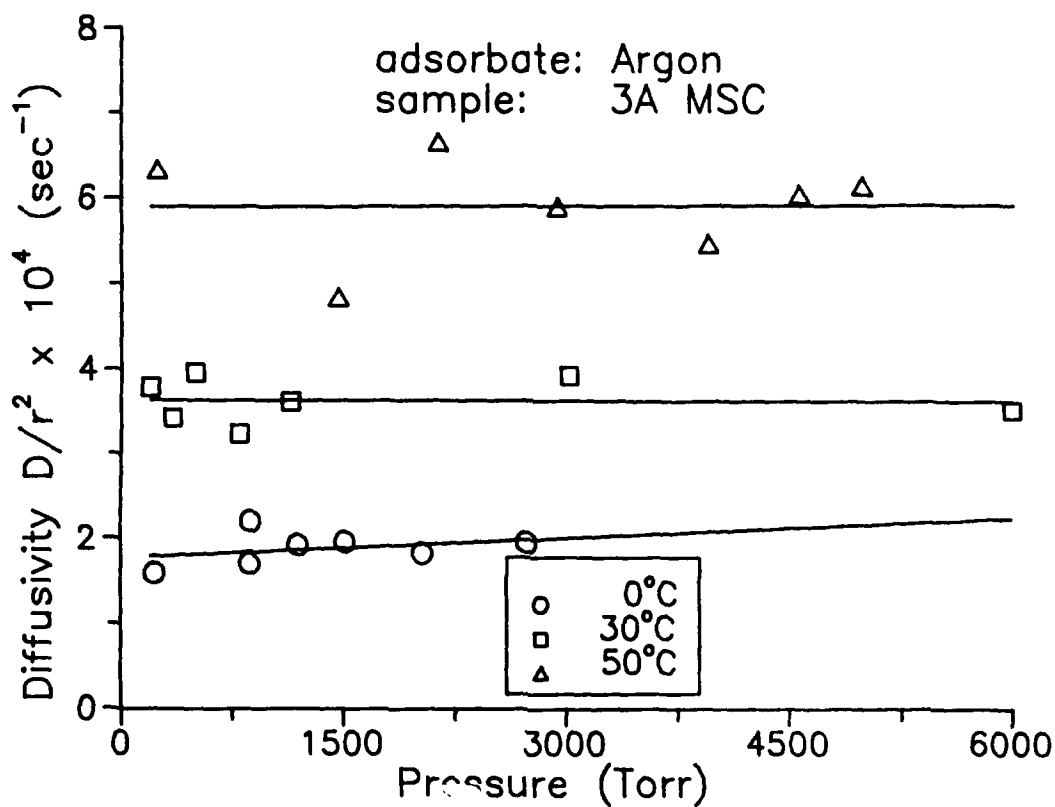


Figure 37. The variation of diffusivity of Ar with pressure.

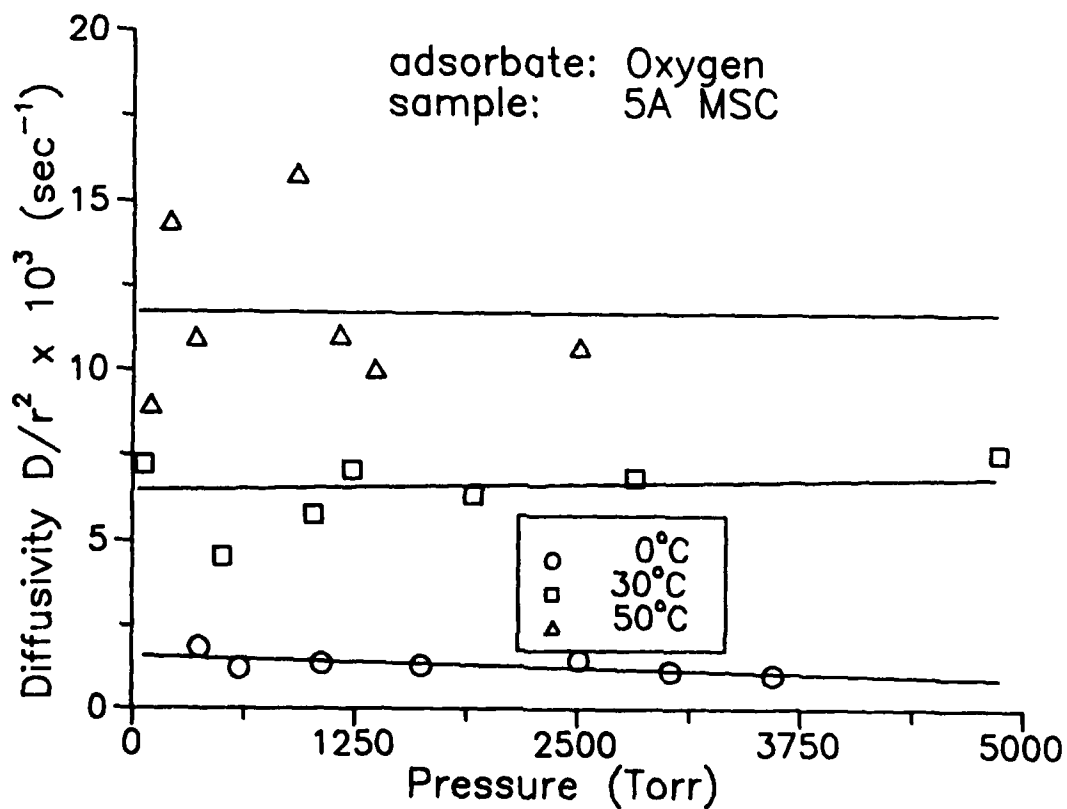


Figure 38. The variation of diffusivity of O_2 with pressure.

dependency observed was in the case of nitrogen adsorbed on 3A MSC at low temperature (0°C). The diffusivity in this case appeared to increase with pressure. The independence of diffusivity with sorbate concentration validates the assumption of an ideal Fickian model for diffusion. It should be noted that Kawazoe et al. (29, 30) previously reported the essential independence of the diffusivity for, as an example, propylene on 5A MSC.

Multicomponent Adsorption

The importance of obtaining information on the adsorption rate of multicomponent systems can be demonstrated by the phenomena of competitive adsorption generally observed in multicomponent systems. The competition for adsorption sites among interacting adsorbates will not only affect the equilibrium adsorption capacity of each individual component, but also influence the diffusion rate of the individual adsorbate. Furthermore, this competitive adsorption causes the displacement phenomena commonly observed in rate studies in a multicomponent system. The result is a maximum in the uptake curve of one of the species until equilibrium is established due to differences in diffusion rates and affinity to the adsorbent. The practical implication of the displacement phenomena is that the displaced species will break through the adsorption bed and reduce the effectiveness of the bed.

The apparatus originally designed to carry out the multicomponent adsorption rate study is described below. The difficulty associated with this setup for obtaining reliable multicomponent adsorption rate data is also discussed. Finally, the new design which will alleviate the difficulties encountered in the original design is presented.

Original Design of the Multicomponent Adsorption Setup

Due to the low adsorption capacity and fast kinetics involved in the diffusion of N_2 , O_2 and Ar (extremely slow kinetics for CH_4), a more sensitive way of detecting the composition change in the gas phase had to be devised. Therefore, a new well-stirred reactor system was designed and constructed.

A well-stirred reactor consisting of a 5-liter cylindrical stainless steel vessel was constructed to study the diffusion and adsorption of gases in multicomponent systems. Either powder or pellets could be placed in two equally spaced adjustable baskets which were attached to the shaft and were rotated at 3300 rev/min. The shaft was driven magnetically by a 1/2 HP motor. A schematic diagram of the adsorption chamber is shown in Figure 39. The adsorbent could be heated by four heating rods placed inside stainless steel castings which also served as baffles to

facilitate mixing. The temperature of the system could be controlled to within $\approx 0.5^\circ\text{C}$.

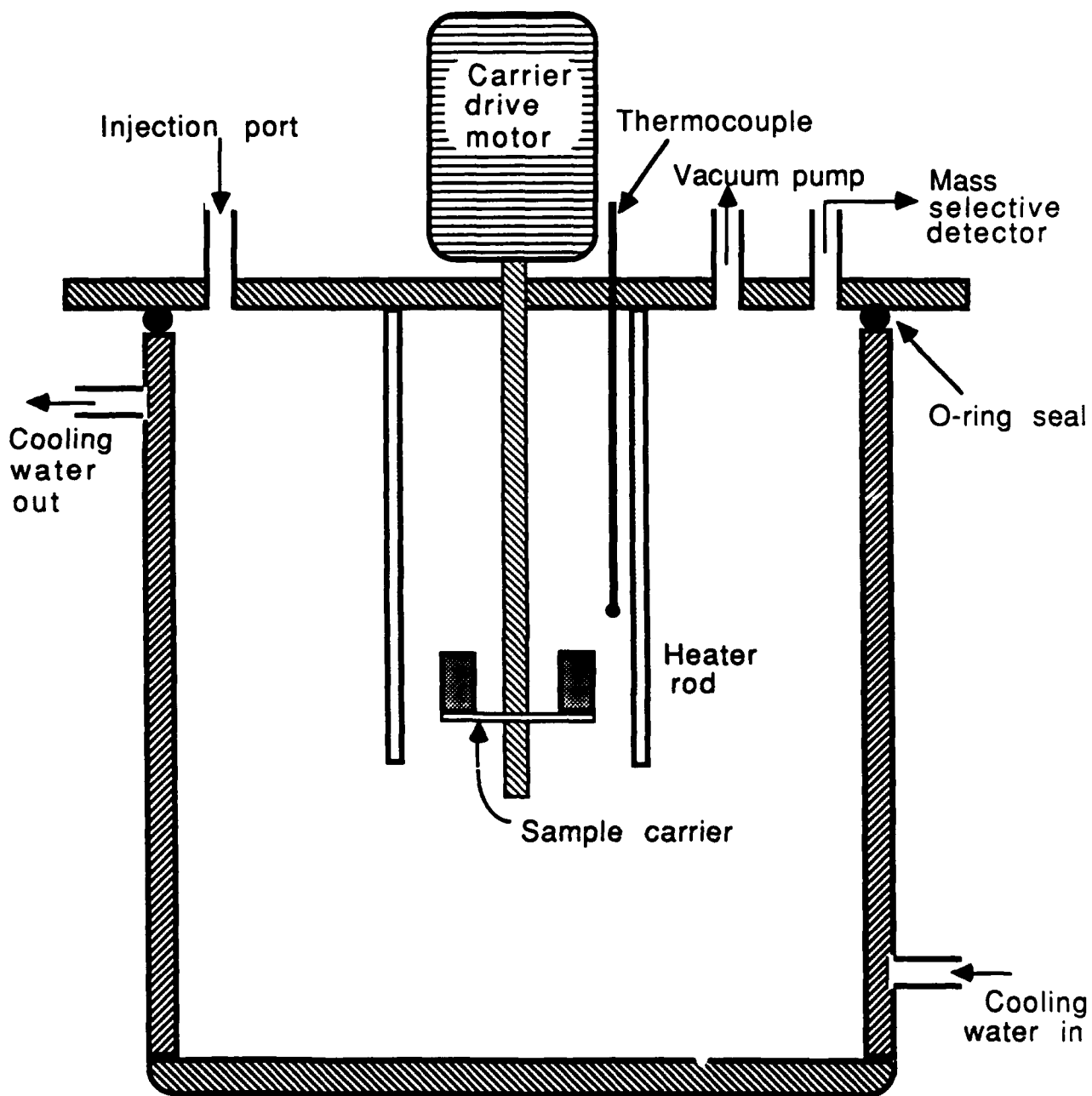


Figure 39. Schematic of the well-stirred reactor.

Adsorption rates were measured by injecting a measured amount of sorbate gases into the adsorption chamber. The amount of each component adsorbed as a function of time could be continuously followed by bleeding a minute quantity of gas from the reactor into a mass selective detector (HP 5970 Series Mass Selective Detector).

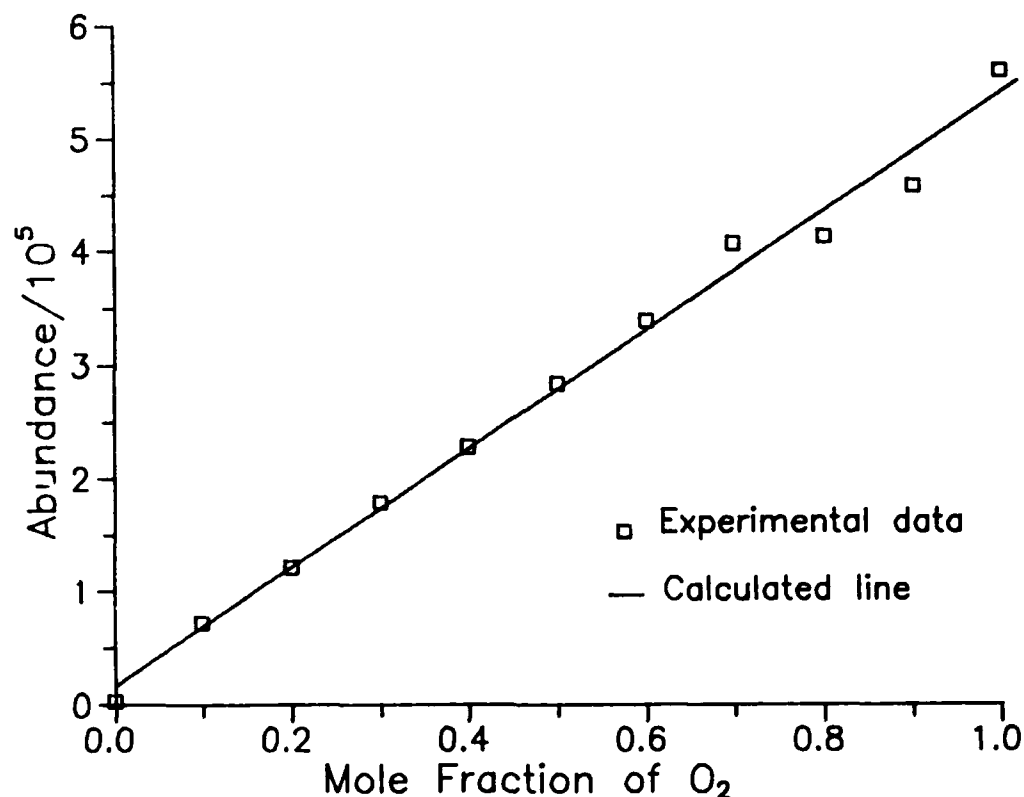


Figure 40. Calibration curve of O₂ in He at 100 Torr.

Difficulty in the Original Design

Since the signal from the mass selective detector is a function of the amount bled into the detector, the signal depends on the gas composition in the reactor as well as on the chamber pressure. Therefore, it is necessary to calibrate the instrument with a known composition under a fixed pressure. A typical calibration curve for O₂ in He at a total pressure of 100 Torr is shown in Figure 40. A good straight line is obtained for the calibration. Calibrations for other gases show similar trends.

The problem arose when the adsorption runs were carried out. The experiments were initiated by activating the sample under vacuum for a fixed period of time. After completing the activation process, a gas mixture was admitted into the reactor creating a sudden surge of chamber pressure which substantially increased the signal from the mass selective detector. The problem is two-fold. First, the sudden increase in the mass spectrometer signal due to the pressure increase made it difficult to determine the initial amount of adsorbate introduced into the system. Second, the subsequent decrease in the MSD signal could be caused by decreased pressure as well as by adsorption. It is essentially impossible to distinguish between these two phenomena due to the sudden surge in initial pressure. After numerous trials, it was decided that a new design would be necessary to obtain accurate, reliable data.

New Design

The purpose of the previous design was to bring a large quantity of gas in contact with the adsorbent and to follow the adsorption process using gas phase composition measurements as a function of time. However, initial pressure changes due to the introduction of the gas interfered with the ability of the MSD to provide signals reflecting the initial gas composition changes. The new design is based on a different concept of bringing together the gas and the adsorbent. After the adsorbent is activated, it is isolated from the gas to be admitted into the chamber. Once the adsorbent is isolated under vacuum, the gas mixture will be admitted to the adsorption chamber. After a steady state is established, the adsorbent is exposed to the gas mixture for the adsorption experiment to eliminate the problem of pressure surge. Thus, the change in the signal from the MSD represents the true composition change in the gas phase. This signal will then be a true measure of the adsorption taking place in the adsorption chamber.

The new design is shown schematically in Figure 41. The main feature of the design is that the sample holder can be isolated from the gas phase by pressing the two plates against the sample holder walls through the two levers. Once the sample is isolated, the gas mixture is released into the chamber. When a steady reading of the signal from the MSD is reached, the adsorbent is exposed to the gas mixture by pulling the two plates away from the sample holder, again through the two levers attached to the chamber. Once the adsorbent is exposed to the gas mixture, the decrease in MSD signals will be continuously recorded. This data will then be used to determine the rate of adsorption and the adsorption equilibrium for a multicomponent system. A photograph of the newly designed multicomponent adsorption system is shown in Figure 42.

IV. CONCLUSIONS

From the results obtained up to date, the following conclusions can be made:

1. It appears that experimental evidence shows that MSC adsorbed relatively small amounts of water when it was exposed to ambient air for an extended period. This phenomenon has been previously stated although experimental data were somewhat scarce.
2. There is no need to activate (heat) the sample after adsorption at low pressures. Desorption under vacuum appears to be sufficient to produce a clean adsorbing surface.
3. Both the Langmuir model and the VSM are used to describe

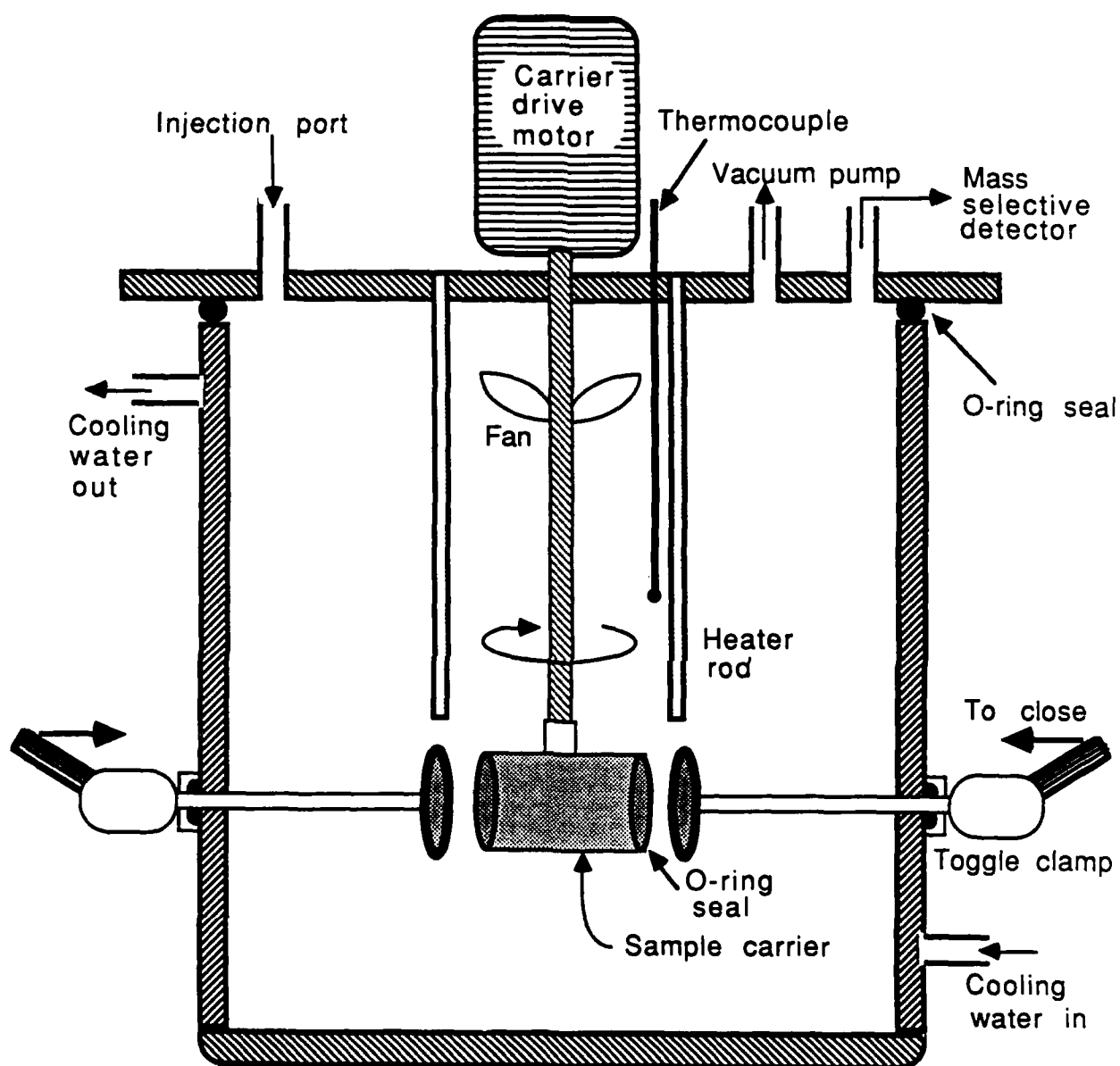


Figure 41. New design for the well-stirred reactor.

the equilibrium adsorption data for the four gases (methane, oxygen, nitrogen and argon) studied over the range of adsorbate pressures 0-10,000 Torr. Some deviation is observed at high pressures for the Langmuir model.

4. The equilibrium adsorption capacities for the four gases are higher for 5A MSC than for 3A MSC.

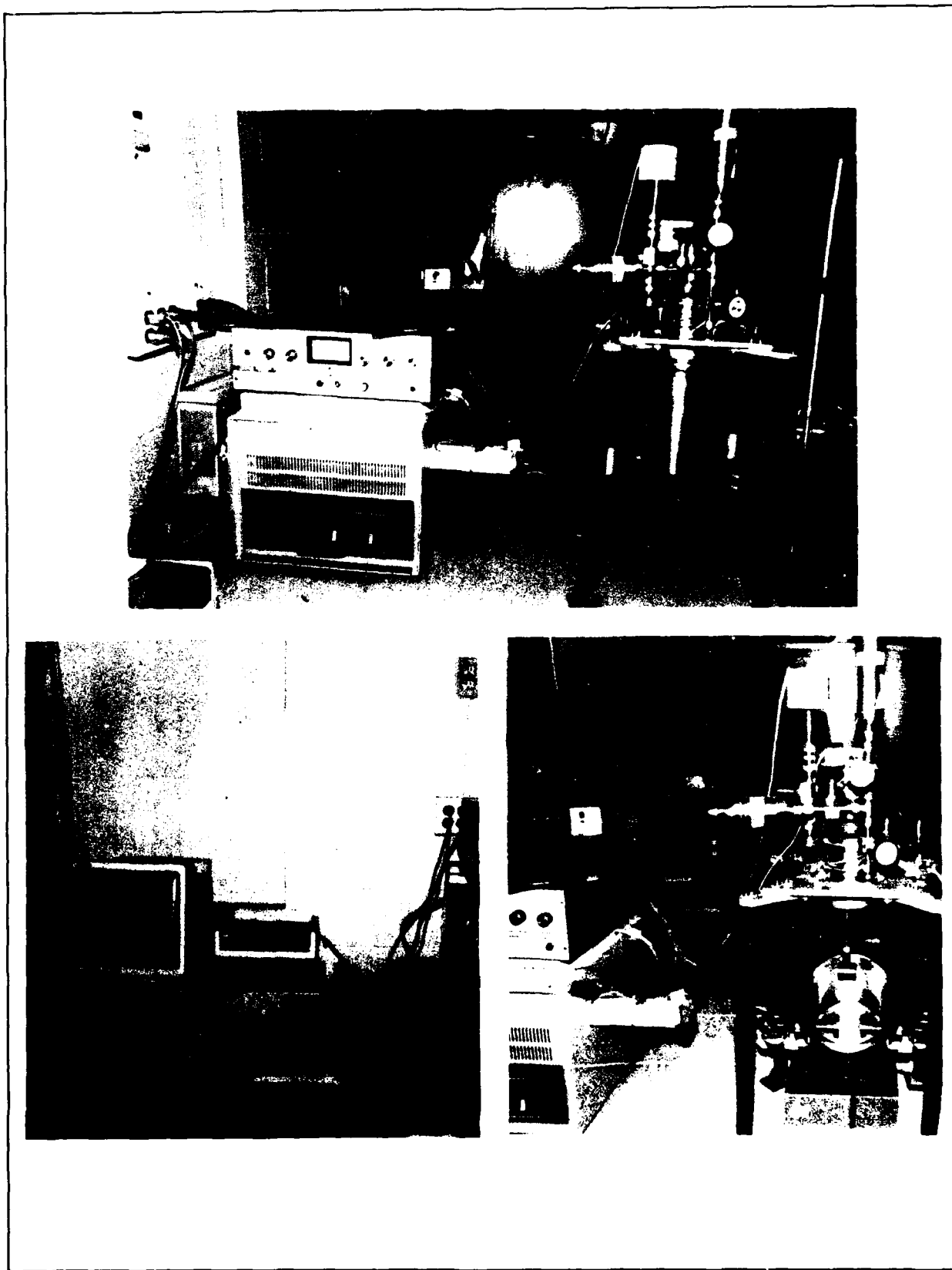


Figure 42. Photographs of the well-stirred reactor.

5. The equilibrium adsorption capacities generally show the expected trend with temperature, *viz.*, the capacities decrease with increasing temperature. Only in the case of methane on 3A MSC, is the capacity at 30°C higher than at 0°C at pressures less than 2,500 Torr, probably because equilibrium was not reached due to the extremely slow diffusion rate of methane at this temperature.
6. The adsorption rate of methane is the slowest of the four gases, while that of oxygen is the fastest. Methane adsorption in 3A is considerably slower than in 5A MSC. The adsorption of oxygen in both 5A and 3A occurs at about the same rate. Nitrogen adsorption in 3A is slower than in 5A, thus making 3A a better adsorbent for kinetic separation of air components in a PSA process.
7. The diffusivity values showed no dependency on the pressure. They increased with increasing temperature as expected.
8. The isosteric heats of adsorption appear to increase slightly with an increase in the surface coverage indicating that there is little energetic heterogeneity toward the gases studied. The slight increase in the isosteric heat of adsorption may be due to the interaction among adsorbed molecules.

V. RECOMMENDATIONS FOR FUTURE WORK

The following research activities are recommended.

Measurement of Adsorption and Diffusion of Binary Gases

The new design described in the previous section should be used to obtain data for the adsorption and diffusion of binary gases at 0°C, 30°C, and 50°C and in a pressure range of 0-10,000 Torr. Both the effects of coadsorption of binary gases and the displacement phenomena should be investigated.

Model Prediction for Multicomponent Adsorption from Single Component Adsorption Data

The Langmuir, VSM, IAST, and modified Langmuir-Sips isotherm equations should be used to predict multicomponent adsorption isotherms from single component data. The mixture adsorption isotherms obtained from the model should be compared with those obtained from experimental measurements.

Mathematical Modeling for Multicomponent Diffusion

A mathematical model for multicomponent diffusion should be developed. This model will then be used to describe the diffusional process occurring in the multicomponent diffusion experiments proposed in Section V; the diffusivity obtained from the multicomponent systems will be compared with those obtained from single component systems.

NOMENCLATURE

b	= a constant in the Langmuir isotherm equation, 1/Torr
b_{01}	= a constant in the VSM equation, mmol/g·Torr
b_1	= Henry's law constant in the VSM equation, mmol/g·Torr
C	= adsorbate concentration in the solid, mmol/cc
D	= diffusion coefficient, cm^2/sec
D_0	= pre-exponential factor in Eq. (11)
E	= activation energy diffusion, KJ/mol
K'	= Henry's law constant, mg/g·Torr
m_1	= a constant in the VSM equation, g/mmol
M_t	= mass adsorbed at time t , g
M_∞	= mass adsorbed at equilibrium, g
n_{01}	= a constant in the VSM equation, mmol/g
n_1	= amount adsorbed, mmol/g
n_1^∞	= limiting amount adsorbed, mmol/g
P	= pressure, Torr
q	= adsorption capacity, mmol/g
q_1	= isosteric heat of adsorption at infinite dilution, KJ/mol
q_m	= monolayer adsorption capacity, mmol/g
q^{st}	= isosteric heat of adsorption, KJ/mol
R	= gas constant, KJ/mol·°K
r	= radial position in the pore, cm; mean particle diameter, cm
R	= radius of the MSC particle, cm
r_1	= a constant in the VSM equation, °K
T	= temperature, °K
t	= time, sec
w	= adsorbed amount, mg/g

Greek Symbols

α_{1v}	= a parameter describing nonideality in the VSM equation
θ	= surface coverage, n_1/n_1^∞

REFERENCES

1. Lamond, T. G., J. E. Metcalf, III, and P. L. Walker, Jr. 6-A molecular sieve properties of Saran-type. Carbon 3:59-63 (1965).
2. Walker, P. L. Jr. Carbon - an old but new material. Carbon 10:369-382 (1972).
3. Kitagawa, H. J., and N. Yuki. Adsorptive properties of carbon molecular sieves from Saran. Carbon 19:470-472 (1981).
4. Franklin, R.E. Fine structure of carbonaceous solids by measurements of true and apparent densities II. Carbonized coals. Trans Faraday Soc 45:668-682 (1949).
5. Dacey, J.R., and D. G. Thomas. Adsorption on Saran charcoal. Trans Faraday Soc 50:740-748 (1954).
6. Walker, P. L., Jr., L. G. Austin and S. P. Nandi. Activated diffusion of gases in molecular-sieve materials, vol. 2, pp. 257-371 In P. L. Walker, Jr. (ed.). Chemistry and physics of carbon. New York: Marcel Dekker, 1966.
7. Spencer, D. H. T. and R. L. Bond. Determination and use of specific surface values for coals. Am Chem Soc - Advances in Chem Ser 55:724-730 (1966).
8. Harrison, I. R., M. Farr and M. E. Jordan. Microporous carbons from polymeric precursors. Proceedings of the 18th Biennial Conf Carbon, Am Carbon Soc, Worcester, Massachusetts, 1987.
9. Marsh, H., and W. F. K. Wynne-Jones. The surface properties of carbon I. The effect of activated diffusion in the determination of surface area. Carbon 1:269-279 (1964).
10. Kipling, J. J. and R. B. Wilson. Adsorptive properties of polymer carbons I. Comparative data. Trans Faraday Soc 56:557-561 (1960).
11. McEnaney, B. and N. Dovaston. The development of porosity in heat-treated polymer carbons upon activation by carbon dioxide. Carbon 13:515-519 (1975).
12. Adams, L. B., E. A. Baucher and D. H. Everett. Adsorption of organic vapors by Saran-carbon fibers and powders. Carbon 8:761-762 (1970).
13. Hirano, S., F. Dachille and P. L. Walker, Jr. Isotropic carbon spherulite formation by pressure carbonization of divinylbenzene. High Temp - High Press 5:207-220 (1973).

14. Patel, R. L. and P. L. Walker, Jr. Preparation of molecular sieve materials from anthracite. (For sale by) Supt of Docs, US Govt Print Off, Washington, 1973.
15. Hosokawa, K. and M. Yamaguchi. The pore structure of the carbons prepared from five kinds of the bamboos. Proceedings of the 18th Biennial Conf Carbon, Am Carbon Soc, Worcester, Massachusetts, 1987.
16. Koresh, J. and A. Soffer. Study of molecular sieve carbons Part 1. Pore structure, gradual pore opening, and mechanism of molecular sieving. J Chem Soc Faraday Trans I 76:2457-2471 (1980).
17. Jüntgen, H. New applications for carbonaceous adsorbents. Carbon 15:273-283 (1977).
18. Suwanayuen, S. and R. P. Danner. A gas adsorption isotherm equation based on vacancy solution theory. AIChE J 26:68-76 (1980).
19. Cochran, T. W., R. L. Kabel and R. P. Danner. The vacancy solution model of adsorption - improvements and recommendations. AIChE J 31:2075-2081 (1985).
20. Cochran, T. W., R. L. Kabel and R. P. Danner. Vacancy solution theory of adsorption using Flory-Huggins activity coefficient equations. AIChE J 31:268-277 (1985).
21. Lucassen-Reynders, E. H. Surface equations of state for mixed surfactant monolayers. J Colloid Interface Sci 41:156-167 (1972).
22. Lucassen-Reynders, E. H. Interactions in mixed monolayers I. Assessment of interaction surfactants. J Colloid Interface Sci 42:554-562 (1973).
23. Lucassen-Reynders, E. H. Adsorption of surfactant monolayers at gas/liquid and liquid/liquid interfaces. Prog Surf Memb Sci 10:253-360 (1976).
24. Ruthven, D. M., N. S. Raghavan and M. M. Hassan. Adsorption and diffusion of nitrogen and oxygen in a carbon molecular sieve. Chem Eng Sci 41:1325-1332 (1986).
25. Kapoor, A. and R. T. Yang. Kinetic separation of methane-carbon dioxide mixture by adsorption on molecular sieve carbon. Chem Eng Sci 44:1723-1733 (1989).
26. Chihara, K., M. Suzuki, and K. Kawazoe. Adsorption rate on molecular sieving carbon by chromatography. AIChE J 24:237-246 (1978).

27. Bird, R. B., W. E. Stewart and E. N. Lightfoot. Transport Phenomena, New York: Wiley, 1960.
28. Crank, J. The Mathematics of Diffusion, Oxford: Clarendon Press, 1976.
29. Kawazoe, K., M. Suzuki, and K. Chihara. Chromatographic study of diffusion in molecular-sieving carbon. J Chem Eng Japan 7:151-157 (1974).
30. Chihara, K., M. Suzuki, and K. Kawazoe. Concentration dependence of micropore diffusivities of propylene in molecular sieving carbon 5A. J Chem Eng Japan 11:153-155 (1978).

APPENDIX A
(Adsorption Data)

Adsorbent : 5A MSC
 Adsorbate : none
 Adsorption Temp : 26°C
 Figure number : 6
 Notes : Weight loss

P (Torr)	Wt. %
750.0	100.000
725.0	99.884
700.0	99.780
673.0	99.734
650.0	99.699
625.0	99.664
600.0	99.618
572.0	99.572
543.0	99.525
513.0	99.468
470.0	99.410
406.0	99.317
351.0	99.236
301.0	99.155
248.0	99.051
198.0	98.935
146.0	98.808
99.0	98.727
48.0	98.646
20.1	98.588
14.0	98.576
10.0	98.565
5.0	98.553
2.0	98.542
0.3	98.530
0.0	98.513

Adsorbent : 5A MSC
 Adsorbate : Oxygen
 Adsorption Temp : 30°C
 Figure number : 7
 Notes : Desorption/ activ.

P (Torr)	q (mmol/g)
670.3	0.3133
604.9	0.2880
559.6	0.2715
495.6	0.2443
405.4	0.2106
295.6	0.1611
192.1	0.1115
98.5	0.0671
22.7	0.0301
0.0	0.0211

Adsorbent : 3A MSC
 Adsorbate : none
 Adsorption Temp : 26°C
 Figure number : 6
 Notes : Weight loss

P (Torr)	Wt. %
750.0	100.000
718.0	99.997
660.0	99.985
595.2	99.953
475.4	99.819
357.7	99.658
233.6	99.511
148.9	99.386
46.7	99.228
18.8	99.180
3.8	99.142
0.8	99.124
0.0	99.086

Adsorbent : 5A MSC
 Adsorbate : Oxygen
 Adsorption Temp : 30°C
 Figure number : 7
 Notes : Activation

P (Torr)	q (mmol/g)
0.0	0.0000
13.2	0.0051
49.4	0.0253
106.9	0.0532
132.7	0.0653
187.4	0.0903
269.4	0.1274
365.8	0.1693
388.6	0.1792
476.0	0.2162
596.4	0.2662
636.0	0.2863
663.1	0.2966
706.2	0.3212

Adsorbent : 5A MSC
 Adsorbate : Oxygen
 Adsorption Temp : 30°C
 Figure number : 7
 Notes : No activation

P (Torr)	q (mmol/g)
0.0	0.0000
12.2	0.0037
49.8	0.0231
87.7	0.0422
214.6	0.1068
361.0	0.1674
510.3	0.2294
539.8	0.2419
666.3	0.2944

Adsorbent : 5A MSC
 Adsorbate : Oxygen
 Adsorption Temp : 30°C
 Figure number : 8
 Notes : 49-107 Torr

Time (sec)	Mt/M _∞
2	0.1139
10	0.5125
18	0.7900
28	0.9039
40	0.9359
50	0.9466
60	0.9537
70	0.9573
80	0.9609

Adsorbent : 5A MSC
 Adsorbate : Oxygen
 Adsorption Temp : 30°C
 Figure number : 8
 Notes : 510-540 Torr

Time (sec)	Mt/M _∞
4	0.4286
10	0.5714
20	0.6349
30	0.6825
40	0.7381
50	0.7698
60	0.7937
80	0.8492
120	0.9048
140	0.9206

Adsorbent : 5A MSC
 Adsorbate : Oxygen
 Adsorption Temp : 30°C
 Figure number : 8
 Notes : 13-49 Torr

Time (sec)	Mt/M _∞
6	0.3191
10	0.3838
20	0.4894
30	0.6117
40	0.7021
50	0.7766
60	0.8245
80	0.8883
100	0.9255
120	0.9415

Adsorbent : 5A MSC
 Adsorbate : Oxygen
 Adsorption Temp : 30°C
 Figure number : 8
 Notes : 366-389 Torr

Time (sec)	Mt/M _∞
6	0.5833
10	0.7500
16	0.8438
20	0.8750
30	0.9167
40	0.9375
60	0.9479

Adsorbent : 5A MSC
 Adsorbate : Oxygen
 Adsorption Temp : 30°C
 Figure number : 8
 Notes : 636-663 Torr

Time (sec)	Mt/M _∞
4	0.3725
10	0.8235
20	0.8824
30	0.9118
40	0.9314
50	0.9412
60	0.9608
80	0.9804

Adsorbent : 5A MSC
 Adsorbate : Oxygen
 Adsorption Temp : 30°C
 Figure number : 9
 Notes : 915-1018

Time (sec)	Mt/M _∞
2.0	0.0862
4.0	0.1385
8.0	0.2864
16.0	0.4953
30.0	0.6693
60.0	0.7389
120.0	0.7737
240.0	0.8260
480.0	0.9217
880.0	0.9800

Adsorbent : 5A MSC
 Adsorbate : Oxygen
 Adsorption Temp : 30°C
 Figure number : 9
 Notes : 2569-2673 Torr

Time (sec)	Mt/M _∞
2.0	0.1328
4.0	0.1756
8.0	0.2506
16.0	0.4219
30.0	0.6574
60.0	0.8109
100.0	0.9072
140.0	0.9643
170.0	0.9929

Adsorbent : 5A MSC
 Adsorbate : Oxygen
 Adsorption Temp : 30°C
 Figure number : 10
 Notes : 1st run at
 high-pressure

P (Torr)	q (mmol/g)
812	0.3308
915	0.3685
1081	0.4430
1380	0.5442
1794	0.6484
2311	0.7844
2828	0.9028
3345	0.9979
3862	1.0929

Adsorbent : 5A MSC
 Adsorbate : Oxygen
 Adsorption Temp : 30°C
 Figure number : 9
 Notes : 1432-1535 Torr

Time (sec)	Mt/M _∞
4.0	0.0008
8.0	0.1266
16.0	0.3648
30.0	0.5765
60.0	0.6625
120.0	0.7287
240.0	0.8147
480.0	0.9074
680.0	0.9868

Adsorbent : 5A MSC
 Adsorbate : Oxygen
 Adsorption Temp : 30°C
 Figure number : 9
 Notes : 3215-3345 Torr

Time (sec)	Mt/M _∞
2.0	0.2454
4.0	0.2779
8.0	0.3223
16.0	0.4318
30.0	0.5916
60.0	0.7810
100.0	0.8994
140.0	0.9349
180.0	0.9763
190.0	0.9941

Adsorbent : 5A MSC
 Adsorbate : Oxygen
 Adsorption Temp : 30°C
 Figure number : 10
 Notes : 2nd run at
 high pressure

P (Torr)	q (mmol/g)
812	0.3483
915	0.3860
1019	0.4296
1432	0.5630
1536	0.5949
2053	0.7426
2570	0.8552
2673	0.8812
3216	1.0003
3345	1.0153
3862	1.0986

Adsorbent : 5A MSC
 Adsorbate : Oxygen
 Adsorption Temp : 30°C
 Figure number : 10
 Notes : 3rd run at
 low-pressure

P (Torr)	q (mmol/g)
13	0.0055
49	0.0255
107	0.0534
133	0.0654
187	0.0903
269	0.1272
366	0.1693
389	0.1791
476	0.2162
596	0.2662
636	0.2863

Adsorbent : 3A MSC
 Adsorbate : Oxygen
 Adsorption Temp : 30°C
 Figure number : 11
 Notes : 1st run
 experimental data

P (Torr)	q (mmol/g)
812	0.3856
915	0.4301
1019	0.4579
1432	0.5859
1536	0.6137
2053	0.7610
2518	0.8483
3087	0.9676
3190	0.9828
3862	1.0964

Adsorbent : 5A MSC
 Adsorbate : Oxygen
 Adsorption Temp : 30°C
 Figure number : 10
 Notes : 4th run at
 low-pressure

P (Torr)	q (mmol/g)
12	0.0040
50	0.0233
88	0.0422
215	0.1067
361	0.1672
510	0.2293
540	0.2418
666	0.2942

Adsorbent : 3A MSC
 Adsorbate : Oxygen
 Adsorption Temp : 30°C
 Figure number : 11
 Notes : 2nd run
 experimental data

P (Torr)	q (mmol/g)
17	0.0798
25	0.0842
66	0.0936
130	0.1202
186	0.1467
252	0.1818
332	0.2089
432	0.2448
577	0.3070
756	0.3867
967	0.4714
1197	0.5274
1424	0.5958
1797	0.6971
2213	0.7954
2575	0.8714
2893	0.9337
3220	0.9921
3536	1.0503
3973	1.1031
4513	1.1836
5046	1.2473
5590	1.3112
6164	1.3750
6591	1.4200

Adsorbent : 5A MSC
 Adsorbate : Oxygen
 Adsorption Temp : 0°C
 Figure number : 12
 Notes : 1st run

P (Torr)	q (mmol/g)
16	0.0889
110	0.1820
184	0.2679
275	0.3587
378	0.4410
495	0.5125
698	0.6415
1066	0.8389
1455	1.0103
1892	1.1297
2509	1.3224
3019	1.4592
3598	1.6000
4180	1.7143

Adsorbent : 5A MSC
 Adsorbate : Oxygen
 Adsorption Temp : 30°C
 Figure number : 12
 Notes : 1st run

P (Torr)	q (mmol/g)
812	0.2934
915	0.3316
1070	0.3711
1277	0.4653
1525	0.5250
1949	0.6662
2352	0.7654
2818	0.8662
3345	0.9982
3862	1.1062

Adsorbent : 5A MSC
 Adsorbate : Oxygen
 Adsorption Temp : 0°C
 Figure number : 12
 Notes : 2nd run

P (Torr)	q (mmol/g)
17	0.0823
72	0.1390
142	0.2094
225	0.2823
340	0.3781
503	0.4884
602	0.5573
737	0.6316
862	0.6989
1147	0.8433
1294	0.9134
1621	1.0677
2065	1.1918
2485	1.3241
2638	1.3679
3105	1.4992
3706	1.6383
4230	1.7445

Adsorbent : 5A MSC
 Adsorbate : Oxygen
 Adsorption Temp : 30°C
 Figure number : 12
 Notes : 2nd run

P (Torr)	q (mmol/g)
812	0.3308
915	0.3685
1081	0.4430
1380	0.5442
1794	0.6484
2311	0.7844
2828	0.9028
3345	0.9979
3862	1.0929

Adsorbent : 5A MSC
 Adsorbate : Oxygen
 Adsorption Temp : 30°C
 Figure number : 12
 Notes : 3st run

P (Torr)	q (mmol/g)
812	0.3483
915	0.3860
1019	0.4296
1432	0.5630
1536	0.5949
2053	0.7426
2570	0.8552
2673	0.8812
3216	1.0003
3345	1.0153
3862	1.0986

Adsorbent : 5A MSC
 Adsorbate : Oxygen
 Adsorption Temp : 30°C
 Figure number : 12
 Notes : 5th run

P (Torr)	q (mmol/g)
12	0.0040
50	0.0233
88	0.0422
215	0.1067
361	0.1672
510	0.2293
540	0.2418
666	0.2942

Adsorbent : 5A MSC
 Adsorbate : Oxygen
 Adsorption Temp : 50°C
 Figure number : 12
 Notes : 2nd run

P (Torr)	q (mmol/g)
22	0.0892
101	0.1156
203	0.1447
347	0.1838
617	0.2527
691	0.2701
920	0.2959
1157	0.3395
1392	0.4208
1754	0.5098
2335	0.6242
2615	0.6800
3201	0.7747
4165	0.9276

Adsorbent : 5A MSC
 Adsorbate : Oxygen
 Adsorption Temp : 30°C
 Figure number : 12
 Notes : 4nd run

P (Torr)	q (mmol/g)
13	0.0055
49	0.0255
107	0.0534
133	0.0654
187	0.0903
269	0.1272
366	0.1693
389	0.1791
476	0.2162
596	0.2662
636	0.2863

Adsorbent : 5A MSC
 Adsorbate : Oxygen
 Adsorption Temp : 50°C
 Figure number : 12
 Notes : 1st run

P (Torr)	q (mmol/g)
22	0.0757
71	0.0925
178	0.1284
387	0.1911
641	0.2617
977	0.3432
1358	0.4413
1670	0.5090
2040	0.5957
2505	0.6982
2991	0.7857
3545	0.8749
4173	0.9749

Adsorbent : 3A MSC
 Adsorbate : Oxygen
 Adsorption Temp : 0°C
 Figure number : 13
 Notes :

P (Torr)	q (mmol/g)
13	0.0913
42	0.2058
123	0.3963
268	0.4455
466	0.5675
680	0.7224
870	0.8929
1143	1.0201
1513	1.1659
2017	1.2892
2786	1.4711
3484	1.6026
4504	1.8266

Adsorbent : 3A MSC
 Adsorbate : Oxygen
 Adsorption Temp : 30°C
 Figure number : 13
 Notes :

P (Torr)	q (mmol/g)
812	0.3856
915	0.4301
1019	0.4579
1432	0.5859
1536	0.6137
2053	0.7610
2518	0.8483
3087	0.9676
3190	0.9828
3862	1.0964

Adsorbent : 3A MSC
 Adsorbate : Oxygen
 Adsorption Temp : 0°C
 Figure number : 13
 Notes :

P (Torr)	q (mmol/g)
5	0.0684
45	0.1084
122	0.3444
226	0.4413
365	0.5781
563	0.7781
767	0.8743
1025	1.0076
1368	1.1626
1732	1.2693
2296	1.4494
2956	1.6579
3737	1.7785
4653	1.9025

Adsorbent : 3A MSC
 Adsorbate : Oxygen
 Adsorption Temp : 30°C
 Figure number : 13
 Notes :

P (Torr)	q (mmol/g)
17	0.0798
25	0.0842
66	0.0936
130	0.1202
186	0.1467
252	0.1818
332	0.2089
432	0.2448
577	0.3070
756	0.3867
967	0.4714
1197	0.5274
1424	0.5958
1797	0.6971
2213	0.7954
2575	0.8714
2893	0.9337
3220	0.9921
3536	1.0503
3973	1.1031
4513	1.1836
5046	1.2473
5590	1.3112

Adsorbent : 3A MSC
 Adsorbate : Oxygen
 Adsorption Temp : 50°C
 Figure number : 13
 Notes : 1st run

P (Torr)	q (mmol/g)
5	0.1631
14	0.1675
46	0.1725
110	0.1825
162	0.1922
283	0.2245
435	0.2534
630	0.2960
857	0.3602
1140	0.4384
1450	0.4923
1840	0.5815
2378	0.6871
2875	0.7749
3400	0.8426
4240	0.9349
4790	1.0157

Adsorbent : 5A MSC
 Adsorbate : Methane
 Adsorption Temp : 30°C
 Figure number : 14
 Notes : No activation

P (torr)	q (mmol/g)
0.0	0.0000
7.2	0.0200
21.2	0.0741
49.1	0.1548
100.0	0.2809
165.2	0.4108
252.4	0.5524
354.4	0.6881
488.2	0.8553
656.4	1.0175
692.5	1.0498

Adsorbent : 3A MSC
 Adsorbate : Oxygen
 Adsorption Temp : 50°C
 Figure number : 13
 Notes : 2nd run

P (Torr)	q (mmol/g)
10	0.0781
79	0.0961
237	0.1617
389	0.2077
695	0.2868
995	0.3495
1510	0.4793
2033	0.5866
2739	0.7213
4165	0.9390

Adsorbent : 5A MSC
 Adsorbate : Methane
 Adsorption Temp : 30°C
 Figure number : 14
 Notes : Activation

P (torr)	q (mmol/g)
12.8	0.0407
79.6	0.2258
151.7	0.3648
284.5	0.5868
304.7	0.6233
398.2	0.7475
532.8	0.9005
563.9	0.9350
672.5	1.0255

Adsorbent : 5A MSC
 Adsorbate : Methane
 Adsorption Temp : 30°C
 Figure number : 14
 Notes : Desorption data

P (torr)	q (mmol/g)
604.4	0.9815
426.0	0.8143
294.0	0.6301
148.0	0.3991
17.3	0.0924

Adsorbent : 3A MSC
 Adsorbate : Methane
 Adsorption Temp : 30°C
 Figure number : 15
 Notes : 1st run

P (Torr)	q (mmol/g)
812	1.4083
915	1.4783
1070	1.5663
1380	1.7592
1794	1.9547
2311	2.0856
2828	2.1660
3345	2.2716

Adsorbent : 3A MSC
 Adsorbate : Methane
 Adsorption Temp : 30°C
 Figure number : 15
 Notes : Desorption data

P (Torr)	q (mmol/g)
0	0.4361
1	0.5337
16	0.5797
108	0.7902
172	0.9351
275	0.9897
473	1.0729
747	1.2165
1077	1.4592
1393	1.6169
1916	1.9555
2431	2.1313
2929	2.3066
3473	2.3985
4008	2.5357

Adsorbent : 3A MSC
 Adsorbate : Methane
 Adsorption Temp : 30°C
 Figure number : 15
 Notes : 2nd run

P (Torr)	q (mmol/g)
18	0.2340
28	0.2510
82	0.3191
123	0.3618
161	0.5964
220	0.6646
280	0.7329
360	0.9268
430	1.0370
525	1.1812
634	1.3258
745	1.4371
877	1.5655
985	1.6934
1250	1.8086
1675	1.9111
1930	2.0010
2493	2.0820

Adsorbent : 5A MSC
 Adsorbate : Methane
 Adsorption Temp : 30°C
 Figure number : 16
 Notes : 1st run at
 high-pressure

P (Torr)	q (mmol/g)
812	0.9480
915	1.0183
1070	1.1587
1381	1.2640
1794	1.4630
2311	1.6269
2829	1.7439
3346	1.8844
3863	1.9546

Adsorbent : 5A MSC
 Adsorbate : Methane
 Adsorption Temp : 30°C
 Figure number : 16
 Notes : 3rd run at
 low-pressure

P (Torr)	q (mmol/g)
7	0.0198
21	0.0741
49	0.1548
100	0.2809
165	0.4108
252	0.5524
354	0.6881
488	0.8553

Adsorbent : 3A MSC
 Adsorbate : Methane
 Adsorption Temp : 30°C
 Figure number : 17
 Notes : 1st run at
 high-pressure

P (Torr)	q (mmol/g)
812	1.044
915	1.097
1019	1.142
1432	1.379
1536	1.407
1949	1.526
2285	1.635
2828	1.884
3190	1.919
3862	2.011

Adsorbent : 5A MSC
 Adsorbate : Methane
 Adsorption Temp : 30°C
 Figure number : 16
 Notes : 2nd run at
 high-pressure

P (Torr)	q (mmol/g)
812	0.9680
915	1.0410
1070	1.1850
1380	1.2990
1749	1.5080
2311	1.6850
2828	1.8150
3345	1.9690
3862	2.0520

Adsorbent : 5A MSC
 Adsorbate : Methane
 Adsorption Temp : 30°C
 Figure number : 16
 Notes : 4th run at
 low-pressure

P (Torr)	q (mmol/g)
13	0.0407
80	0.2258
152	0.3648
285	0.5868
305	0.6233
398	0.7475
533	0.9005

Adsorbent : 3A MSC
 Adsorbate : Methane
 Adsorption Temp : 30°C
 Figure number : 17
 Notes : 2nd run at
 high pressure

P (Torr)	q (mmol/g)
822	1.249
915	1.294
1019	1.347
1380	1.549
1701	1.616
2311	1.792
2828	1.923
3345	2.003
3862	2.084

Adsorbent : 3A MSC
 Adsorbate : Methane
 Adsorption Temp : 30°C
 Figure number : 17
 Notes : 3rd run at
 low-pressure

P (Torr)	q (mmol/g)
44	0.410
530	0.774
590	0.808
690	0.869
876	1.000

Adsorbent : 5A MSC
 Adsorbate : Methane
 Adsorption Temp : 0°C
 Figure number : 18
 Notes :

P (Torr)	q (mmol/g)
14	0.2128
52	0.4262
93	0.5954
150	0.7739
205	0.9080
272	1.0381
359	1.1908
459	1.3305
586	1.5063
715	1.6645
920	1.8954
1153	2.0916
1614	2.2892
2323	2.5196
3145	2.7175

Adsorbent : 3A MSC
 Adsorbate : Methane
 Adsorption Temp : 30°C
 Figure number : 17
 Notes : 4th run at
 low-pressure

P (Torr)	q (mmol/g)
10	0.342
25	0.384
90	0.453
130	0.454
210	0.464
320	0.542
471	0.621
648	0.792

Adsorbent : 5A MSC
 Adsorbate : Methane
 Adsorption Temp : 30°C
 Figure number : 18
 Notes : 1st run at
 low pressure

P (Torr)	q (mmol/g)
13	0.0407
80	0.2258
152	0.3648
285	0.5868
305	0.6233
398	0.7475
533	0.9005
564	0.9350
673	1.0255

Adsorbent : 5A MSC
 Adsorbate : Methane
 Adsorption Temp : 30°C
 Figure number : 18
 Notes : 3rd run at
 high pressure

P (Torr)	q (mmol/g)
812	0.9680
915	1.0410
1070	1.1850
1380	1.2990
1749	1.5080
2311	1.6850
2828	1.8150
3345	1.9690
3862	2.0520

Adsorbent : 5A MSC
 Adsorbate : Methane
 Adsorption Temp : 30°C
 Figure number : 18
 Notes : 2nd run at
 high pressure

P (Torr)	q (mmol/g)
7	0.0198
21	0.0741
49	0.1548
100	0.2809
165	0.4108
252	0.5524
354	0.6881
488	0.8553
656	1.0175
693	1.0498
812	0.9480
915	1.0183
1070	1.1587
1381	1.2640
2829	1.7439
3346	1.8844
3863	1.9546

Adsorbent : 3A MSC
 Adsorbate : Methane
 Adsorption Temp : 0°C
 Figure number : 19
 Notes : 1st run

P (Torr)	q (mmol/g)
8	0.2330
47	0.3051
108	0.4683
229	0.6589
375	0.8048
628	0.9599
917	1.1160
1216	1.3370
1428	1.5234
1753	1.8290
2086	2.0056
2505	2.1520
2963	2.2283
3603	2.4385
4122	2.5680

Adsorbent : 5A MSC
 Adsorbate : Methane
 Adsorption Temp : 50°C
 Figure number : 18
 Notes :

P (Torr)	q (mmol/g)
13	0.1422
76	0.2191
159	0.3187
275	0.4324
454	0.5832
651	0.7212
908	0.8740
1571	1.1655
2262	1.4268
3223	1.6817

Adsorbent : 3A MSC
 Adsorbate : Methane
 Adsorption Temp : 0°C
 Figure number : 19
 Notes : 2nd run

P (Torr)	q (mmol/g)
4	0.1039
87	0.3006
167	0.4583
308	0.6434
643	0.8919
1204	1.5612
2133	1.9740
3146	2.2850
3938	2.4997

Adsorbent : 3A MSC
 Adsorbate : Methane
 Adsorption Temp : 30°C
 Figure number : 19
 Notes : 1st run

P (Torr)	q (mmol/g)
812	1.4083
915	1.4783
1070	1.5663
1380	1.7592
1794	1.9547
2311	2.0856
2828	2.1660
3345	2.2716

Adsorbent : 3A MSC
 Adsorbate : Methane
 Adsorption Temp : 50°C
 Figure number : 19
 Notes : 1st run

P (Torr)	q (mmol/g)
10	0.3670
25	0.3840
90	0.4020
130	0.4040
210	0.4640
320	0.5420
471	0.6210
648	0.7920
845	0.9310
1070	1.0950
1315	1.2190
1481	1.2480
1710	1.2870
2040	1.3790
3270	1.5770

Adsorbent : 3A MSC
 Adsorbate : Methane
 Adsorption Temp : 30°C
 Figure number : 19
 Notes : 2nd run

P (Torr)	q (mmol/g)
18	0.2340
28	0.2510
82	0.3191
123	0.3618
161	0.5964
220	0.6646
280	0.7329
360	0.9268
430	1.0370
525	1.1812
634	1.3258
745	1.4371
877	1.5655
985	1.6934
1250	1.8086
1675	1.9111
1930	2.0010
2493	2.0820

Adsorbent : 3A MSC
 Adsorbate : Methane
 Adsorption Temp : 50°C
 Figure number : 19
 Notes : 2nd run

P (Torr)	q (mmol/g)
44	0.4106
530	0.7740
590	0.8090
690	0.8700
867	0.9998
1045	1.0879
1340	1.1957
1610	1.2778
2470	1.5336

Adsorbent : 5A MSC
 Adsorbate : Nitrogen
 Adsorption Temp : 0°C
 Figure number : 21
 Notes : 1st run

P (Torr)	q (mmol/g)
23	0.1424
79	0.2122
143	0.2797
230	0.3629
357	0.4649
508	0.5726
665	0.6703
924	0.7933
1162	0.8880
1445	0.9914
1791	1.0989
2204	1.2133
2624	1.3201
3125	1.4190
3631	1.5179
4232	1.6268

Adsorbent : 5A MSC
 Adsorbate : Nitrogen
 Adsorption Temp : 30°C
 Figure number : 21
 Notes :

P (Torr)	q (mmol/g)
23	0.0916
108	0.1317
227	0.1853
418	0.2584
693	0.3589
1007	0.4554
1337	0.5522
1696	0.6549
2129	0.7847
2483	0.8619
2995	0.9862
3543	1.1164
4112	1.1814
4526	1.2399
5330	1.3387
6100	1.3936

Adsorbent : 5A MSC
 Adsorbate : Nitrogen
 Adsorption Temp : 0°C
 Figure number : 21
 Notes : 2nd run

P (Torr)	q (mmol/g)
11	0.1422
110	0.2587
193	0.3368
314	0.4438
480	0.5570
629	0.6520
810	0.7402
1097	0.8742
1384	0.9727
1740	1.0932
2142	1.1845
2453	1.2886
3006	1.4167
3475	1.5021
4087	1.6063
4724	1.6908
5617	1.7870

Adsorbent : 5A MSC
 Adsorbate : Nitrogen
 Adsorption Temp : 50°C
 Figure number : 21
 Notes : 1st run

P (Torr)	q (mmol/g)
750	0.4233
1034	0.4985
1427	0.5501
1858	0.6290
2288	0.6852
2762	0.7577
3493	0.8594
4181	0.9486
5623	1.1287

Adsorbent : 5A MSC
 Adsorbate : Nitrogen
 Adsorption Temp : 50°C
 Figure number : 21
 Notes : 2nd run

P (Torr)	q (mmol/g)
24	0.0790
71	0.1156
163	0.1634
337	0.2083
594	0.2932
1055	0.4137
1438	0.4790
2061	0.6187
2791	0.7434
3972	0.9099
5915	1.1337

Adsorbent : 3A MSC
 Adsorbate : Nitrogen
 Adsorption Temp : 0°C
 Figure number : 22
 Notes : 2nd run

P (Torr)	q (mmol/g)
16	0.1376
64	0.1982
120	0.2701
243	0.3956
406	0.5184
632	0.6651
919	0.8096
1355	0.9802
2087	1.1545
3113	1.3400
4595	1.5000
6826	1.6641

Adsorbent : 3A MSC
 Adsorbate : Nitrogen
 Adsorption Temp : 30°C
 Figure number : 22
 Notes : 1st run

P (Torr)	q (mmol/g)
812	0.3975
915	0.4871
1019	0.4994
1432	0.6259
1536	0.6382
1872	0.6950

Adsorbent : 3A MSC
 Adsorbate : Nitrogen
 Adsorption Temp : 0°C
 Figure number : 22
 Notes : 1st run

P (Torr)	q (mmol/g)
10	0.1042
73	0.1800
153	0.2748
305	0.4308
485	0.5727
667	0.6663
907	0.7689
1334	0.8873
1823	1.0185
2438	1.1565
3039	1.2423
4025	1.3638
5392	1.5060
7021	1.6661

Adsorbent : 3A MSC
 Adsorbate : Nitrogen
 Adsorption Temp : 30°C
 Figure number : 22
 Notes : 2nd run

P (Torr)	q (mmol/g)
290	0.3364
580	0.4487
1000	0.5786
1700	0.7538
2500	0.9076
3500	1.0665
4500	1.1729
5470	1.2834
6490	1.3569
7580	1.4275

Adsorbent : 3A MSC
 Adsorbate : Nitrogen
 Adsorption Temp : 50°C
 Figure number : 22
 Notes :

P (Torr)	q (mmol/g)
85	0.1674
200	0.2110
425	0.2776
735	0.3492
1065	0.4417
1545	0.5611
1990	0.6652
2450	0.7378
2910	0.8335
3440	0.9079
3895	0.9716
5000	1.0779
5630	1.1287
6030	1.1794

Adsorbent : 5A MSC
 Adsorbate : Argon
 Adsorption Temp : 0°C
 Figure number : 23
 Notes : 1st run

P (Torr)	q (mmol/g)
142	0.1754
225	0.2465
321	0.3233
456	0.4206
553	0.4850
684	0.5627
810	0.6385
970	0.7170
1168	0.8052
1342	0.8858
1496	0.9410
1637	0.9960
2071	1.1398
2514	1.2714
2994	1.4022
3506	1.5126
4004	1.6014
5005	1.7631
5935	1.8858
7145	2.0015

Adsorbent : 3A MSC
 Adsorbate : Nitrogen
 Adsorption Temp : 50°C
 Figure number : 22
 Notes :

P (Torr)	q (mmol/g)
139	0.2264
252	0.2590
406	0.3037
614	0.3647
942	0.4362
1456	0.5495
2215	0.6987
2881	0.8011
3854	0.9557
4981	1.0437

Adsorbent : 5A MSC
 Adsorbate : Argon
 Adsorption Temp : 0°C
 Figure number : 23
 Notes : 2nd run

P (Torr)	q (mmol/g)
145	0.1913
233	0.2626
360	0.3667
459	0.4400
560	0.5063
775	0.6285
1210	0.8378
1714	1.0347
2586	1.3081
3661	1.5619
4857	1.7533
6012	1.9118
7198	2.0286

Adsorbent : 5A MSC
 Adsorbate : Argon
 Adsorption Temp : 30°C
 Figure number : 23
 Notes : 1st run

P (Torr)	q (mmol/g)
13	0.1191
36	0.1381
103	0.1847
174	0.2102
312	0.2691
530	0.3591
810	0.4401
1167	0.5890
1273	0.6286
2016	0.8189
2147	0.8539
2885	0.9254
3200	0.9809
4150	1.0894
4397	1.1326
5736	1.2879
6957	1.4218

Adsorbent : 5A MSC
 Adsorbate : Argon
 Adsorption Temp : 50°C
 Figure number : 23
 Notes :

P (Torr)	q (mmol/g)
980	0.3194
1533	0.4488
2035	0.5308
2545	0.6218
3178	0.7319
3633	0.8038
4167	0.8918
5145	1.0213
6100	1.1165
7420	1.2636
8147	1.3264
9520	1.4339

Adsorbent : 5A MSC
 Adsorbate : Argon
 Adsorption Temp : 30°C
 Figure number : 23
 Notes : 2nd run

P (Torr)	q (mmol/g)
22	0.0928
77	0.1172
175	0.1676
315	0.2350
530	0.3184
782	0.4100
1010	0.5079
1530	0.6382
2025	0.7624
2505	0.8757
3157	1.0057
3570	1.0765

Adsorbent : 5A MSC
 Adsorbate : Argon
 Adsorption Temp : 50°C
 Figure number : 23
 Notes :

P (Torr)	q (mmol/g)
31	0.0309
105	0.0505
236	0.0892
407	0.1325
610	0.1855
895	0.2583
1225	0.3357
1689	0.4467
2168	0.5403
3045	0.6901
4296	0.8794
5260	1.0066
6429	1.1319
7973	1.2720
9974	1.4804

Adsorbent : 3A MSC
 Adsorbate : Argon
 Adsorption Temp : 0°C
 Figure number : 24
 Notes : 1st run

P (Torr)	q (mmol/g)
227	0.2936
368	0.3750
614	0.5498
877	0.6861
1288	0.8392
1656	0.9886
2111	1.1738
2762	1.2967
3537	1.4227
6167	1.7824

Adsorbent : 3A MSC
 Adsorbate : Argon
 Adsorption Temp : 30°C
 Figure number : 24
 Notes :

P (Torr)	q (mmol/g)
50	0.2390
100	0.2600
200	0.3100
350	0.3670
550	0.4460
800	0.5330
1150	0.6250
1800	0.7890
2240	0.8740
3040	1.0150
4300	1.1980
5980	1.3610
8030	1.5110
9960	1.6470

Adsorbent : 3A MSC
 Adsorbate : Argon
 Adsorption Temp : 0°C
 Figure number : 24
 Notes : 2nd run

P (Torr)	q (mmol/g)
40	0.1463
146	0.2553
365	0.4139
616	0.5318
867	0.6523
1196	0.7903
1512	0.9203
2029	1.1097
2292	1.1761
2737	1.2963
3269	1.3902
3717	1.5053
4312	1.5878
4969	1.6693
5647	1.7669
6322	1.8307

Adsorbent : 3A MSC
 Adsorbate : Argon
 Adsorption Temp : 30°C
 Figure number : 24
 Notes :

P (Torr)	q (mmol/g)
400	0.3388
770	0.4555
1210	0.5774
1870	0.7383
2980	0.9945
4290	1.1619
5750	1.3599
8180	1.5590
9980	1.6147

Adsorbent : 3A MSC
 Adsorbate : Argon
 Adsorption Temp : 50°C
 Figure number : 24
 Notes :

P (Torr)	q (mmol/g)
58	0.1352
90	0.1786
170	0.1988
290	0.2302
500	0.2822
820	0.3673
1155	0.4305
1560	0.5157
1985	0.5772
2420	0.6490
2780	0.7169
3060	0.7625
3520	0.8288
3950	0.8721
4560	0.9606
4980	0.9975
6010	1.0622

Adsorbent : 5A MSC
 Adsorbate : Oxygen
 Adsorption Temp : 30°C
 Figure number : 25
 Notes : 1st run

P (torr)	q (mmol/g)
0.0	0.0000
13.2	0.0051
49.4	0.0253
106.9	0.0532
132.7	0.0653
187.4	0.0903
269.4	0.1274
365.8	0.1693
388.6	0.1792
476.0	0.2162
636.0	0.2863
706.2	0.3212

Adsorbent : 3A MSC
 Adsorbate : Argon
 Adsorption Temp : 50°C
 Figure number : 24
 Notes :

P (Torr)	q (mmol/g)
9	0.0496
79	0.1085
240	0.1593
535	0.2395
858	0.3178
1461	0.4525
2130	0.5915
2935	0.7054
4776	0.9234
6710	1.1308

Adsorbent : 5A MSC
 Adsorbate : Oxygen
 Adsorption Temp : 30°C
 Figure number : 25
 Notes : 2nd run

P (torr)	q (mmol/g)
0.0	0.0000
12.2	0.0037
49.8	0.0231
87.7	0.0422
214.6	0.1068
361.0	0.1674
510.3	0.2294
539.8	0.2419
666.3	0.2944
596.4	0.2662
663.1	0.2966

Adsorbent : 5A MSC
 Adsorbate : Nitrogen
 Adsorption Temp : 30°C
 Figure number : 25
 Notes : 1st. run

P (torr)	q (mmol/g)
0.2	0.0940
1.8	1.4410
3.9	3.1260
8.1	5.9930
12.6	8.6210

Adsorbent : 3A MSC
 Adsorbate : Methane
 Adsorption Temp : 30°C
 Figure number : 26
 Notes :

P (Torr)	q (mmol/g)
812	1.4083
915	1.4783
1070	1.5663
1380	1.7592
1794	1.9547
2311	2.0856
2828	2.1660
3345	2.2716

Adsorbent : 5A MSC
 Adsorbate : Methane
 Adsorption Temp : 30°C
 Figure number : 26
 Notes :

P (Torr)	q (mmol/g)
812	0.9686
915	1.0415
1070	1.1858
1380	1.2990
1794	1.5085
2311	1.6855
2828	1.8156
3345	1.9692
3862	2.0525

Adsorbent : 5A MSC
 Adsorbate : Nitrogen
 Adsorption Temp : 30°C
 Figure number : 25
 Notes : 2nd. run

P (torr)	q (mmol/g)
23.4	0.0138
77.5	0.0448
172.8	0.0954
274.7	0.1466
299.3	0.1590
451.1	0.2268
610.1	0.2930

Adsorbent : 3A MSC
 Adsorbate : Methane
 Adsorption Temp : 30°C
 Figure number : 26
 Notes :

P (Torr)	q (mmol/g)
18	0.2340
28	0.2510
82	0.3191
123	0.3618
161	0.5964
220	0.6646
280	0.7329
360	0.9268
430	1.0370
525	1.1812
634	1.3258
745	1.4371
877	1.5655
985	1.6934
1250	1.8086
1675	1.9111
1930	2.0010
2493	2.0820

Adsorbent : B-F MSC
 Adsorbate : Methane
 Adsorption Temp : 30°C
 Figure number : 26
 Notes :

P (Torr)	q (mmol/g)
18	0.0184
273	0.4311
521	0.6007
732	0.7297
981	0.8734
1427	1.0781
2037	1.1609
3239	1.3341
4220	1.4262
5221	1.4815

Adsorbent : 3A MSC
 Adsorbate : Oxygen
 Adsorption Temp : 30°C
 Figure number : 27
 Notes : 1st run

P (Torr)	q (mmol/g)
812	0.3856
915	0.4301
1019	0.4579
1432	0.5859
1536	0.6137
2053	0.7610
2518	0.8483
3087	0.9676
3190	0.9828
3862	1.0964

Adsorbent : 5A MSC
 Adsorbate : Oxygen
 Adsorption Temp : 30°C
 Figure number : 27
 Notes : 1st run

P (Torr)	q (mmol/g)
812	0.2934
915	0.3316
1070	0.3711
1277	0.4653
1525	0.5250
1949	0.6662
2352	0.7654
2818	0.8662
3345	0.9982
3862	1.1062

Adsorbent : 5A MSC
 Adsorbate : Methane
 Adsorption Temp : 30°C
 Figure number : 26
 Notes :

P (Torr)	q (mmol/g)
25	0.1325
60	0.2520
125	0.2800
230	0.4871
305	0.5549
472	0.7041
712	0.8684
970	1.0398
1186	1.1705
1500	1.3037
1874	1.4582
1980	1.4939
2383	1.6557
2682	1.7358
2928	1.8014
3402	1.9123
3922	2.0441

Adsorbent : 3A MSC
 Adsorbate : Oxygen
 Adsorption Temp : 30°C
 Figure number : 27
 Notes : 2nd run

P (Torr)	q (mmol/g)
17	0.0798
25	0.0842
66	0.0936
130	0.1202
186	0.1467
252	0.1818
332	0.2089
432	0.2448
577	0.3070
756	0.3867
967	0.4714
1197	0.5274
1424	0.5958
1797	0.6971
2213	0.7954
2575	0.8714
2893	0.9337
3220	0.9921
3536	1.0503
3973	1.1031
4513	1.1836
5046	1.2473
5590	1.3112
6164	1.3750
6591	1.4200

Adsorbent : 5A MSC
 Adsorbate : Oxygen
 Adsorption Temp : 30°C
 Figure number : 27
 Notes : 2nd run

P (Torr)	q (mmol/g)
812	0.3308
915	0.3685
1081	0.4430
1380	0.5442
1794	0.6484
2311	0.7844
2828	0.9028
3345	0.9979
3862	1.0929

Adsorbent : 5A MSC
 Adsorbate : Oxygen
 Adsorption Temp : 30°C
 Figure number : 27
 Notes : 4nd run

P (Torr)	q (mmol/g)
13	0.0055
49	0.0255
107	0.0534
133	0.0654
187	0.0903
269	0.1272
366	0.1693
389	0.1791
476	0.2162
596	0.2662
636	0.2863

Adsorbent : 5A MSC
 Adsorbate : Oxygen
 Adsorption Temp : 30°C
 Figure number : 27
 Notes : 3nd run

P (Torr)	q (mmol/g)
812	0.3483
915	0.3860
1019	0.4296
1432	0.5630
1536	0.5949
2053	0.7426
2570	0.8552
2673	0.8812
3216	1.0003
3345	1.0153
3862	1.0986

Adsorbent : 5A MSC
 Adsorbate : Oxygen
 Adsorption Temp : 30°C
 Figure number : 27
 Notes : 5nd run

P (Torr)	q (mmol/g)
12	0.0040
50	0.0233
88	0.0422
215	0.1067
361	0.1672
510	0.2293
540	0.2418
666	0.2942

Adsorbent : B-F MSC
 Adsorbate : Oxygen
 Adsorption Temp : 30°C
 Figure number : 27
 Notes :

P (Torr)	q (mmol/g)
8	0.1100
72	0.1520
178	0.1890
344	0.2390
645	0.3220
1097	0.4360
1553	0.5800
2116	0.6850
2748	0.7510
3108	0.8220
3643	0.9060
4298	0.9880
4505	1.0160

Adsorbent : 3A MSC
 Adsorbate : Nitrogen
 Adsorption Temp : 30°C
 Figure number : 28
 Notes :

P (Torr)	q (mmol/g)
35	0.2203
130	0.2609
290	0.3364
580	0.4487
1000	0.5786
1700	0.7538
2500	0.9076
3500	1.0665
4500	1.1729
5470	1.2834
6490	1.3569
7580	1.4275
9870	1.5285

Adsorbent : B-F MSC
 Adsorbate : Nitrogen
 Adsorption Temp : 30°C
 Figure number : 28
 Notes :

P (Torr)	q (mmol/g)
8	0.1230
67	0.1500
181	0.1900
397	0.2440
721	0.2560
1160	0.3520
1951	0.5070
2717	0.6290
3558	0.7190
4243	0.8110
5113	0.8760
5492	0.8910
6892	0.9840
8419	1.0720
9468	1.1300

Adsorbent : 5A MSC
 Adsorbate : Nitrogen
 Adsorption Temp : 30°C
 Figure number : 28
 Notes :

P (Torr)	q (mmol/g)
23	0.0916
108	0.1317
227	0.1853
418	0.2584
693	0.3589
1007	0.4554
1337	0.5522
1696	0.6549
2129	0.7847
2483	0.8619
2995	0.9862
3543	1.1164
4112	1.1814
4526	1.2399
5330	1.3387
6100	1.3936

Adsorbent : 3A MSC
 Adsorbate : Argon
 Adsorption Temp : 30°C
 Figure number : 29
 Notes : 1st run

P (Torr)	q (mmol/g)
50	0.2390
100	0.2600
200	0.3100
350	0.3670
550	0.4460
800	0.5330
1150	0.6250
1800	0.7890
2240	0.8740
3040	1.0150
4300	1.1980
5980	1.3610
8030	1.5110
9960	1.6470

Adsorbent : 5A MSC
 Adsorbate : Argon
 Adsorption Temp : 30°C
 Figure number : 29
 Notes : 1st run

P (Torr)	q (mmol/g)
13	0.1191
36	0.1381
103	0.1847
174	0.2102
312	0.2691
530	0.3591
810	0.4401
1167	0.5890
1273	0.6286
2016	0.8189
2147	0.8539
2885	0.9254
3200	0.9809
4150	1.0894
4397	1.1326
5736	1.2879
6957	1.4218

Adsorbent : B-F MSC
 Adsorbate : Argon
 Adsorption Temp : 30°C
 Figure number : 29
 Notes :

P (Torr)	q (mmol/g)
18	0.0646
63	0.0818
135	0.0996
278	0.1614
515	0.2195
965	0.3251
1421	0.4550
1828	0.5334
2729	0.6966
3019	0.7300
4079	0.7970
4321	0.8211
4525	0.8484
6604	1.0213
6817	1.0428
8519	1.1561
9654	1.2309

Adsorbent : 3A MSC
 Adsorbate : Argon
 Adsorption Temp : 30°C
 Figure number : 29
 Notes : 2nd run

P (Torr)	q (mmol/g)
400	0.3388
770	0.4555
1210	0.5774
1870	0.7383
2980	0.9945
4290	1.1619
5750	1.3599
8180	1.5590
9980	1.6147

Adsorbent : 5A MSC
 Adsorbate : Argon
 Adsorption Temp : 30°C
 Figure number : 29
 Notes : 3rd run

P (Torr)	q (mmol/g)
22	0.0928
77	0.1172
175	0.1676
315	0.2350
530	0.3184
782	0.4100
1010	0.5079
1530	0.6382
2025	0.7624
2505	0.8757
3157	1.0057
3570	1.0765

Adsorbent : 3A MSC
 Adsorbate : Nitrogen
 Adsorption Temp : 0°C
 Figure number : 33
 Notes : 153 Torr

Time (sec)	Mt/M _∞
1	0.0004
2	0.0151
3	0.0230
4	0.0276
5	0.0351
6	0.0362
8	0.0399
10	0.0435
10	0.0450
14	0.0519
16	0.0619
18	0.0667
20	0.0772
25	0.0860
30	0.0926
35	0.1010
40	0.1108
45	0.1224
50	0.1332
60	0.1792
30	0.2186
100	0.2564
150	0.2920
200	0.3263
250	0.3552
300	0.3840
350	0.4120
400	0.4332
450	0.4597
550	0.5039
700	0.5446
850	0.5789
1000	0.6147
1150	0.6457
1300	0.6823
1450	0.7080
1600	0.7421
1800	0.7632
2000	0.7858
2200	0.8120
2400	0.8287
2600	0.8536
2800	0.8699
3000	0.8887

Adsorbent : 3A MSC
 Adsorbate : Argon
 Adsorption Temp : 0°C
 Figure number : 33
 Notes : 227 Torr

Time (sec)	Mt/M _∞
2	0.0593
4	0.0663
6	0.0671
10	0.1445
20	0.1607
30	0.1832
50	0.3190
100	0.4144
140	0.4600
160	0.4900
180	0.5200
200	0.5600
300	0.6000
400	0.6542
500	0.6900
600	0.7300
700	0.7600
800	0.8000
900	0.8300
1000	0.8500
1100	0.8700
1200	0.8900
1300	0.9200
1400	0.9400
1500	0.9500
1600	0.9600
1700	0.9700
1800	0.9780

Adsorbent : 3A MSC
 Adsorbate : Oxygen
 Adsorption Temp : 0°C
 Figure number : 33
 Notes : 680 Torr

Time (sec)	Mt/M _∞
2	0.0339
3	0.0486
4	0.1101
5	0.1629
6	0.2138
7	0.2463
8	0.2915
9	0.3304
10	0.3612
12	0.3934
14	0.4229
16	0.4714
18	0.5349
20	0.5831
25	0.6194
30	0.6579
35	0.6886
40	0.7089
45	0.7305
50	0.7604
70	0.7938
270	0.9672
370	0.9828
770	0.9982

Adsorbent : 3A MSC
 Adsorbate : Methane
 Adsorption Temp : 0°C
 Figure number : 33
 Notes : 510 Torr

Time (sec)	Mt/M _∞
2	0.0218
52	0.0453
152	0.1044
202	0.1549
352	0.1982
452	0.2298
552	0.2526
652	0.2737
852	0.3258
1052	0.3666
1152	0.3901
1352	0.4075
1452	0.4192
1552	0.4516
1652	0.4853
1852	0.5108
2352	0.5515
2852	0.5776

Adsorbent : 3A MSC
 Adsorbate : Argon
 Adsorption Temp : 30°C
 Figure number : 34
 Notes : 400 Torr

Time (sec)	Mt/M _∞	Time (sec)	Mt/M _∞
40	0.2998	400	0.8447
40	0.3877	440	0.8663
60	0.4319	480	0.8848
80	0.4689	520	0.9003
100	0.5059	560	0.9141
120	0.5383	600	0.9388
140	0.5718	680	0.9568
160	0.5985	760	0.9681
180	0.6278	840	0.9784
200	0.6751	920	0.9846
240	0.7188	1000	0.9913
280	0.7573	1080	0.9964
320	0.7887		
360	0.8170		

Adsorbent : 3A MSC
 Adsorbate : Nitrogen
 Adsorption Temp : 30°C
 Figure number : 34
 Notes : 650 Torr

Time (sec)	Mt/M _∞
24	0.0006
70	0.4575
80	0.4822
100	0.5019
120	0.5217
160	0.5759
200	0.6252
240	0.6548
280	0.6992
320	0.7337
360	0.7534
600	0.8767
840	0.9310

Adsorbent : 3A MSC
 Adsorbate : Oxygen
 Adsorption Temp : 30°C
 Figure number : 34
 Notes : 1540 Torr

Time (sec)	Mt/M _∞
15	0.0058
10	0.6012
20	0.8585
30	0.9061
40	0.9307
50	0.9465
60	0.9578
70	0.9654
80	0.9722
90	0.9794
100	0.9870
120	1.0000
140	1.0000
160	1.0000
180	1.0000
200	1.0000

Adsorbent : 3A MSC
 Adsorbate : Methane
 Adsorption Temp : 30°C
 Figure number : 34
 Notes : 815 Torr

Time (sec)	Mt/M _∞
5	0.0000
10	0.0117
20	0.0273
30	0.0468
40	0.0640
50	0.0824
60	0.0976
70	0.1259
80	0.1539
90	0.1790
100	0.2038
120	0.2100
140	0.2200
160	0.2300
180	0.2400
200	0.250
220	0.2600

Time (sec)	Mt/M _∞
240	0.2700
260	0.2800
280	0.2900
300	0.3000
350	0.3200
400	0.3400
450	0.3600
500	0.3800
600	0.4000
700	0.4200
800	0.4500
1000	0.4700
1200	0.5200
1400	0.5500
1600	0.5800
2000	0.6100

Adsorbent : 3A MSC
 Adsorbate : Nitrogen
 Adsorption Temp : 50°C
 Figure number : 35
 Notes : 200 Torr

Time (sec)	Mt/M _∞
2	0.0901
3	0.1636
5	0.1994
7	0.2209
10	0.2533
13	0.2762
17	0.2986
20	0.3301
23	0.3568
27	0.3778
30	0.4074
33	0.4365
37	0.4580
44	0.4857
51	0.5210
57	0.5243
64	0.5539
71	0.5935
77	0.6064
84	0.6355
91	0.6631
97	0.6903
104	0.7118
111	0.7180
127	0.7500
144	0.7800
161	0.8000
177	0.8250
194	0.8500
244	0.8800
261	0.9000
277	0.9200
311	0.9400
411	0.9600

Adsorbent : 3A MSC
 Adsorbate : Argon
 Adsorption Temp : 50°C
 Figure number : 35
 Notes : 1461 Torr

Time (sec)	Mt/M _∞
2	0.0899
4	0.1072
6	0.1339
8	0.1611
13	0.2161
18	0.2566
23	0.2859
28	0.3137
33	0.3502
43	0.4124
53	0.4636
63	0.5000
73	0.5373
83	0.5680
93	0.5959
103	0.6196
113	0.6390
123	0.6605
133	0.6723
183	0.7436
233	0.7987
283	0.8473
333	0.8897
383	0.9210
433	0.9442
483	0.9631
533	0.9772
583	0.9902
633	0.9981
733	1.0000

Adsorbent : 3A MSC
 Adsorbate : Oxygen
 Adsorption Temp : 50°C
 Figure number : 35
 Notes : 725 Torr

Time (sec)	Mt/M _∞
1	0.1783
2	0.3545
3	0.4817
4	0.5939
5	0.6822
7	0.7592
10	0.8561
14	0.9388
18	0.9666
22	0.9736
26	0.9869
35	0.9901
50	0.9957
70	0.9983
90	1.0000
120	1.0000
150	1.0000
200	1.0000

Adsorbent : 3A MSC
 Adsorbate : Methane
 Adsorption Temp : 50°C
 Figure number : 35
 Notes : 962 Torr

Time (sec)	Mt/M _∞
10	0.0441
20	0.1360
30	0.2278
40	0.2577
50	0.2638
60	0.2756
70	0.2883
80	0.2997
130	0.3510
200	0.4031
230	0.4249
260	0.4485
290	0.4789
350	0.5133
400	0.5460
500	0.5772
600	0.6013
700	0.6305
800	0.6530
900	0.6747
1000	0.6960
1200	0.7174
1400	0.7509
1600	0.7821
1800	0.8109
2000	0.8378
2200	0.8658
2400	0.8895
2600	0.9053
2800	0.9218

Adsorbent : 3A MSC
 Adsorbate : Argon
 Adsorption Temp : 0°C
 Figure number : 36
 Notes : 227 Torr

Time (sec)	Mt/M _∞
2	0.0593
4	0.0663
6	0.0671
10	0.1445
20	0.1607
30	0.1832
50	0.3190
100	0.4144
140	0.4600
160	0.4900
180	0.5200
200	0.5600
300	0.6000
400	0.6542
500	0.6900
600	0.7300
700	0.7600
800	0.8000
900	0.8300
1000	0.8500
1100	0.8700
1200	0.8900
1300	0.9200
1400	0.9400
1500	0.9500
1600	0.9600
1700	0.9700
1800	0.9780

Adsorbent : 3A MSC
 Adsorbate : Argon
 Adsorption Temp : 50°C
 Figure number : 36
 Notes : 1461 Torr

Time (sec)	Mt/M _∞
2	0.0899
4	0.1072
6	0.1339
8	0.1611
13	0.2161
18	0.2566
23	0.2859
28	0.3137
33	0.3502
43	0.4124
53	0.4636
63	0.5000
73	0.5373
83	0.5680
93	0.5959
103	0.6196
113	0.6390
123	0.6605
133	0.6723
183	0.7436
233	0.7987
283	0.8473
333	0.8897
383	0.9210
433	0.9442
483	0.9631
533	0.9772
583	0.9902
633	0.9981
733	1.0000

Adsorbent : 3A MSC
 Adsorbate : Argon
 Adsorption Temp : 30°C
 Figure number : 36
 Notes : 350 Torr

Time (sec)	Mt/M _∞	Time (sec)	Mt/M _∞
16	0.0004	140	0.6073
30	0.2988	160	0.6413
40	0.3343	200	0.7048
50	0.3652	240	0.7564
60	0.4051	300	0.8125
70	0.4346	370	0.8598
80	0.4656	490	0.9011
100	0.5217	610	0.9365
120	0.5660		

Adsorbent : 5A MSC
 Adsorbate : Oxygen
 Adsorption Temp : 0°C
 Figure number : none
 Notes : 602 Torr

Time (sec)	Mt/M _∞
3	0.1021
4	0.1710
5	0.1916
8	0.2229
9	0.2856
10	0.3196
11	0.3268
12	0.3384
13	0.3456
14	0.3483
15	0.3778
20	0.4924
25	0.5067
30	0.5389
35	0.5739
40	0.6276
50	0.6759
60	0.7466
70	0.7834
80	0.8241
90	0.8554
120	0.9155
340	0.9973
440	0.9973
490	0.9982
590	1.0000

Diffusivity (D/r²) = 0.0012 s⁻¹

Adsorbent : 5A MSC
 Adsorbate : Oxygen
 Adsorption Temp : 0°C
 Figure number : none
 Notes : 1066 Torr

Time (sec)	Mt/M _∞
2	0.1091
3	0.2329
4	0.2654
5	0.2842
6	0.2973
7	0.3116
8	0.3219
9	0.3316
10	0.3441
11	0.3578
12	0.3721
13	0.3840
14	0.4000
15	0.4125
20	0.4719
25	0.5084
30	0.5705
35	0.5825
40	0.6179
50	0.6812
60	0.7405
70	0.7781
80	0.8124
90	0.8272
100	0.8409
110	0.8688
120	0.9036
130	0.9281
190	0.9470
240	0.9652
290	0.9721
590	0.9772
640	0.9937
740	0.9954
1040	1.0000

Diffusivity (D/r²) = 0.0014 s⁻¹

Adsorbent : 5A MSC
 Adsorbate : Oxygen
 Adsorption Temp : 0°C
 Figure number : none
 Notes : 2509 Torr

Time (sec)	Mt/M _∞
2	0.1285
3	0.2318
4	0.2626
5	0.2789
6	0.3003
7	0.3160
8	0.3270
9	0.3294
10	0.3508
11	0.3764
12	0.3950
13	0.4124
14	0.4199
15	0.4287
20	0.4867
25	0.5622
30	0.5825
35	0.6243
40	0.6481
50	0.7062
60	0.7654
70	0.7886
80	0.8026
90	0.8531
100	0.8653
110	0.9036
120	0.9065
190	0.9065
240	0.9501
290	0.9512
340	0.9628
390	0.9704
440	0.9750
490	0.9779
590	0.9866
640	0.9977
740	1.0000

Diffusivity (D/r²) = 0.0015 s⁻¹

Adsorbent : 5A MSC
 Adsorbate : Oxygen
 Adsorption Temp : 0°C
 Figure number : none
 Notes : 3019 Torr

Time (sec)	Mt/M _∞
1	0.0815
2	0.1786
5	0.1801
6	0.1831
7	0.2072
8	0.2343
9	0.2607
10	0.2938
11	0.3239
12	0.3555
13	0.3683
15	0.3811
20	0.4368
25	0.5144
30	0.5626
35	0.5701
40	0.5957
50	0.6875
60	0.7003
70	0.7613
80	0.7809
90	0.8065
110	0.8509
140	0.8785
190	0.9302
340	0.9532
390	0.9613
440	0.9735
640	0.9788
740	0.9824
940	1.0000

Diffusivity (D/r²) = 0.0012 s⁻¹

Adsorbent : 5A MSC
 Adsorbate : Oxygen
 Adsorption Temp : 50°C
 Notes : 203 Torr

Time (sec)	Mt/M _∞
15	0.3674
55	0.8125
60	0.8131
65	0.8155
75	0.8186
95	0.8204
105	0.8289
115	0.8295
125	0.8379
135	0.8458
145	0.8579
155	0.8627
215	0.9002
265	0.9196
315	0.9565
365	0.9728
415	0.9825
465	0.9958
615	1.0000

Diffusivity (D/r²) = 0.014 s⁻¹

Adsorbent : 5A MSC
 Adsorbate : Oxygen
 Adsorption Temp : 50°C
 Notes : 920 Torr

Time (sec)	Mt/M _∞
2	0.2866
3	0.4649
4	0.6164
5	0.7175
6	0.7926
7	0.8470
8	0.8858
9	0.9135
10	0.9347
11	0.9478
13	0.9627
15	0.9692
17	0.9726
19	0.9740
76	0.9778
86	0.9858
96	0.9965
116	0.9975
126	0.9993
146	1.0000

Diffusivity (D/r²) = 0.016 s⁻¹

Adsorbent : 5A MSC
 Adsorbate : Oxygen
 Adsorption Temp : 50°C
 Notes : 347 Torr

Time (sec)	Mt/M _∞
2	0.0186
3	0.3115
4	0.5123
5	0.6497
6	0.7483
8	0.8660
10	0.9200
12	0.9258
14	0.9444
16	0.9506
21	0.9593
36	0.9652
131	0.9668
141	0.9700
191	0.9761
291	0.9803
341	0.9909
441	0.9945
541	0.9967
591	0.9986
641	1.0000

Diffusivity (D/r²) = 0.011 s⁻¹

Adsorbent : 5A MSC
 Adsorbate : Oxygen
 Adsorption Temp : 50°C
 Notes : 2505 Torr

Time (sec)	Mt/M _∞
2	0.2593
3	0.4664
5	0.6869
7	0.7917
9	0.8395
11	0.8595
13	0.8655
18	0.8704
23	0.8837
28	0.8837
118	0.9667
128	0.9724
138	0.9734
188	0.9789
238	0.9830
288	0.9903
338	0.9958
488	0.9964

Diffusivity (D/r²) = 0.011 s⁻¹

APPENDIX B

(Computer Program for VSM Calculations)

C SIMULATION OF ADSORPTION EQUILIBRIA BY VSM
 C SEE PAGE 11 FOR EQUATIONS AND REFERENCES
 C JIN_QU WANG, DEPT. OF CHEMICAL ENG. WORCESTER POLYTECHNIC
 C INSTITUTE, WORCESTER, MA 01609, 1989
 C

```

    PROGRAM AVSM3P
    REAL N1IN,N(50),NC(50),N1INO,N1INF,NN0,NN,NCC(150)
    DIMENSION F0(50),F1(50),F2(50),DALF1N(50),DALF1B(50),
    *           DALF1A(50),DALF2N(50),DALF2B(50),DALF2A(50),
    *           DALF3N(50),DALF3B(50),DALF3A(50),A(10,10)
    DIMENSION F3(50),P(50),X(4),
    *           BB(50),BB1(50),CC(50),CC1(50),CC2(50),CC3(50),
    *           PC(50),CC4(50),DD(50),DD1(50),DAL1(50),DAL2(50),
    *           DAL3(50),PCC(150)
    COMMON /FOUR/ A
    WRITE (*,300)
300  FORMAT(4X,'INPUT SWITCH NUMBER: IF THE UNIT OF PRESSURE')
    WRITE (*,302)
302  FORMAT(4X,'IS psia, INPUT 1; IF THE UNIT OF PRESSURE')
    WRITE (*,304)
304  FORMAT(4X,'IS torr, INPUT 3')
    READ (*,*) SW
    WRITE (*,1)
    1  FORMAT (6X,'INPUT N1INO, B10,AV0,M')
    READ (*,*) N1INO,B10,AV0,M
    OPEN (1,FILE='VSMDATA')
    DO 2 I=1,M
    2  READ (1,*) P(I),N(I)
    CONTINUE
    CLOSE (1)
    WRITE (*,310)
310  FORMAT (6X,'INPUT THE MOLECULAR WEIGHT')
    READ (*,*) WM
    WRITE (*,3)
    3  FORMAT (6X,'N1INO',10X,'B10',10X,'AV0',6X,'WM','M')
    WRITE (*,4)N1INO,B10,AV0,WM,M
    4  FORMAT (1X,4F12.4,I8,/)
    WRITE (*,5)
    5  FORMAT (10X,'P',14X,'N',)
    DO 9 I=1,M
    8  WRITE (*,8) P(I),N(I)
    8  FORMAT (4X, 2F12.5)
    IF (SW.LT.2) GOTO 9
    P(I)=P(I)/51.71
    N(I)=N(I)*22.4
    9  CONTINUE
    J=1
10  N1IN=N1INO
    B1=B10
    ALFA1V=AV0
    AA=N1IN/B1
    SF0=0.0
    SF1=0.0
    SF2=0.0
  
```

```

SF3=0.0
SDF1N=0.0
SDF1B=0.0
SDF1A=0.0
SDF2N=0.0
SDF2B=0.0
SDF2A=0.0
SDF3N=0.0
SDF3B=0.0
SDF3A=0.0
DO 30 I=1,M
BB(I)=N1IN-N(I)
BB1(I)=N(I)/BB(I)
CC(I)=N1IN+ALFA1V*N(I)
CC1(I)=ALFA1V**2*N(I)
CC2(I)=CC1(I)/CC(I)
CC3(I)=ALFA1V*N(I)
CC4(I)=2*N1IN+ALFA1V*N(I)
DD(I)=N1IN*N(I)*ALFA1V
DD1(I)=DD(I)/CC(I)**2
F0(I)=P(I)-AA*BB1(I)*EXP(CC2(I))
F1(I)=F0(I)*(ALFA1V**2*N(I)**2*N1IN*EXP(CC2(I))
*      /(B1*BB(I)*CC(I)**2)-BB1(I)*EXP(CC2(I))/B1+
*      N(I)*N1IN*EXP(CC2(I))/B1/(N1IN-N(I))**2)
SF1=SF1+F1(I)
F2(I)=F0(I)*N(I)*N1IN*EXP(CC2(I))/B1**2/(N1IN-
*      N(I))
SF2=SF2+F2(I)
F3(I)=-F0(I)*N(I)*N1IN*(2*CC3(I)/CC(I)-CC1(I)*N(I)/
*      CC(I)**2)*EXP(CC2(I))/(B1*BB(I))
SF3=SF3+F3(I)
DALF1N(I)=2*(2*CC3(I)**2*EXP(CC2(I))/(B1*BB(I)*CC(I)**
*      2)-2*CC3(I)**2*N1IN*EXP(CC2(I))/(B1*BB(I)
*      **2*CC(I)**2)-2*CC3(I)**2*N1IN*EXP(CC2(I))/(B1*
*      BB(I)*CC(I)**3)-ALFA1V**4*N(I)**3*N1IN*EXP(CC2(I))/
*      (B1*BB(I)*CC(I)**4)+2*N(I)*EXP(CC2(I))/(B1*BB(I)**2)
*      -2*N(I)*N1IN*EXP(CC2(I))/(B1*BB(I)**3))*F0(I)+2*
*      (CC3(I)**2*N1IN*EXP(CC2(I))/(B1*BB(I)*CC(I)**2)-
*      N(I)*EXP(CC2(I))/(B1*BB(I))+N(I)*N1IN*EXP(CC2(I))/
*      (B1*BB(I)**2))**2
SDF1N=SDF1N+DALF1N(I)
DALF1B(I)=2*(-CC3(I)**2*N1IN*EXP(CC2(I))/(B1**2*BB(I)
*      *CC(I)**2)+N(I)*EXP(CC2(I))/(B1**2*BB(I))-
*      N(I)*N1IN*EXP(CC2(I))/(B1**2*BB(I)**2))*F0(I)+2*
*      N(I)*N1IN*EXP(CC2(I))*(CC3(I)**2*N1IN*EXP(CC2(I))/
*      (B1*BB(I)*CC(I)**2)-N(I)*EXP(CC2(I))/(B1*BB(I))+
*      N(I)*N1IN*EXP(CC2(I))/(B1*BB(I)**2))/(B1**2*
*      BB(I))
SDF1B=SDF1B+DALF1B(I)
DALF1A(I)=2*(CC3(I)**2*N1IN*(2*CC3(I)/CC(I)-CC3(I)**
*      2/CC(I)**2)*EXP(CC2(I))/(B1*BB(I)*CC(I)**2)
*      -N(I)*(2*CC3(I)/CC(I)-CC3(I)**2/CC(I)**2)*EXP(CC2(I))/
*      (B1*BB(I))+N(I)*N1IN*(2*CC3(I)/CC(I)-CC3(I)**2/
*      CC(I)**2)*EXP(CC2(I))/(B1*BB(I)**2)+2*DD(I)*N(I)*

```

```

* EXP(CC2(I))/(B1*BB(I)*CC(I)**2)-2*CC3(I)**2*N(I)*
* N1IN*EXP(CC2(I))/(B1*BB(I)*CC(I)**3))*F0(I)-2*
* N(I)*N1IN*(2*CC3(I)/CC(I)-CC3(I)**2/CC(I)**2)*EXP(
* CC2(I))*(CC3(I)**2*N1IN*EXP(CC2(I))/(B1*BB(I)*
* CC(I)**2)-N(I)*EXP(CC2(I))/(B1*BB(I))+N(I)*N1IN*
* EXP(CC2(I))/(B1*BB(I)**2))/(B1*BB(I))
SDF1A=SDF1A+DALF1A(I)
DALF2N(I)=-2*CC3(I)**2*N1IN*EXP(CC2(I))*F0(I)/(B1**
* 2*BB(I)*CC(I)**2)+2*N(I)*EXP(CC2(I))*F0(I)/
* (B1**2*BB(I))-2*N(I)*N1IN*EXP(CC2(I))*F0(I)/(B1**
* 2*BB(I)**2)+2*N(I)*N1IN*EXP(CC2(I))*(CC3(I)**2*
* N1IN*EXP(CC2(I))/(B1*BB(I)*CC(I)**2)-N(I)*EXP(
* CC2(I))/(B1*BB(I))+N(I)*N1IN*EXP(CC2(I))/(B1*
* BB(I)**2))/(B1**2*BB(I))
SDF2N=SDF2N+DALF2N(I)
DALF2B(I)=2*(N(I)*N1IN)**2*EXP(2*CC2(I))/(B1**4*
* BB(I)**2)-4*N(I)*N1IN*EXP(CC2(I))*F0(I)/
* (B1**3*BB(I))
SDF2B=SDF2B+DALF2B(I)
DALF2A(I)=2*N(I)*N1IN*(2*CC3(I)/CC(I)-CC3(I)**2/CC(I)
* **2)*EXP(CC2(I))*F0(I)/(B1**2*BB(I))-2*
* (N(I)*N1IN)**2*(2*CC3(I)/CC(I)-CC3(I)**2/CC(I)**2)*
* EXP(2*CC2(I))/(B1**3*BB(I)**2)
SDF2A=SDF2A+DALF2A(I)
DALF3N(I)=2*CC3(I)**2*N1IN*(2*CC3(I)/CC(I)-CC3(I)**2/
* CC(I)**2)*EXP(CC2(I))*F0(I)/(B1*BB(I)*CC(I)
* **2)-2*N(I)*(2*CC3(I)/CC(I)-CC3(I)**2/CC(I)**2)*EXP(
* CC2(I))*F0(I)/(B1*BB(I))+2*N(I)*N1IN*(2*CC3(I)/
* CC(I)-CC3(I)**2/CC(I)**2)*EXP(CC2(I))*F0(I)/
* (B1*BB(I)**2)-2*N(I)*N1IN*(2*CC3(I)**2/CC(I)**3-2*
* CC3(I)/CC(I)**2)*EXP(CC2(I))*F0(I)/(B1*BB(I))-2*N(I)*
* N1IN*(2*CC3(I)/CC(I)-CC3(I)**2/CC(I)**2)*EXP(CC2(I))*
* (CC3(I)**2*N1IN*EXP(CC2(I))/(B1*BB(I)*CC(I)**2)-
* N(I)*EXP(CC2(I))/(B1*BB(I))+N(I)*N1IN*EXP(CC2(I))/
* (B1*BB(I)**2))/(B1*BB(I))
SDF3N=SDF3N+DALF3N(I)
DALF3B(I)=2*N(I)*N1IN*(2*CC3(I)/CC(I)-(CC3(I)/CC(I))
* **2)*EXP(CC2(I))*F0(I)/(B1**2*BB(I))-2*
* (N(I)*N1IN)**2*(2*CC3(I)/CC(I)-(CC3(I)/CC(I))**2)*
* EXP(2*CC2(I))/(B1**3*BB(I)**2)
25 SDF3B=SDF3B+DALF3B(I)
DALF3A(I)=-2*N(I)*N1IN*(2*CC3(I)/CC(I)-(CC3(I)/CC(I))
* **2)**2*EXP(CC2(I))*F0(I)/(B1*BB(I))-2*N(I)
* *N1IN*(2*N(I)/CC(I)-4*CC3(I)*N(I)/CC(I)**2+2*CC3(I)**
* 2*N(I)/CC(I)**3)*EXP(CC2(I))*F0(I)/(B1*BB(I))+2*(N(I)
* *N1IN)**2*(2*CC3(I)/CC(I)-CC3(I)**2/CC(I)**2)**2*
* EXP(2*CC2(I))/(B1*BB(I))**2
SDF3A=SDF3A+DALF3A(I)
30 CONTINUE
WRITE (*,40)
40 FORMAT (10X,'I',6X,'J',6X,'SF1',6X,'SF2',6X,'SF3',/)
WRITE (*,45) I,J,SF1,SF2,SF3
45 FORMAT (2X,2I8,3E12.4)
A(1,1)=SDF1N

```

```

A(1,2)=SDF1B
A(1,3)=SDF1A
A(1,4)=-SF1
A(2,1)=SDF2N
A(2,2)=SDF2B
A(2,3)=SDF2A
A(2,4)=-SF2
A(3,1)=SDF3N
A(3,2)=SDF3B
A(3,3)=SDF3A
A(3,4)=-SF3
K=3
NP1=K+1
CALL GAUSS (X,K,NP1)
DAL TAN=X(1)
DAL TAB=X(2)
DAL TAA=X(3)
N1INF=N1IN+DAL TAN
B1F=B1+DAL TAB
ALF1VF=ALFA1V+DAL TAA
WRITE(*,55)
55  FORMAT(/,8X,'DAL TAN',10X,'DAL TAB',10X,'DAL TAA')
WRITE(*,60) DAL TAN,DAL TAB,DAL TAA
60  FORMAT(1X,3E15.6 )
WRITE(*,65)
65  FORMAT(/,8X,'N1INF',10X,'B1F',10X,'ALFA1VF' )
WRITE(*,70) N1INF,B1F,ALF1VF
70  FORMAT(1X,3E15.6)
IF (ABS(DAL TAN).GT.0.000001) GOTO 72
IF (ABS(DAL TAB).GT.0.000001) GOTO 72
IF (ABS(DAL TAA).LT.0.000001) GOTO 80
72  IF (ABS(SF1).GT.0.001 ) GOTO 75
IF (ABS(SF2).GT.0.001 ) GOTO 75
IF (ABS(SF3).LT.0.001 ) GOTO 80
75  N1INO=N1INF
B10=B1F
AV0=ALF1VF
J=J+1
GOTO 10
80  WRITE(*,85)
85  FORMAT(6X,'J',6X,'N1INF',8X,'B1F',8X,'ALFA1VF')
WRITE(*,90) J,N1INF,B1F,ALF1VF
90  FORMAT(1X,I8,3F15.4,/)
SR=0.0
DO 100 K=1,M
PC(K)=N(K)*N1INF*EXP(ALF1VF**2*N(K)/(N1INF+ALF1VF*N(K)))/
*      (B1F*(N1INF-N(K)))
SR=SR+(P(K)-PC(K))**2
100  CONTINUE
ER0=SR/M
ER=(ER0)**(0.5)
WRITE (*,101) N1INF,B1F,ALF1VF
101  FORMAT (4x,'VSM Parameter: N1INF=',E9.4,3X,'B1F=',E9.4,
*          3X,'ALF1VF=',E10.4,/)

```

```

102     PAUSE 102
103     WRITE(*,105)
104     FORMAT(6X,'I',8X,'P',14X,'PC',16X,'N',/)
105     DO 115 I=1,M
106         P(I)=P(I)*51.71
107         PC(I)=PC(I)*51.71
108         N(I)=N(I)/22.4
109         WRITE(*,110) I,P(I),PC(I),N(I)
110     FORMAT(1X,I6,3F15.8)
111     CONTINUE
112     WRITE (*,120) ER
113     FORMAT (/,6X,'ER=',F12.6)
114     NCC(1)=0.0
115     PCC(1)=0.0
116     DAN=(N(M)*22.4+5)/100
117     DO 130 I=2,100
118         NCC(I)=NCC(I-1)+DAN
119         PCC(I)=NCC(I)*N1INF*EXP(ALF1VF**2*NCC(I)/(N1INF+
120 *           ALF1VF*NCC(I)))/(B1F*(N1INF-NCC(I)))
121     CONTINUE
122     OPEN (2,FILE='VSMC100.DAT')
123     DO 150 I=1,100
124         PCC(I)=PCC(I)*51.71
125         NCC(I)=NCC(I)/22.4
126         WRITE (2,*) PCC(I),NCC(I)
127     CONTINUE
128     CLOSE (2)
129     END

```

```

C-----
      SUBROUTINE GAUSS (X,N1,NP1)
      DIMENSION X(10),A(10,10)
      COMMON /FOUR/ A
C      THIS SUBROUTINE SOLVES A SYSTEM OF N LINEAR
      DO 100 K=1,N1
      IF(K.EQ.N1) GOTO 30
      KP1=K+1
      L=K
      DO 10 I=KP1,N1
      IF(ABS(A(I,K)).GT.ABS(A(L,K))) L=I
10     CONTINUE
      IF(L.EQ.K) GOTO 30
      DO 20 J=K,NP1
      C=A(K,J)
      A(K,J)=A(L,J)
      A(L,J)=C
20     CONTINUE
30     PIVOT=A(K,K)
      DO 40 J=K,NP1
      A(K,J)=A(K,J)/PIVOT
40     CONTINUE
      DO 60 I=1,N1
      IF(I.EQ.K) GOTO 60
      FACTOR=A(I,K)
      DO 50 J=K,NP1

```



```
      A(I,J)=A(I,J)-FACTOR*A(K,J)
50    CONTINUE
60    CONTINUE
100   CONTINUE
      DO 200 I=1,N1
      X(I)=A(I,NP1)
200   CONTINUE
      RETURN
      END
```